63-3-4

GD|C-63-060

DEVELOPMENT OF A TELEMETERING OCEANOGRAPHIC BUOY

PROGRESS REPORT

FEBRUARY 1963

GENERAL DYNAMICS | CONVAIR
Post Office Box 1950, San Diego 12, California

GDC-63-060

DEVELOPMENT OF A TELEMETERING OCEANOGRAPHIC BUOY

PROGRESS REPORT

February 1963

Sponsored by
United States Navy
Office of Naval Research
Contract Nonr-3062(00)
NR 083-147

Robert Devereux

W. R. Hoover

J. T. Lack

K. A. Morgan

N. W. Reed

V. J. Schack

S. E. Sowers

L. Turchick

F. E. Wilson

The authors express their appreciation for the particularly intelligent and industrious efforts of Mr. J. L. Hemming, Research and Development Technician for this project.

CONTENTS

TABLES

ILLUSTRATIONS

1 | INTRODUCTION

For many years buoys have been used at sea as aids to navigation, and, more recently, as moored or drifting platforms for collection of oceanographic data. Most of these efforts have met with success. Ordinary aid-to-navigation (ATN) buoys, moored in shallow water by brute-force methods that are truly classic, remain on station reliably for periods as long as a year in all kinds of weather. Many oceanographic buoys moored in deep water have successfully remained on station for similar periods. In these cases brute-force methods had been abandoned in favor of a more sophisticated design philosophy.

As the capability requirements for oceanographic buoys increased, in terms of the number of measurements to be sampled and the rate of their sampling, of telemetering data long distances by radio to shore, and of remaining on station for a year or more, it became necessary to study the entire buoy question in a more systematic way than had been done before. In this way the many factors influencing design and total performance of a buoy system could be properly taken into account. Only if this were done could the success of continued development of oceanographic buoys be assured.

Accordingly, General Dynamics/Convair proposed to conduct a series of studies to investigate the major problems standing in the way of development of buoy systems. It was proposed to conduct: 1. a comparative study of the drag of shapes proposed for buoy hulls, 2. a life test at sea of an unattended electric power system, 3. a study of antennas for long-distance ionospheric telemetry from buoys, and 4. a study into the methods and equipment available to give an oceanographic buoy the data capability required.

No investigation of this kind could be planned or conducted without having information about the nature of the task the buoy system would be expected to perform. Preliminary specifications for the capability of the buoy were suggested by Oceanographic Office (then Hydrographic Office) and Office of Naval Research, in a meeting of some members of the Guidance Committee at Washington, D.C., in December 1961. It was determined that each buoy should have a capability of accepting 100 channels of data, of telemetering these data 4 times each 24 hours over distances as great as 2000 miles on command from shore, and of storing the data in the buoy for its design station endurance of one year.

The work was begun in March, 1962, and is continuing. This report presents results of work completed as of February 1963, for which final data processing has been done. It also presents preliminary results of the electric power system tests at sea, which are still in progress.

2 | BUOY HULL MODEL TESTS

2.1 GENERAL

To establish a successful mooring in deep water, where the weight and fluid-dynamic drag of the mooring line itself are important considerations, requires a surface float that places small tensile demands upon the mooring line. As part of the study program at General Dynamics/Convair, a comparative evaluation of the drag and stability of various shapes and sizes of buoy hulls was conducted. The work was begun in May 1962. Final processing of data is complete and the results are presented here.

2.2 DRAG STUDIES

Tests of buoy hull drag were conducted in the Convair Hydrodynamics Towing Basin. Fourteen scale-models were tested. In testing some of them at different densities to arrive at different full-scale sizes, a total of 24 configurations was tested, involving 957 gravity tows and 147 carriage runs in the towing basin.

2.2.1 PROCEDURE — To obtain preliminary data, each shape was gravity towed by calibrated weights and monofilament line over a system of pulleys, as shown in Figure 1. Velocity was determined by timing the run over a measured distance, after acceleration to constant speed. Final data were obtained by towing each model from an underwater sting moved by the towing basin carriage (Figure 2).

Mooring line angle was kept at approximately 45° during the carriage runs. Actual mooring-line tension was recorded on an oscillograph on the carriage.

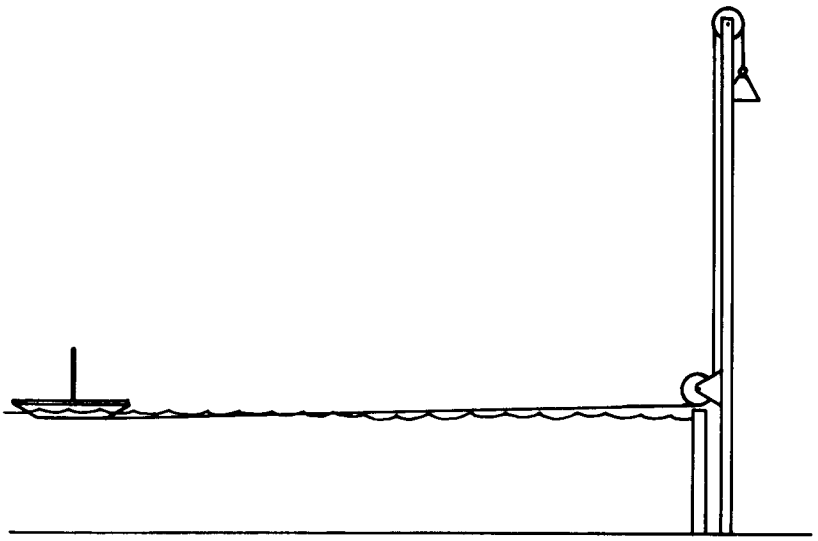

Figure 1. Method of Gravity Tow

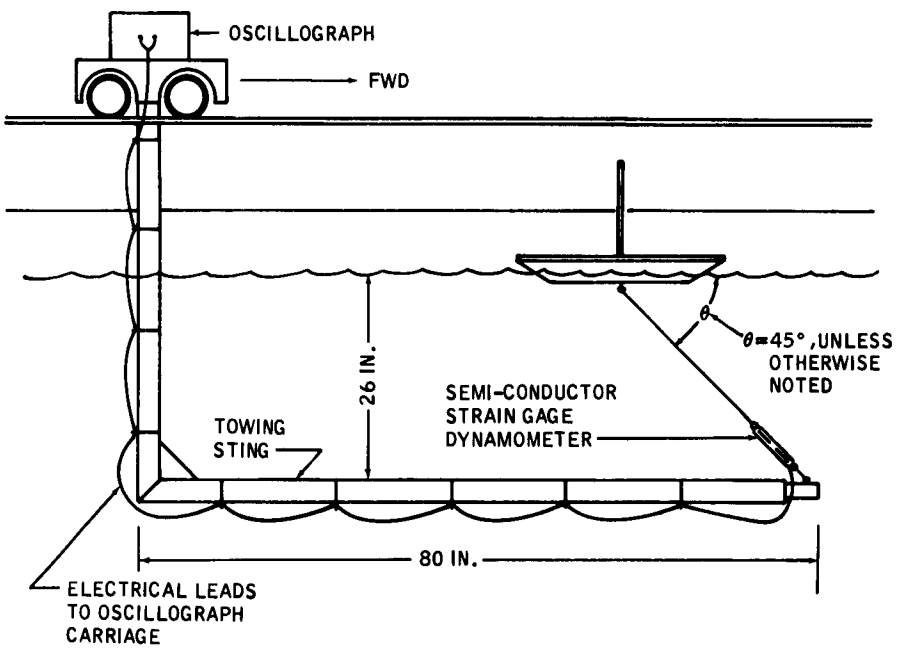

Figure 2. Test Method for Comparative Drag Data

Signals from a small, precision dynamometer in the mooring line were fed to the recorder.

The dynamometer, in addition to being carefully calibrated in the laboratory before the runs, was given a complete resistance-substitution R_{cal} calibration before and after each run. The dynamometer is a solid-state strain gage unit designed and built at Convair especially for these tests. It has good sensitivity and was found to be stable.

Each carriage run was a constant acceleration from rest to a velocity equivalent to 10 kt full scale, or until towing-under of the model, if that occurred first. Acceleration was very gradual, requiring in some cases two passes of the entire 300-ft. length of the towing basin. (One pass 0 - 5 kt., another 5 - 10 kt., equivalent full-scale velocity.)

Towing was conducted in smooth water and in the presence of waves. Ciné photographs were made of the runs to record the behavior of each model. Data correlation between oscillograms and ciné films was accomplished by recording timing pulses on the paper record; the pulses also advanced a counter in the field of the ciné camera.

Oscillograms and associated ciné footage were analyzed and the data given a preliminary processing to compare the drag of each hull shape. Data from those shapes exhibiting low drag were then given rigorous final processing. Processing of data consisted of extrapolation to the full scale of the drag values obtained from the models.

All model data were extrapolated to full scale, using the Schoenherr Mean-Line Method according to the Uniform Procedure set forth in Technical and Research Bulletin No. 1-2 (reprinted by Society of Naval Architects and Marine Engineers, March 1952).

Full scale was taken as the actual size and gross weight of the shapes tested that are already in use at sea. (In one case, extrapolation was also made to a

size and gross weight exceeding that of the buoy actually in use.) In the case of new shapes proposed for use at sea, test data were extrapolated to several different full-scale sizes and gross weights in an attempt to find an optimum. A net or payload weight of 4,000 pounds (full scale) was used as a guide in establishing full-scale density. In new shapes, full-scale tare or bare-hull weight was computed from state-of-the-art structural standards. Extrapolation to different full-scale sizes and gross weights was made possible by towing the same model at correspondingly different densities.

2.2.2 RESULTS — Preliminary testing of models showed large differences in the drag of the various shapes. In general, the cylinder spar and related shapes such as the aid-to-navigation (ATN) buoys exhibited the greatest drag of all the shapes tested. For this reason only the drag test results of the spars are illustrated in this report, as a comparison for the several shapes which exhibited relatively low drag.

Measurements were made of the drag of each model in the presence of surface waves. Attempts to extrapolate these data have been inconclusive. Only the observations and qualitative results of wave test drag are presented.

Final results of smooth-water test data are shown in Figures 3 and 4.

Figure 3 compares eight different shapes — plotting actual, predicted full-scale mooring-line tension (at 45° mooring angle) as a function of equivalent, full-scale current velocity in knots. Full-scale gross weights are also indicated. Except for the two 8-ft. toroids and the 45-in.-diameter cylinder spar, payload weight (gross weight minus bare-hull-plus-ballast weight) used in computing full-scale hull density was 4,000 pounds.

Figure 4 compares the same shapes, plotting the ratio of horizontal drag to gross weight (again full scale) as a function of equivalent, full-scale current velocity in knots.

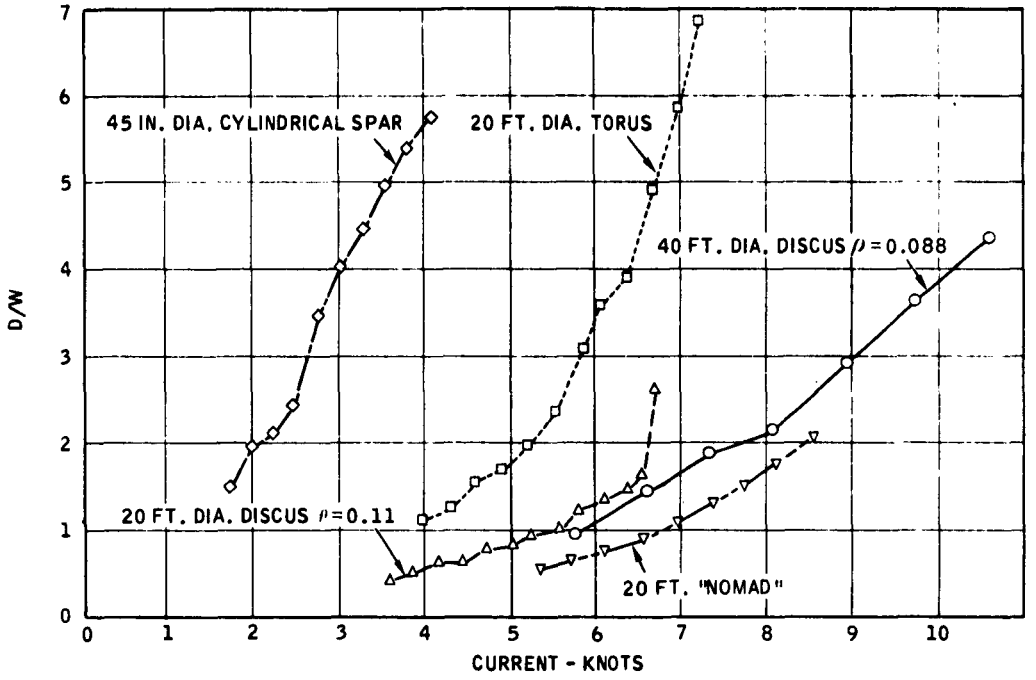

Figure 3. Buoy Mooring Loads in Ocean Currents

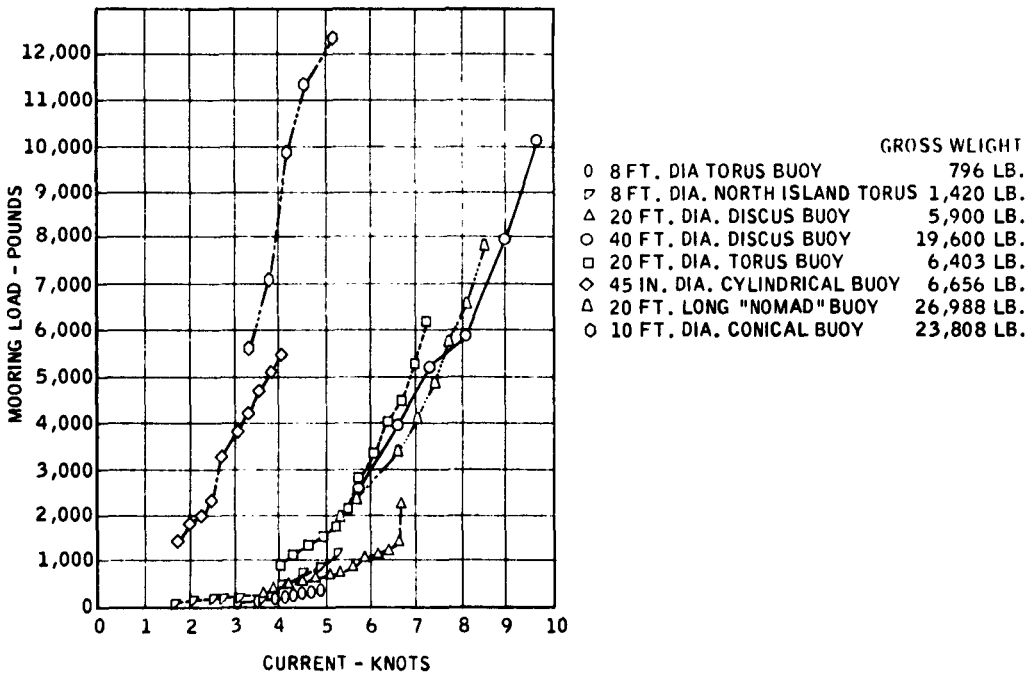

Figure 4. Drag Weight Ratio of Several Buoy Shapes

2.2.2.1 Aid-To-Navigation (ATN) Buoy — A 1/27-scale model of an ATN buoy such as a standard lighted bell buoy was tested. Shape, dimensions, and gross weight were obtained from U. S. Coast Guard Civil Engineering Report No. 33, Performance Characteristics of Buoys (CG-250-33, February 1959). Figure 5 shows this model.

Preliminary towing tests of the ATN buoy showed its drag to be high (nearly identical to that of the cylinder spar); consequently, test results for this shape were not processed rigorously. Preliminary processing of data was accomplished to arrive at scale velocities for the towing tests. Horizontal tows using the gravity method, and subsequent carriage tows using a mooring-line angle of 45°, produced towing-under of the model at an equivalent full-scale velocity of approximately 4 kt.

Figure 5. Aid-To-Navigation Buoy Model

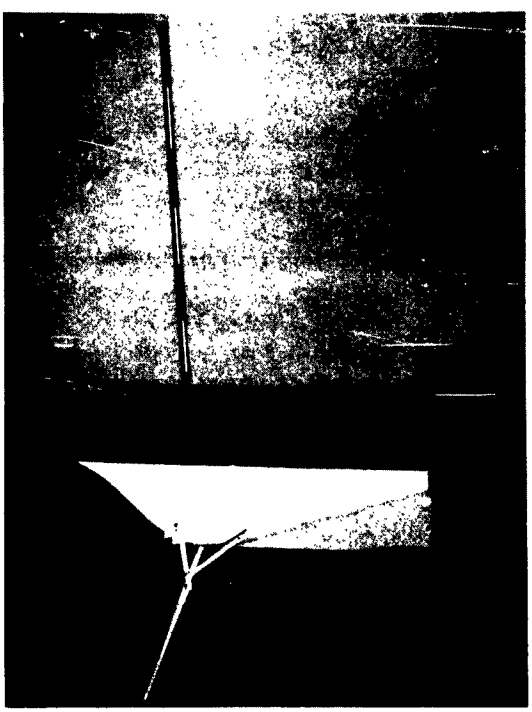

Figure 6. NOMAD Boat-Type Buoy Model

Large eddies from shed vortices were observed in the wake. At equivalent full-scale velocities exceeding 2 kt., shedding of vortices produced side-to-side deviations from the towing path, and pendular oscillations exceeding 30°. Because of its great drag, this shape exhibited no large increment of drag associated with towing under.

Towing of this model in the presence of waves produced significant periodic variation in mooring-line tension. Except at resonance waves appeared to have little effect upon the velocity at which towing-under occurred. Because of its small freeboard or reserve buoyancy, wave crests continually swept over the model at towing velocities much less than those at which towing under occurred in smooth water.

2.2.2.2 Boat Buoy — A 1/40-scale model of the NOMAD buoy hull was tested. Exact shape, dimensions and design gross weight were obtained from David Taylor Model Basin Report No. 550, Characteristics of the NRL Mk 3 Boat-Type Buoy and Determination of Mooring-Line Sizes, Ensign P. Eisenberg, September 1945, describing the original tests of this hull. Figure 6 shows this model.

Preliminary towing tests showed that the drag of the NOMAD hull is low. Rigorous processing of gravity tow and carriage tow data (Figure 4) revealed that the NOMAD hull has the lowest drag/weight ratio of all the shapes tested.

Observations of the model confirmed the behavior described in the DTMB report (stated to be a design objective), in that towing-under of the model occurred. Repeated attempts to cause the model to plane out again after towing under (also designated a design objective and demonstrated in the DTMB tests) were not successful. Towing under was often associated with development of instability in yaw, and then deviation from the towing path in one direction or the other, so that the model veered steadily to left or to right, rolled down in the same direction, and left the surface (downward) at a roll attitude of approximately 40°. With the center of gravity located slightly farther aft than indicated in the DTMB reports, this divergence did not occur — the model simply towed under. Some

increment of drag was associated with attachment of flow of water to the deck surface and additional production of waves at the moment of towing under.

Towing of the model in the presence of waves showed large periodic variations in mooring-line tension. Because of its relatively small freeboard or reserve buoyancy, the model was occasionally swept over by wave crests at velocities less than that at which towing under occurred in smooth water. Otherwise the model appeared to behave well.

2.2.2.3 Discus Buoys — Four discus hull models were tested: three of 1/40 scale and one of 1/20 scale relative to full-scale diameter of 50 feet. The first was a simple cylindrical disc resembling a coin, tested to obtain baseline data for this shape (Figure 7). The second and third models had beveled edges (Figures 8, 9). The latter model was used extensively during the tests. The fourth model (Figure 10) was used to obtain scaling data.

Shape of the model was determined arbitrarily. Except for establishing the 15:1 ratio of diameter to thickness and determining the 30° angle of the beveled edge, no attempt was made to optimize the shape.

Preliminary towing tests showed the drag of the discus with beveled edge to be low. Figure 4 shows the results of rigorous processing of towing data. Figure 3 shows the mooring line tension of a 40-ft. discus of 19,600 pounds full-scale gross weight.

The discus models were tested at several different gross weights, permitting extrapolation of data to correspondingly different full-scale sizes. Variation of gross weight was computed to account for the fixed value of 4,000-pound payload common to all, assuming the basic structure weight varies as the cube of the scale. Figure 11 shows a comparison of four different full-scale sizes of discus, plotting mooring line tension as a function of equivalent full-scale current velocity.

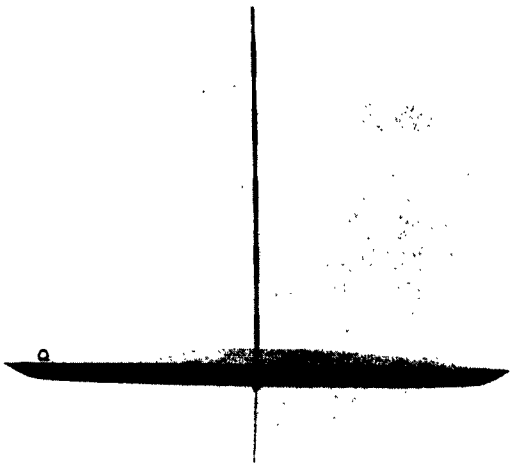

Figure 7. Discus Buoy Model, Preliminary

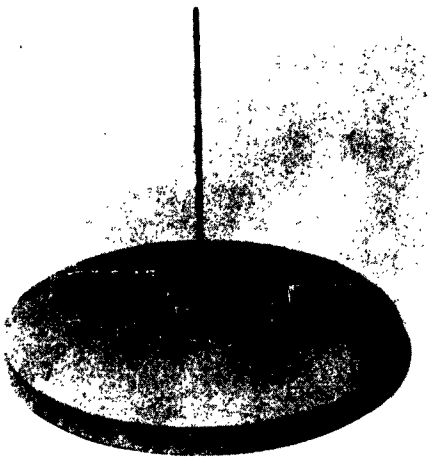

Figure 8. Discus Model For Baseline Data

Figure 9. Discus Buoy 15-Inch Model

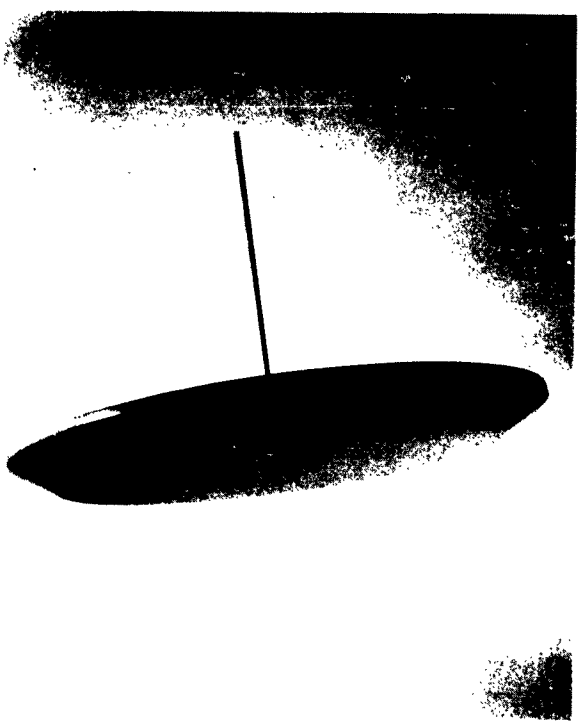

Figure 10. Discus Buoy 30-Inch Model

Observation of the models showed that below a certain density, towing-under of the discus could not be induced within the range of velocities used in the tests and the range of wave characteristics that could be produced in the towing basin. As shown in Figure 3, the drag of the 20-ft. full-scale discus increases abruptly upon towing under at approximately 6.5 kt. equivalent full-scale velocity, in smooth water. The 30-ft., full-scale discus model was observed to tow under occasionally only in rough water. With model density adjusted to correspond to a 40-ft. full-scale diameter, and a hull gross weight of 19,600 lb., towing under could not be induced.

The models were towed from a point at the exact center of the bottom of the disc. No preferred orientation in rotation was observed, although small random perturbations, of the order of ±40° in rotation, sometimes occurred. No sustained rotation was observed.

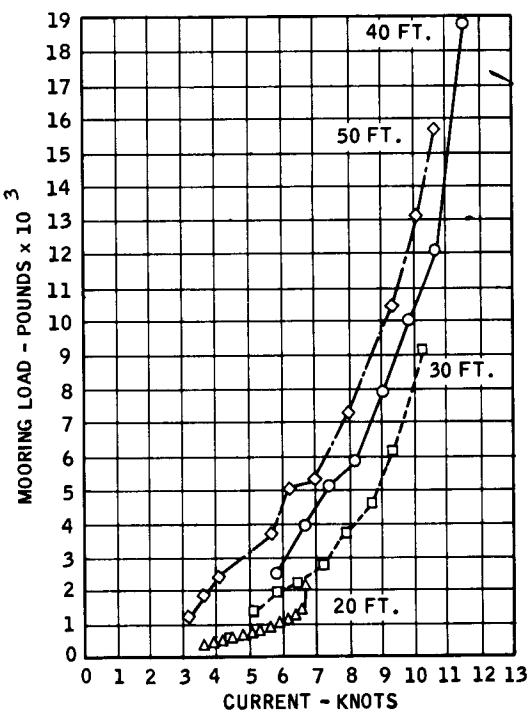

Figure 11. Mooring Loads for Various Diameter Discus Buoys

With the density of the model adjusted to correspond to a 40-ft. -diameter full scale, the model behaved as a planing hull,above a certain equivalent full-scale velocity depending upon surface roughness. A significant reduction in mooring-line tension was associated with this phenomenon.

Towing of the discus models in the presence of waves showed large variations in mooring-line tension. Because of its relatively large reserve buoyancy, the model was never swept over by wave crests if model density was low enough to prevent towing under. Above that density, towing under usually occurred the first time a large wave crest swept the hull. Towing under was an abrupt phenomenon associated with a large increase of mooring-line tension.

2.2.2.4 Spar Buoys — Models of two types of spar buoy were tested, one a 1/16-scale cylinder spar and the other a 1/40-scale conical spar (Figures 12, 13). Shape and full-scale size of the conical spar were determined experimentally, in an effort to improve stability by placing the center of buoyancy as high as possible and the center of gravity as low as possible. The constriction at the waterline was designed to give a non-linear positive variation in restoring force both up and down from rest, to prevent vertical resonance.

Preliminary towing tests showed the drag of both shapes to be great. In spite of this fact, both shapes were tested in carriage runs and the data given rigorous processing. The results are shown in Figures 3 and 4.

Because of placement of the tow point at the center of lateral resistance of both shapes, there was little tendency to tow under during the gravity tows, which produced purely horizontal towing force. During the carriage tows, with the mooring line at 45° , towing under of both shapes occurred at 4 and 5 kt. equivalent full-scale velocity, respectively. No large increment of drag was associated with towing under.

Large eddies were observed in the wake of both models. Vortex shedding induced side-to-side deviations from the towing path in the case of the cylinder spar, and large pendular oscillations in both shapes.

Towing of these models in the presence of waves produced a significant periodic variation in mooring-line tension. In the case of the cylinder spar, which has three possible modes of resonant motion (described in this report), the variation was complex.

2.2.2.5 Torus Buoys — Four types of torus buoy shapes were tested: two had small minor diameters relative to the major diameters, but had different cross-section shapes of the minor diameter. (See Figures 14 and 15.) The other two had minor diameters that were approximately 30% of the major diameter, one of which had the hole of the donut occupied by a cylinder beneath which a rigid tripod and ballast mass were suspended. A fifth torus model was also tested, twice the size of those whose minor diameter was 30% of major diameter. (See Figures 16, 17 and 18.)

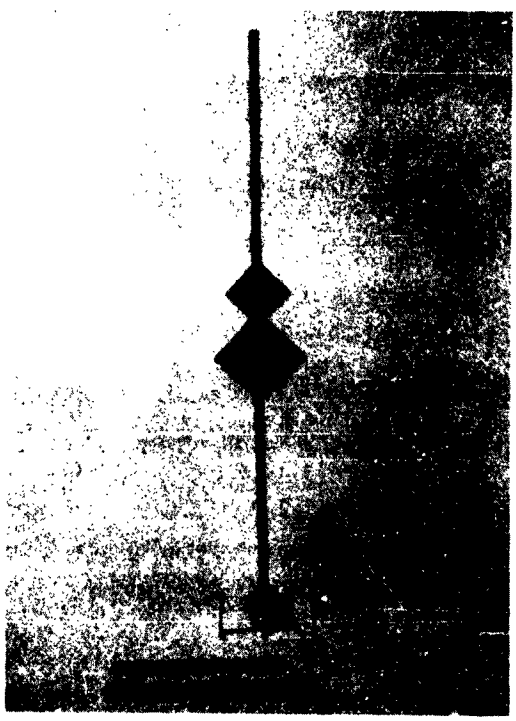

Figure 12. Cylinder Spar Buoy Model Figure 13. Conical Spar Buoy Model

Shape and full-scale size of the two thin toroids were established arbitrarily, purely on the basis of structural density and a full-scale major diameter to afford maximum stability at sea. The two fat toroids represent the buoy designed by Richardson of Woods Hole Oceanographic Institution, and the modification of it being studied by Robinson, of the Fleet Weather Facility, North Island Naval Air Station.

Preliminary towing tests indicated that the torus in any form or proportion is not a low-drag shape. Rigorous processing of data revealed that its drag/weight ratio lies about midway between the high-drag spars and the low-drag shapes, as shown in Figure 4. The indicated 20-ft. full-scale torus is a Richardson torus scaled to accept a 4,000-lb. payload. It has the same density as those presently in use, and is representative of the torus shape.

Observation of towing tests of all toroids with open centers shows large pitch oscillations at some critical velocity. This oscillation seems to be associated with waves or vortices produced by the leading minor diameter of the torus interfering with the trailing minor diameter. It is often accompanied by an increment of drag. In the case of the thin toroids, this phenomenon was seen to induce towing under. In the case of the fat toroids, towing under occurred at a higher velocity, having passed through the phase of oscillations.

The torus having the cylinder situated in the central hole was towed from the lower end of the ballast mass, which was attached to the hull by a rigid tripod. The drag of this torus was comparable to the others, and it towed under at approximately the same equivalent full-scale velocity.

Towing of the models in the presence of waves showed moderately large variations in mooring-line tension. In the case of the thin toroids, towing under was induced by waves and was associated by a large increment of drag. In the case of the fat toroids, the model was swept over by wave crests at a velocity lower than that at which towing under occurred.

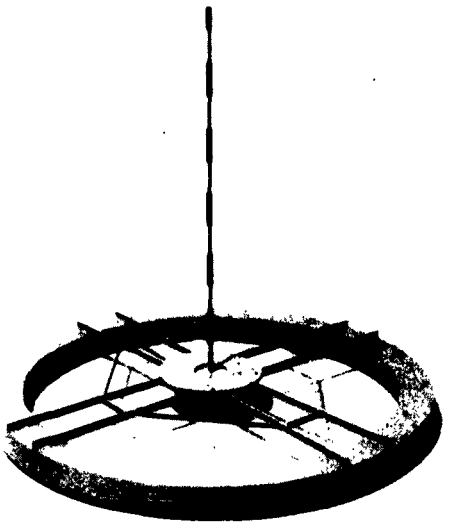

Figure 14. Thin Torus Buoy Model, Square Section

Figure 15. Thin Torus Buoy Model, Semicircular Section

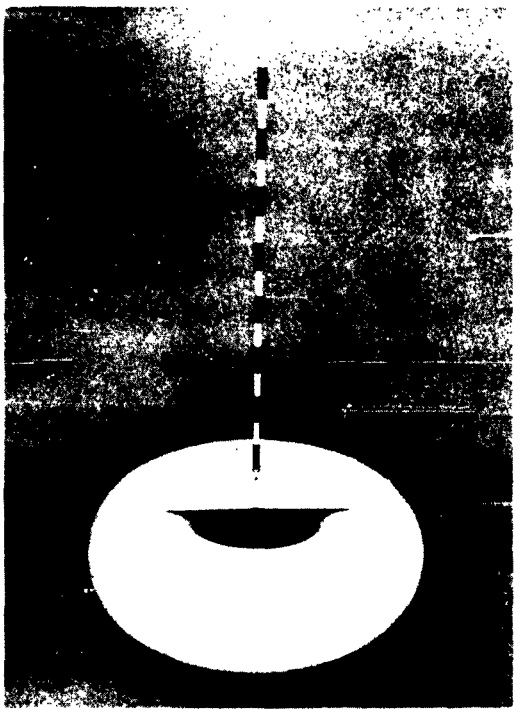

Figure 16. Richardson Torus Buoy Model

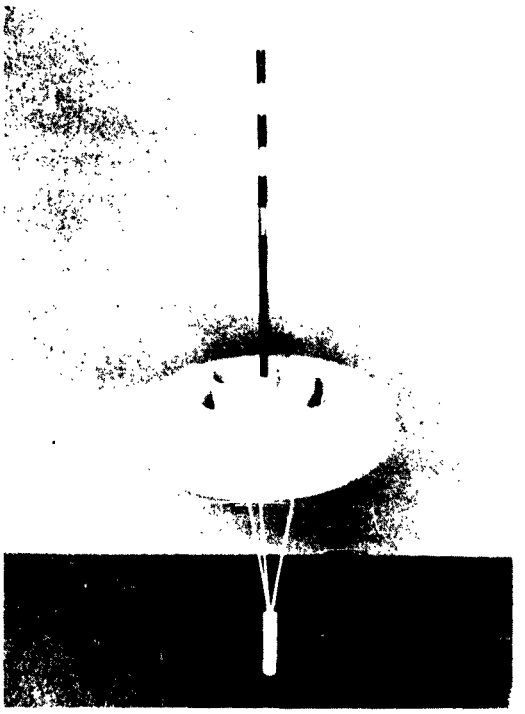

Figure 17. North Island Torus Buoy Model

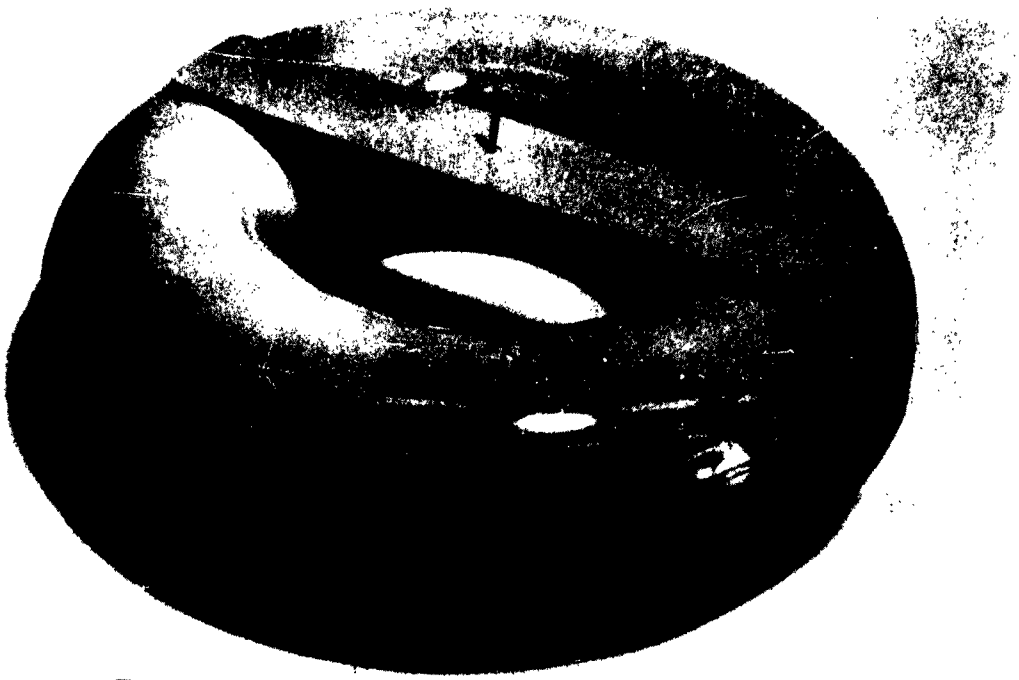

Figure 18. Large Model, Richardson Torus Buoy

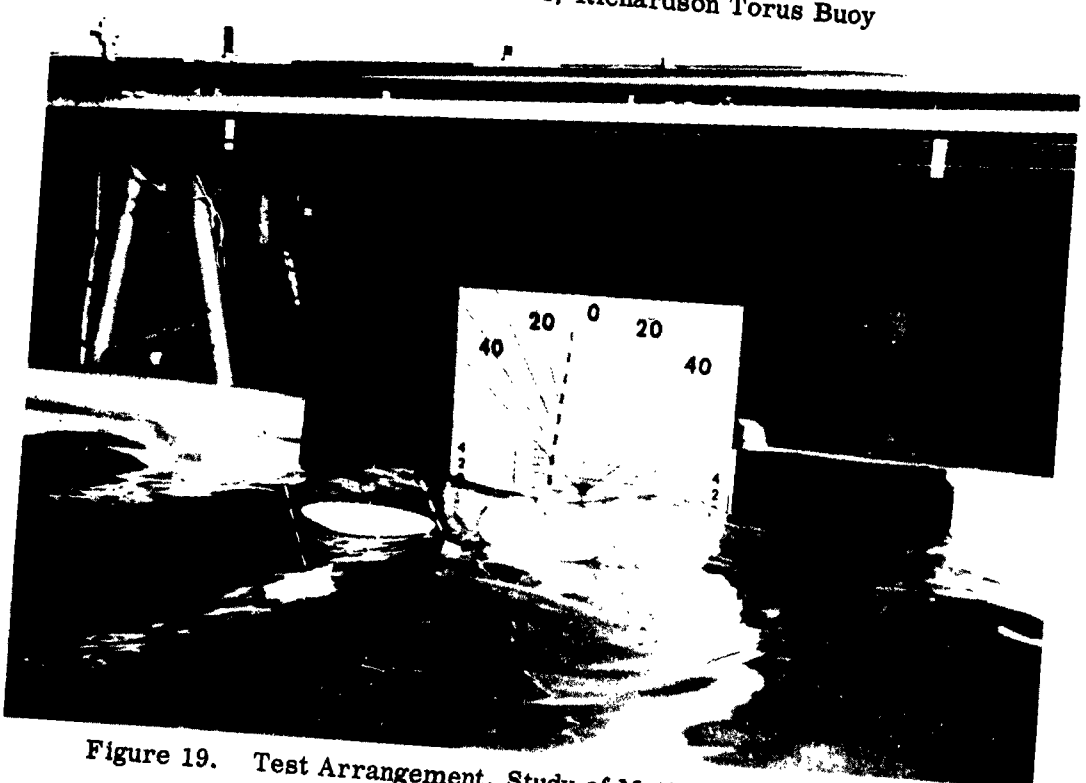

Figure 19. Test Arrangement, Study of Motions of Buoy Models

2.3 MOTION STUDIES

Tests of buoy hull model stability in the presence of surface waves were also conducted in the Convair Hydrodynamics Towing Basin. Eight scale models were tested, selected from those used in the drag studies. (Each of these models was discussed previously in this section.)

2.3.1 PROCEDURE — To obtain preliminary data, each model was tested with a compliant mooring set at an angle of 45° , and the wave-making machine slowly tuned through its entire range of frequency in an attempt to observe resonant motion of the model. Final data were obtained by photographing the model at resonance, or while it was subjected to its worst wave conditions, in front of a protractor board, using the high-speed Millikan ciné camera (Figure 19). The films were analyzed and plots of wave slope and buoy antenna inclination were prepared. Wave height, period and length were also measured.

2.3.2 RESULTS — Preliminary testing of models moored in the towing basin in the presence of waves showed significant differences in the behavior of the various shapes. In general, the cylinder and conical spars, and the ATN buoy, exhibited the greatest motion because they became resonant at some characteristic wave period. The boat buoy in its pitch mode, the discus buoys, and particularly the thin toroids showed least motion in that they most nearly followed the slope of the waves and could not be induced to exhibit resonant motion. Figure 20 shows a comparison of the general behavior of the shapes tested.

2.3.2.1 Aid-To-Navigation (ATN) Buoy — Preliminary wave testing showed that the ATN buoy is capable of resonant pendular motion. To a somewhat less extent, resonance in vertical motion could also be observed. It was found that parametric oscillation could often be observed in pendular motion. This phenomenon is discussed in subparagraph 2.3.2.4 (Spar Buoys) and in paragraph 2.4 (Conclusions).

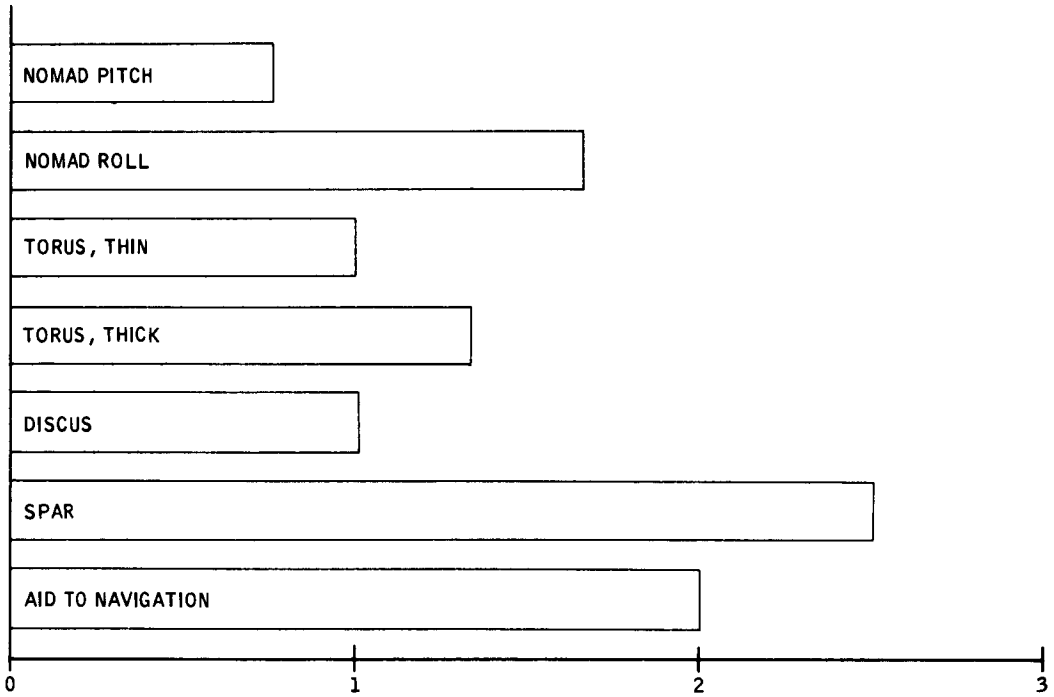

Figure 20. Comparison of Antenna Angle and Wave Slope

Data obtained from tests of the ATN buoy (Figure 21) were rigorously processed. The buoy inclination and wave slope typically associated with it at each instant are shown in Figure 21. The data were taken during resonance in pendular motion in its fundamental mode. Antenna angles of 30° are associated with wave slopes of 15°.

2.3.2.2 Boat Buoy — Preliminary wave tests showed that the boat hull is capable of some resonant motion in roll, but is practically free of resonance in pitch. Figure 22 shows a typical plot resulting from rigorous processing of ciné film exposed during final tests. Pitch motion of 15° is shown, associated with wave slopes of the order of 20°. Figure 23 is a plot showing roll motion approaching 20° associated with waves of slope approximately 15°.

2.3.2.3 Discus Buoys — Two models of the discus shape were tested, identical except that one was twice the diameter and eight times the weight of the other. Preliminary tests indicated that the discus is not capable of resonant behavior,

regardless of wave period or shape.

Analysis of ciné records of the wave tests of the small model showed that in the presence of unstable waves antenna angle could be made to exceed wave slope by as much as 10°, suggesting the possibility of resonance when wave length equals hull diameter (Figure 24). Tests with the large model failed to show resonance. Using this model, large waves (the lengths of which were the same as model diameter) were generated by the wave machine. Figure 25 shows the results of evaluating the typical data obtained. Antenna angle equals wave slope.

Observation of both models, in waves, and analysis of the ciné films, showed slamming when the edge of the disc went into the trough after the buoy had gone over an unstable crest. Digging in of the leading edge or flooding of the upper surface of the buoy were not observed, even with the wave machine set to produce the most precipitous waves within its capability, except when the model was ballasted to several times its normal gross weight.

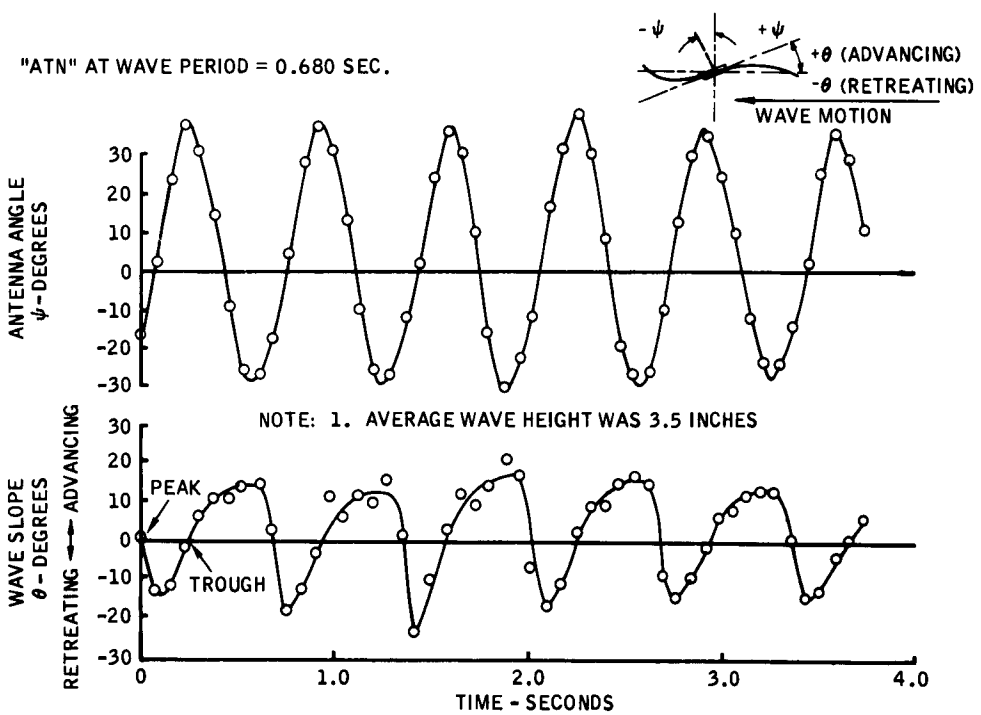

Figure 21. ATN Buoy Model Resonant Motion

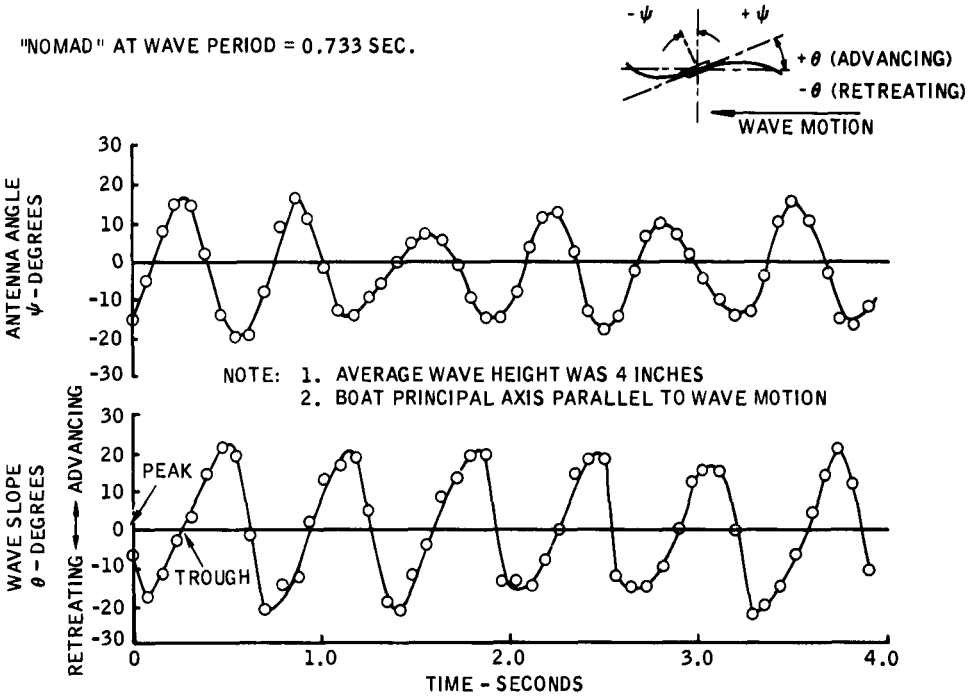

Figure 22. NOMAD Boat-Type Buoy Model Motions, Pitch

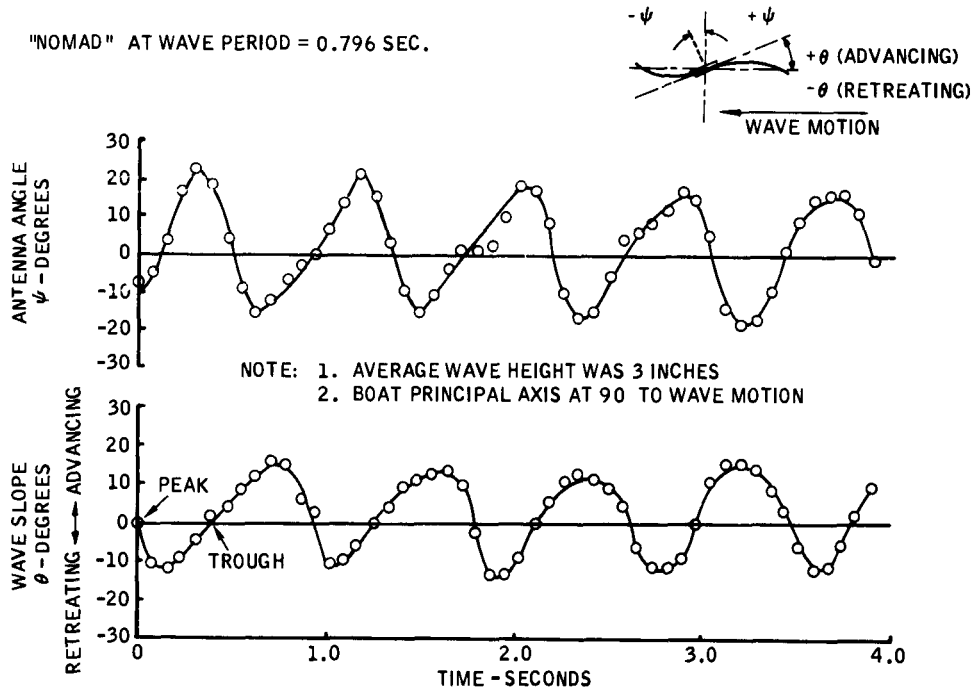

Figure 23. NOMAD Boat-Type Buoy Model Motions, Roll

No rotation of either model was observed during the wave tests.

2.3.2.4 Spar Buoys — Preliminary wave tests of the cylinder spar and the conical spar showed that both shapes are capable of resonant motion. The conical spar model had been especially designed to avoid vertical oscillation. Its non-linear center of buoyancy was concentrated at the surface, with the center of mass concentrated as low as possible. This model could not be made to resonate in vertical oscillation, but it had two modes of pendular resonance: fundamental and parametric.

The cylinder spar model was simply a hollow tube closed at each end with enough lead ballast at the bottom to allow 25% of its length to remain above the surface. Ratio of total length to diameter was 6.65:1. The model' s center of gravity was located approximately 25% from the lower end. The mooring attach point was the same as in the drag studies: at the center of buoyancy, mid-way between the waterline and the lower end of the tube.

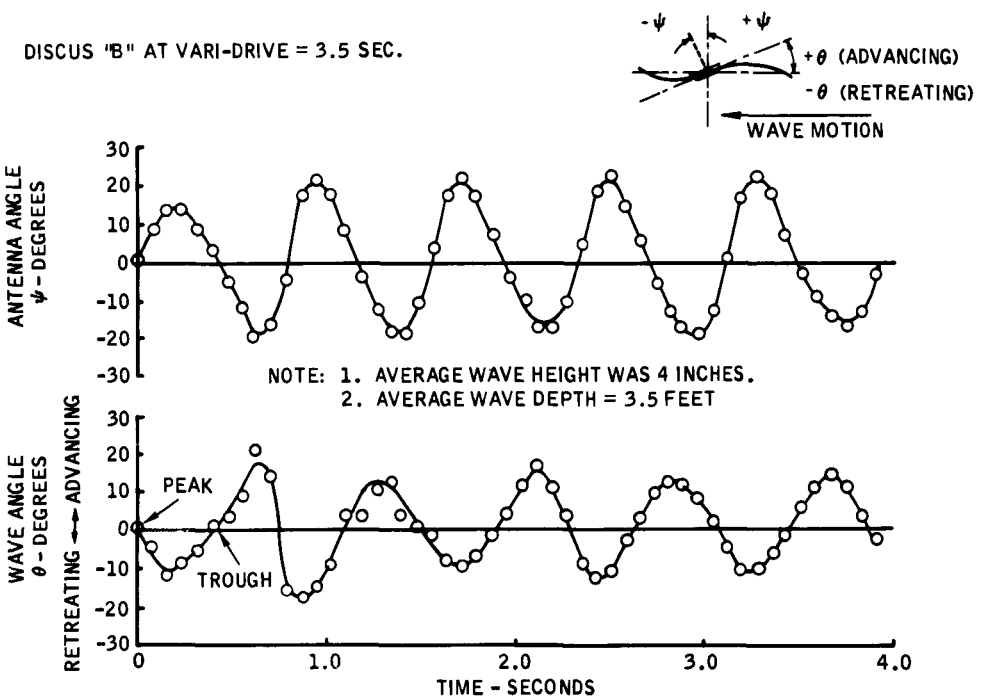

Figure 24. Discus Buoy 15-In. Model Motions

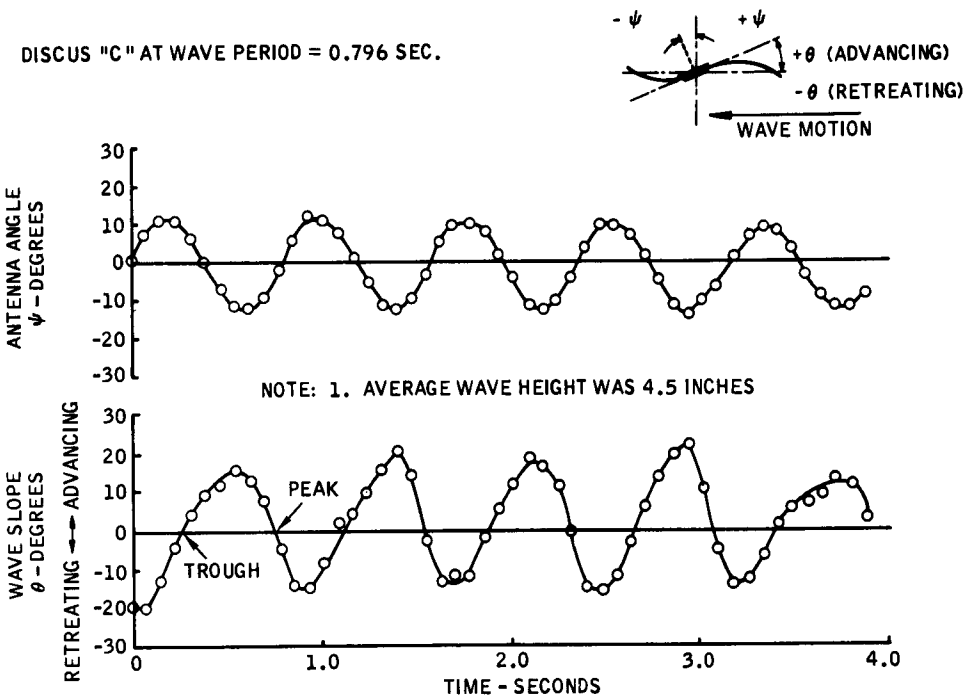

Figure 25. Discus Buoy 30-In. Model Motions

Preliminary wave studies indicated that the cylinder spar had two modes of oscillation: vertical and pendular. In pendular motion it had two modes of resonance: fundamental and parametric.

When the model was studied in the presence of single-frequency waves whose frequency was twice that which usually caused resonance in pendular motion, the model was observed to resonate at its natural or fundamental frequency of pendular motion. This type of motion is known as parametric oscillation. It is a well understood physical phenomenon, having been described by Lord Rayleigh in the case of the pendulum in air, The Theory of Sound, Vol. 1, 68b., published in 1877.

Figure 26 shows a typical plot prepared from the results of processed ciné data obtained during wave tests of the conical spar buoy model. The buoy was at fundamental resonance in pendular motion. Antenna angles exceeding 25° are associated with wave slopes of 10°.

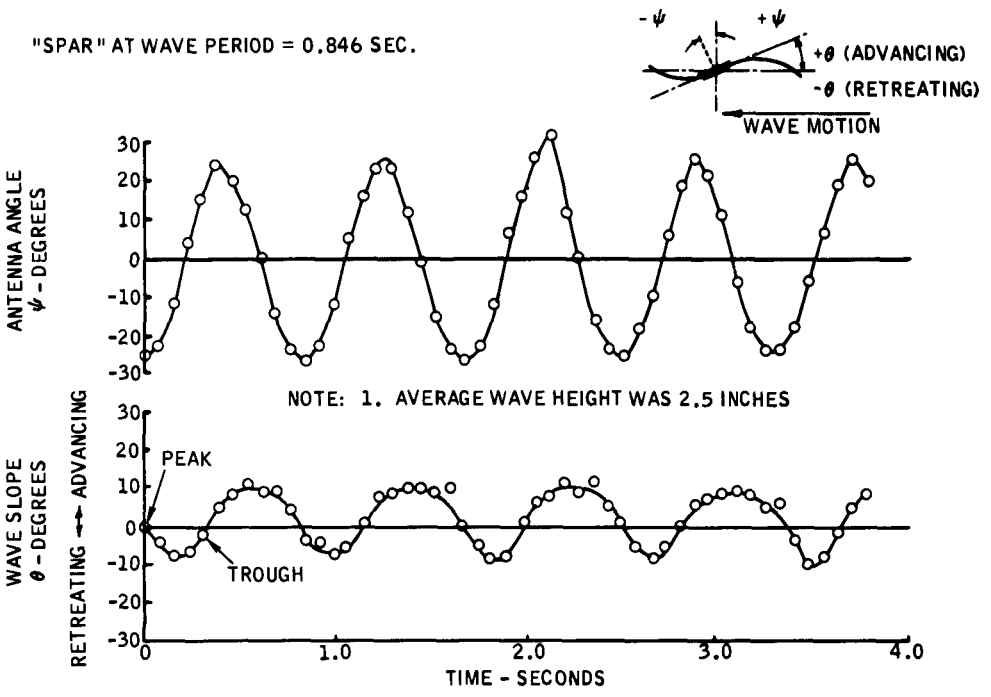

Figure 26. Conical Spar Buoy Model Resonant Motion

2.3.2.5 Torus Buoys — Five models of torus buoys were given preliminary testing. Models with a minor diameter that was a relatively large fraction of the major diameter (fat donut) appeared to be less well coupled to the surface than those whose minor diameter was small compared to the major diameter (thin donut). The thin toroids showed the least motion of any models tested.

Processed ciné data produced typical plots such as those shown in Figure 27, which shows a thin torus in its worst wave condition within the capability of the wave machine in the basin. Antenna angle is the same as wave slope.

2.4 CONCLUSIONS

Attempts to find a hull shape that would remain motionless in waves have not been successful. Shapes that remain vertical in the presence of some waves display resonant motions in response to others. In hull sizes practical for use as unattended oceanographic buoys, the hulls respond to waves of one or more

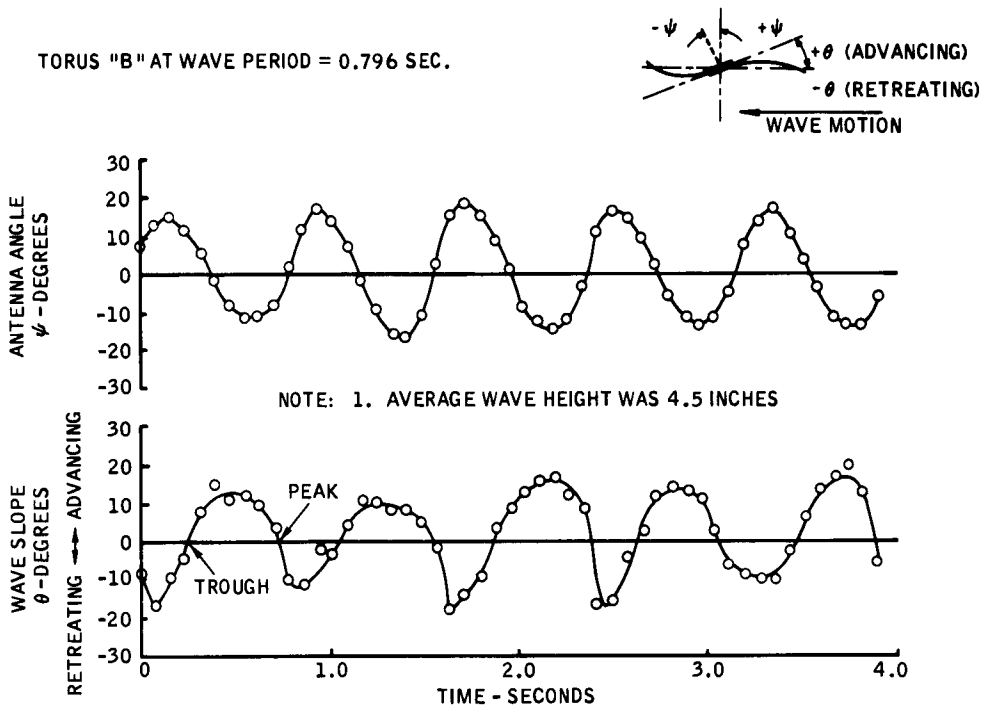

Figure 27. Thin Torus Buoy Model Motions

critical periods. These shapes are characterized by their deep immersion in the water, using ballast to achieve a low center of gravity and a high center of buoyancy, assuming the form of a pendulum in an effort to gain stability. At resonance, the motions of these shapes are often extreme, exceeding the slope of the waves producing the motion. This presents certain practical problems if the buoy is to support a radio antenna for long-distance communication, or if it is to support meteorologic sensors for wind direction and velocity.

Studies of the comparative drag of shapes for buoy hulls show that the same ones that are capable of resonant behavior usually have high drag as well.

Boat hulls, toroids and discs that float upon rather than within the water are never motionless, but they may be made to follow wave slope closely coupled and highly damped, never exhibiting resonant motion. These shapes also have comparatively low drag. Boat hulls have the most favorable drag/weight ratio

of all, and in the pitch mode follow wave slope fairly well, although they do exhibit resonance in roll.

The choice is between high-drag shapes that sometimes achieve resonant motion, and low-drag shapes that never become resonant.

It will be obvious that to use a device that is capable of resonant behavior in the presence of an energy spectrum containing components of that frequency is to be avoided, if resonance produces undesirable effects. In the case of spar buoys and related shapes to avoid resonance the buoy should have a natural period of motion either less than 3 seconds or more than 25 seconds if these are to be considered the practical limits of the spectrum of energy contained in surface waves at sea. More than that, it implies that the natural period of pendular motion of a spar should be at least twice 25 seconds, or 50 seconds if parametric resonance is to be avoided. A spar buoy having a natural period of pendular motion of 50 seconds would be very large, perhaps as large as FLIP, the large manned spar built by Scripps Institution of Oceanography. At the opposite end of the spectrum, a spar having a natural period of motion in any mode of 3 seconds would be quite small. A spar having a draft of 2.4 meters has a natural period of vertical motion of 3.0 seconds, independent of diameter. Natural period of pendular motion depends upon location of the center of gravity with respect to center of buoyancy, ratio of diameter to draft, etc., but a buoy having a diameter of 12 ft and a draft of 3 ft would have a natural period of pendular motion of the order of 3 seconds.

Observation of models in the towing basin indicates that a symmetrical shape is to be preferred over an irregular one such as a boat hull. Avoidance of preferred orientation and of cross coupling between possible modes of motion simplifies the response of symmetrical shapes to waves and other forces. This is particularly true when several forces are arriving from conflicting directions.

This observation has also been made in full scale on a 36-ft. boat hull moored in the open ocean for another test, and is corroborated by records of pitch, roll and mooring load obtained during telemetering of test data from the boat. A typical storm record is shown in Figure 28. The comparison of pitch data to roll data clearly shows the difference between resonant response and non-resonant response to the same forcing function. Mooring-load maxima will be seen to correlate with roll oscillations as well as pitch motions.

Of additional interest is data taken from a ciné photopanel in the boat, which shows excursions through 90° of the relative wind direction indicator — reading from a Bendix-Friez Aerovane situated 30 ft. above the waterline, at the same time the telemetering records were obtained. Magnetic heading at that time was holding steady, and wind velocity was steady at 30 kt. The roll-attitude indicator agreed with the telemetry record and correlates with the oscillations of indicated relative wind direction.

Based upon results of all tests it appears that a suitable compromise is the low-drag circular disc. The disc has no ballast and may be designed as a simple, low-density structure having large reserve buoyancy. However, the disc should have slightly more thickness than the models tested. In a size practical for use as a moored telemetering buoy carrying a 4,000-lb. payload, the low-drag circular disc would have a diameter of 40 ft., a gross weight or displacement of 19,600 lb., a freeboard or reserve buoyancy of 193,400 lb., and would draw approximately 4 inches of water.

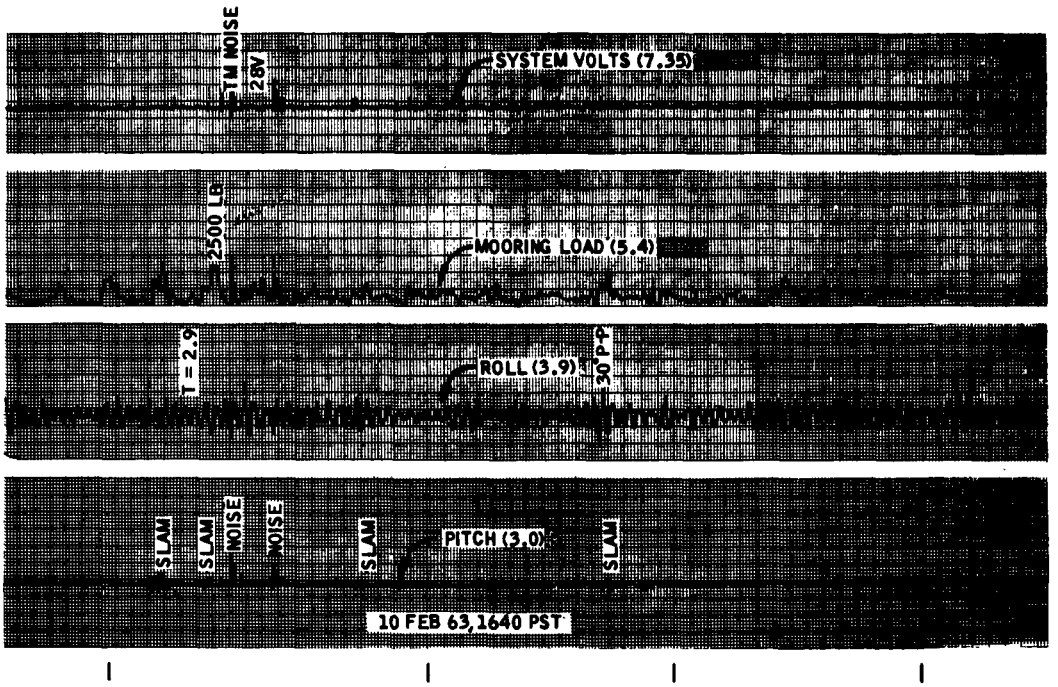

Figure 28. Telemetry Record Obtained During Storm

3 | RADIATION PATTERNS FROM TILTED ANTENNAS

3.1 GENERAL

Choice of antennas is an important part of the design of a system of telemetering buoys. On the buoy, one is restricted to antennas having omnidirectional patterns, that is that send out equal energy in every horizontal direction. For long-distance ionospheric radio transmission, the amount of energy radiated at low angles, that is, toward the horizon rather than upward, is especially important. Certain omnidirectional antennas permit successful communication with half the transmitter power required by others. The radio transmitters being a significant portion of the load upon the electrical power system in a buoy, it is worth considerable effort to optimize antenna design.

A thorough search of the literature revealed that nothing had ever been published on the performance of antennas near ground plane when their tilt orientation relative to the ground plane changes periodically, as when the antenna is on a boat hull or buoy moving in response to waves.

Because any one buoy must be capable of transmitting on more than one radio frequency, it is important that the antenna selected be efficient at each frequency, and that the radiation pattern be more or less the same at each frequency.

To study the relative importance of these things, and to select the optimum antenna for radiotelemetry from buoys at sea, a series of antenna-pattern tests was conducted at General Dynamics/Convair. Because studies of full-scale

antennas is not feasible at the frequencies to be used, patterns were plotted from scale-model antennas operating over an artificial ground plane.

The primary purpose of the test was to look for pattern nulls as a function of antenna tilt and radiation angle, and to compare the shape of the whip and discone patterns. Although both the discone and whip are vertically polarized it was felt that under conditions of severe tilt appreciable energy would be radiated with horizontal polarization. Either horizontal or vertical polarization is useful for ionspheric propagation, even though a plane-polarized antenna is used at the receiving station, because plane-polarized waves striking the ionosphere are reflected as elliptically polarized waves. As a result of this reasoning, both horizontal and vertical antenna patterns were measured and the combined effects taken into consideration.

Knowledge of these pattern shapes provides the information required to help make a selection between the two antennas for buoy applications.

Radiation patterns were made at 900 and 2,300 mc. The whips tested were cut to one quarter wavelength at 900 mc which made them approximately 0.64 wavelength at 2,300 mc. The discone antenna was designed for a 900 to 2,700 mc range.

3.2 DESCRIPTION OF TEST

A 100:1 scale-model discone antenna and five 100:1 whip antennas were constructed for the test. The whip antennas were all the same length but were bent at angles of 0°, 10°, 20°, 30°, and 40° to simulate the corresponding tilt angles. The model discone was adjustable in tilt angle. A 0.2-inch-square wire mesh screen (20 feet in diameter) was stretched over a wooden frame to simulate an ocean ground plane (Figures 29 through 32). The model antennas were located at the center of the screen, where they were linked to a geared-down motor drive system located below the screen. The discone mounting shaft was fed through a hole in the screen (as shown in Figure 29), and inserted into a

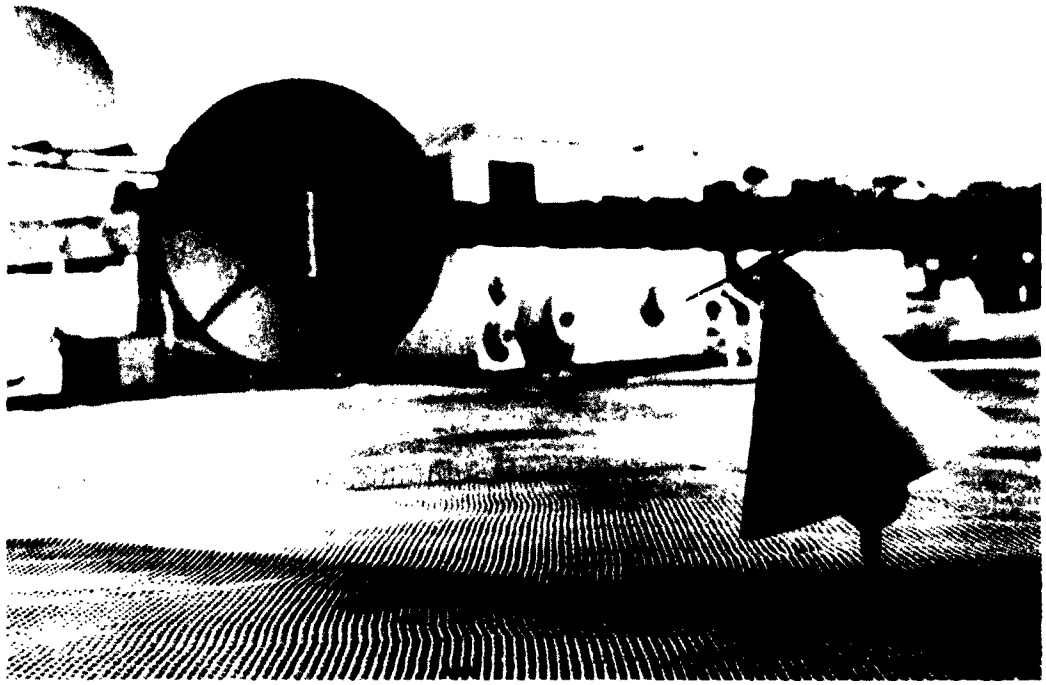

Figure 29. Discone Antenna Tilted 20° Off Perpendicular to Ground Plane

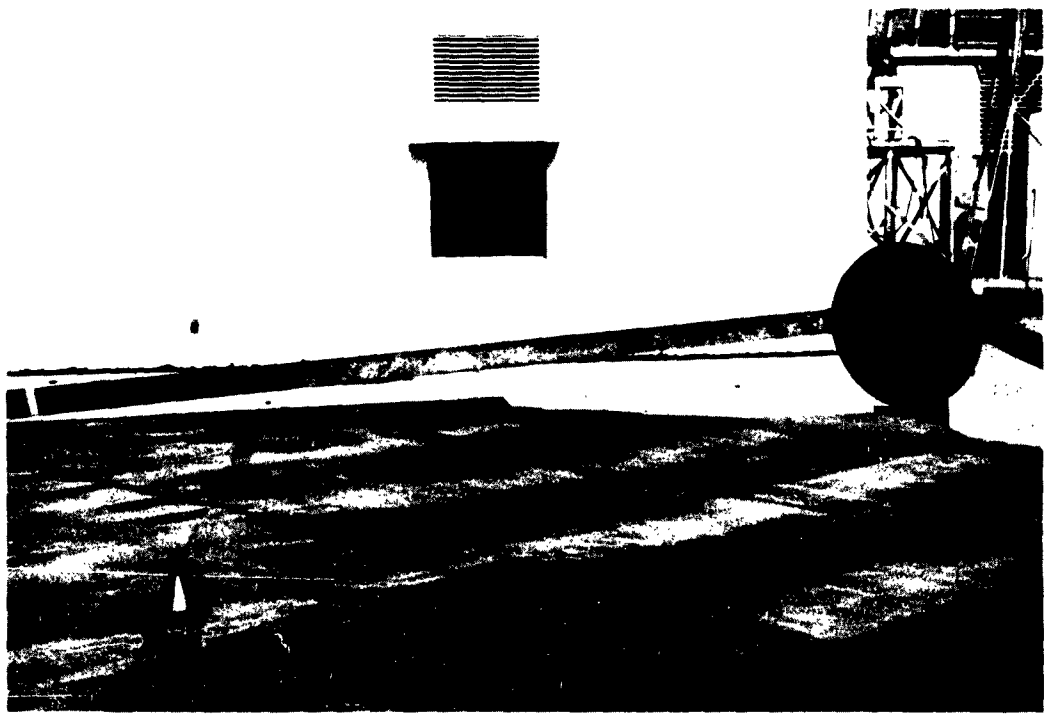

Figure 30. Discone at 0° Tilt With Illuminating Source Horizontally Polarized

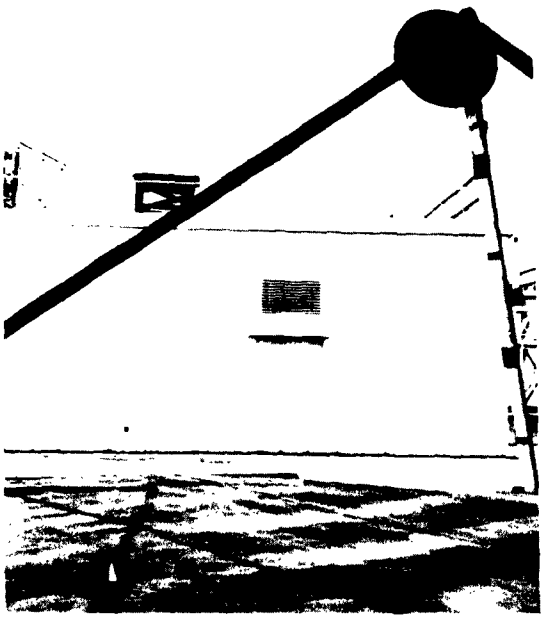

Figure 31. Discone Antenna at 0° Tilt, Receiving Radiation From A High Angle, Illuminating Source Vertically Polarized

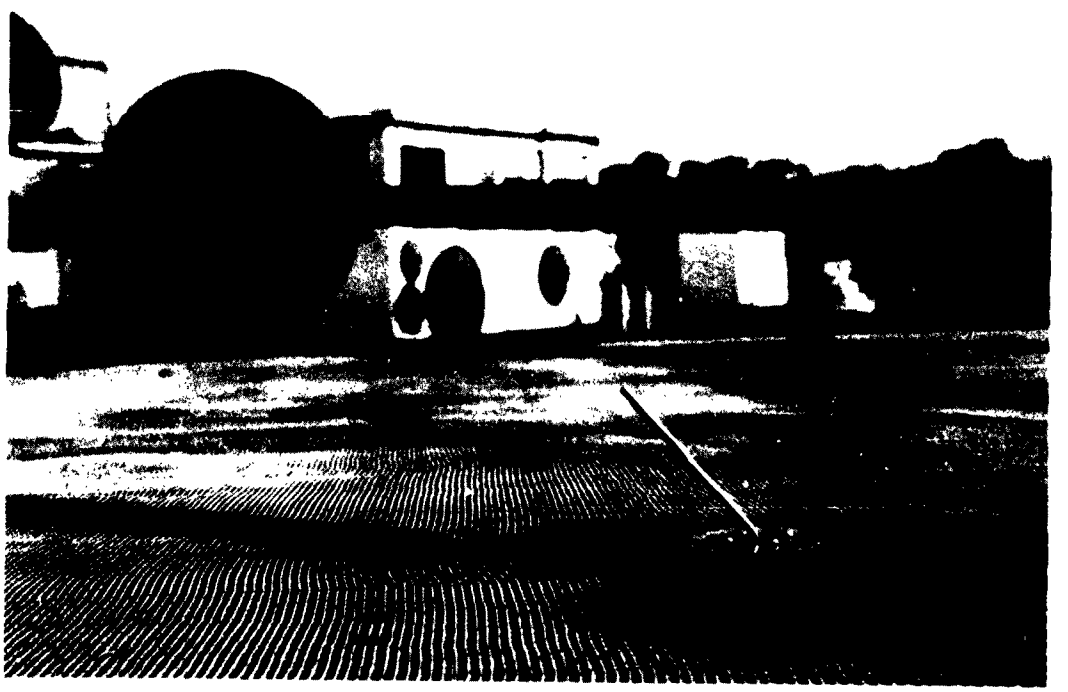

Figure 32. Whip Antenna Tilted 40° Off Perpendicular to Ground Plane Illuminating Source Vertically Polarized

mounting collar in the rotating drive mechanism. When a tilted whip antenna was tested it was rotated through an RF slip joint mounted at the center of the screen, such that the screen was an integral part of the vertical antenna (Figure 32).

Antenna patterns were run with the antennas mounted vertical to the ground plane and tilted from the vertical, 10°, 20°, 30° and 40° toward the ground plane. The tilted antennas had a nutating type of action when rotated, in that the center of the disc and the tip of the whip described a circle whose center was directly over the rotator drive shaft.

A 2.5-ft.-diameter parabolic reflector with a dipole feed mounted at the dish focal point (Figures 29 through 32) was used as a transmitting antenna to illuminate the discone or whip which was set up as a receiving antenna. The dish was mounted so that it could be elevated above the ground screen, subtending radiation angles of from 5° to 50° with respect to the test antenna while maintaining a constant distance of 10 feet from the antenna and pointing directly at it (as shown in Figure 33).

A signal generator set at one of the two test frequencies (900 or 2,300 mc) supplied RF energy to the parabolic antenna feed for illumination of the antenna under test. The feed was positioned perpendicular to the ground plane (Figures 29, 31, 32) for the vertical radiation patterns and parallel to the ground plane (Figure 30) for the horizontal patterns. The output of the antenna being tested was fed through a short length of coax cable to a bolometer detector and 1-kc selective amplifier. The output of the amplifier was connected by cable to the polar plotter where its amplitude determined the position of the plotting pen along a radial from the center of the polar graph paper to its outermost concentric circle. When the antenna motor drive system rotated the test antenna 360° in azimuth, the polar plotter table rotated 360° in synchronism. The maximum signal conditions were determined by checking the test antenna under extreme settings of tilt radiation angle and azimuth angle. Plotter gain adjustment was

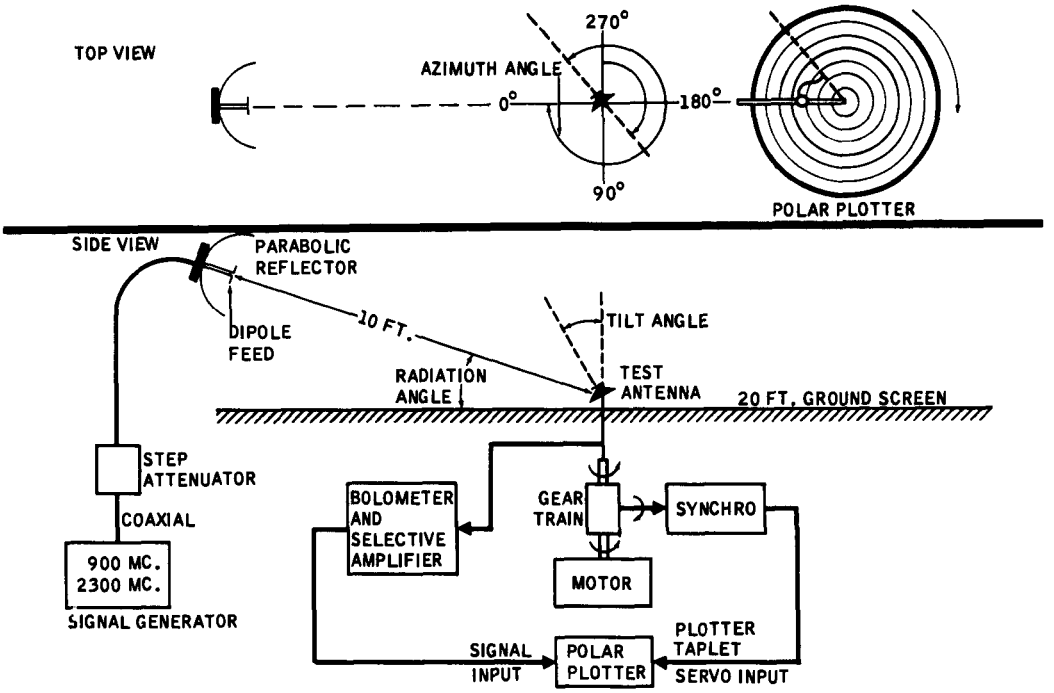

Figure 33. Antenna Test Setup

set to place the inking pen at the outermost circle position under the maximum signal conditions, and all plots were relative to this point. The entire system was calibrated by setting the RF attenuator (Figure 33) in 3 db steps ranging from 0 to 24 db.

The following antenna patterns were measured:

Azimuth Angle	Tilt Angle	Radiation Angle	Polarization
0 through 360°	0°	5, 10, 15, 20, 30, 40 & 50°	Vertical
0 through 360°	10°	5, 10, 15, 20, 30, 40 & 50°	Vertical
0 through 360°	20°	5, 10, 15, 20, 30, 40 & 50°	Vertical
0 through 360°	30°	5, 10, 15, 20, 30, 40 & 50°	Vertical
0 through 360°	40°	5, 10, 15, 20, 30, 40 & 50°	Vertical
0 through 360°	0°	5, 10, 15, 20, 30, 40 & 50°	Horizontal
0 through 360°	10°	5, 10, 15, 20, 30, 40 & 50°	Horizontal

Azimuth Angle	Tilt Angle	Radiation Angle	Polarization
0 through 360°	20°	5, 10, 15, 20, 30, 40 & 50°	Horizontal
0 through 360°	30°	5, 10, 15, 20, 30, 40 & 50°	Horizontal
0 through 360°	40°	5, 10, 15, 20, 30, 40 & 50°	Horizontal

The previous table shows one condition of azimuth, five conditions of tilt angle, (0°, 10°, 20°, 30° and 40°) seven conditions of radiation angle (5°, 10°, 15°, 20°, 30°, 40° and 50°) and two conditions of polarization (vertical and horizontal). This makes a total of 5 x 7 x 2 = 70 plots.

Figures 29, 32 and 33 show these variables. In Figure 29 the discone tilt angle is 20°, the radiation angle is 5° and the polarization is vertical. In Figure 30, the discone tilt angle is 0°, the radiation angle is 5° and the polarization is horizontal. In Figure 3 the discone tilt angle is 0°, the radiation angle is 50° and the polarization is vertical. In Figure 32 the whip tilt angle is 40°, the radiation angle is 5° and the polarization is vertical.

3.3 TEST PROCEDURE

The following procedure was used to obtain the radiation patterns.

1. Test antenna was placed in the center of the ground plane and adjusted for a tilt angle of zero degrees.
2. Transmitting antenna array (dipole and the parabolic reflector) was set for a radiation angle of five degrees.
3. Dipole was used as a feed for the parabolic reflector and adjusted for vertical polarization (perpendicular to the ground screen, as in Figure 29).
4. Signal generator power was adjusted to make the recorder pen indicate full scale (zero db) on the polar graph paper.
5. The antenna rotation drive motor was engaged and kept running until the antenna had rotated through a 360° azimuth angle.

6. Step 5 was then repeated for radiation angles of 10°, 15°, 20°, 30°, 40° and 50°. At the end of each of these runs the parabolic reflector was returned to the 5 degree setting to check calibration. Linearity was checked occasionally by means of the step attenuator.

7. The dipole used as a feed for the parabolic reflector was then adjusted for horizontal polarization (parallel to the ground screen, as in Figure 30).

8. Steps 2, 5 and 6 were repeated.

9. Excluding Step 4, Steps 1 through 8 were repeated with the test antenna tilted at 10°, 20°, 30° and 40°.

10. Steps 1 through 9 were followed for the whip and discone at both 900 and 2,300 mc.

3.4 TEST RESULTS

The data obtained from running the patterns are in the form of vertical and horizontal components. Since it is the total energy that is of interest in this application, the sets of orthogonal plots are combined vectorially and replotted as total energy plots.

Plots of this type are shown in Figures 34 through 55. Figures 34 through 53 are families of horizontal patterns, and Figures 54 and 55 are vertical patterns derived from the horizontal patterns.

Considering the discone patterns at 900 mc, the discone patterns at 2,300 mc, the whip patterns at 900 mc and the whip patterns at 2,300 mc, there is a scale factor difference between these four sets of plots. This is due to full scale being set up for each family of curves as a function of maximum output for the particular antenna and frequency used.

By comparing the shapes of the discone and whip patterns, a good estimate of the scale factor difference can be obtained, in that both antennas have similar

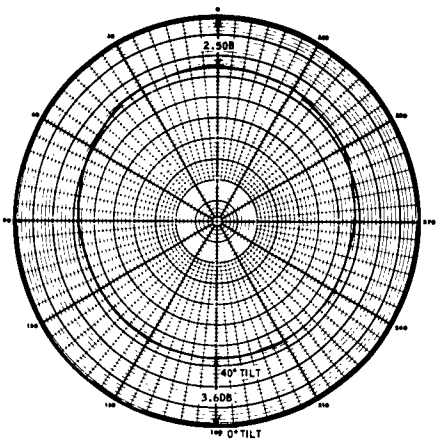

Figure 34. Radiation Angle 5°

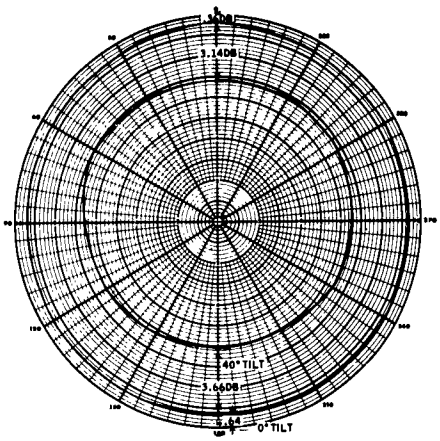

Figure 35. Radiation Angle 10°

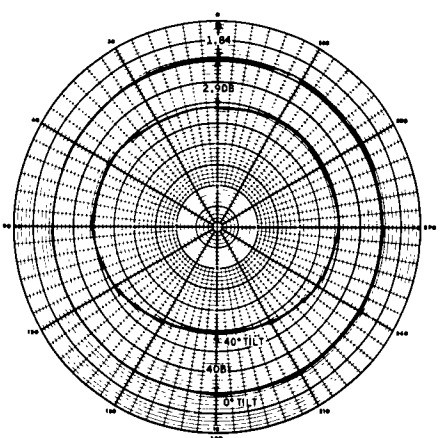

Figure 36. Radiation Angle 15°

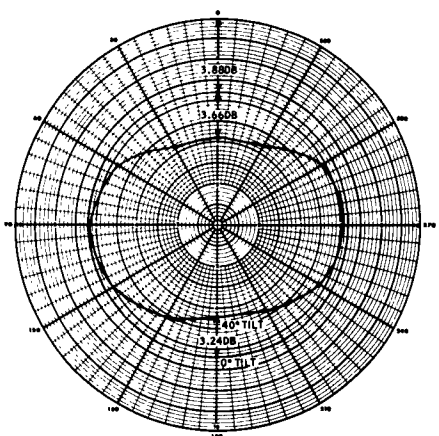

Figure 37. Radiation Angle 30°

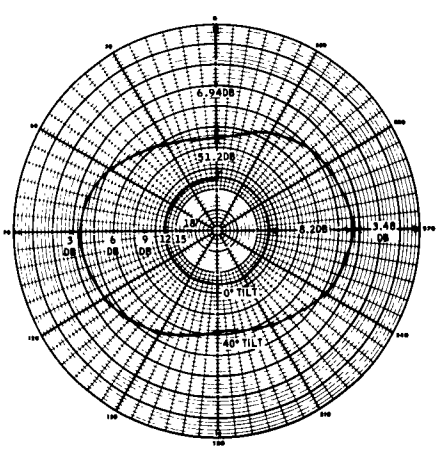

Figure 38. Radiation Angle 50°

Figure:	**Discone**
Design Frequency:	**9.0 mc**
Model Frequency:	**900 mc**
Scale Factor:	**100:1**
Polarization:	**Combined vertical and horizontal.**

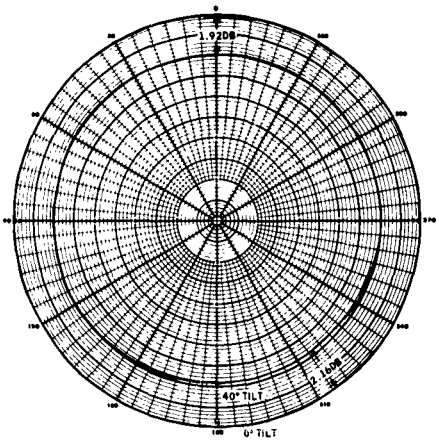

Figure 39. Radiation Angle 5°

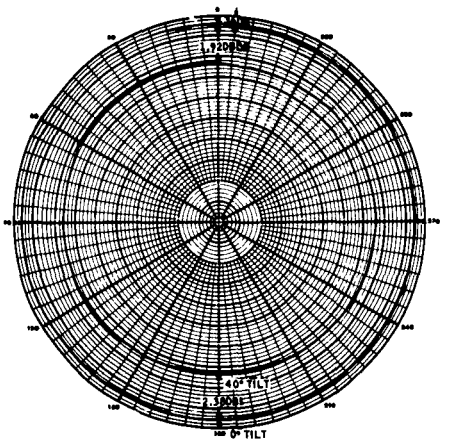

Figure 40. Radiation Angle 10°

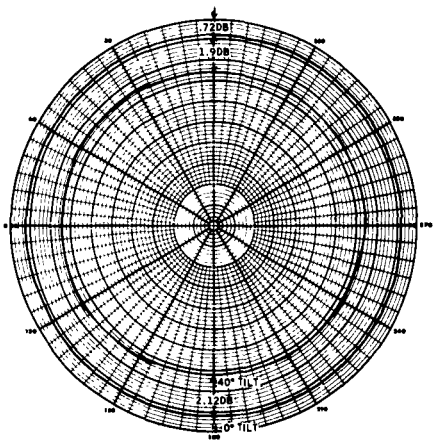

Figure 41. Radiation Angle 15°

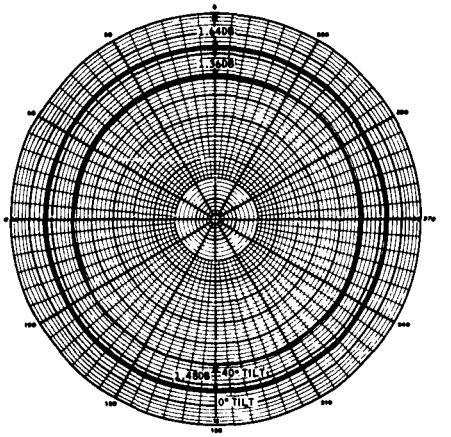

Figure 42. Radiation Angle 30°

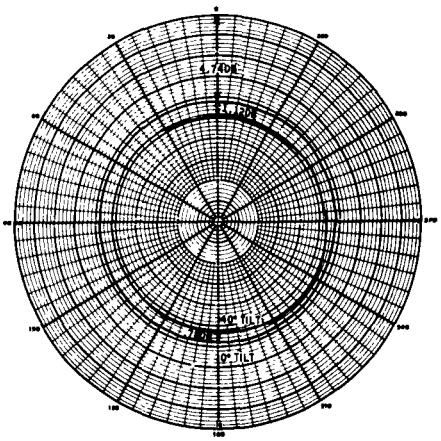

Figure 43. Radiation Angle 50°

Figure:	**Whip**
Design Frequency:	**9.0 mc**
Model Frequency:	**900 mc**
Scale Factor:	**100:1**
Polarization:	**Combined vertical and horizontal.**

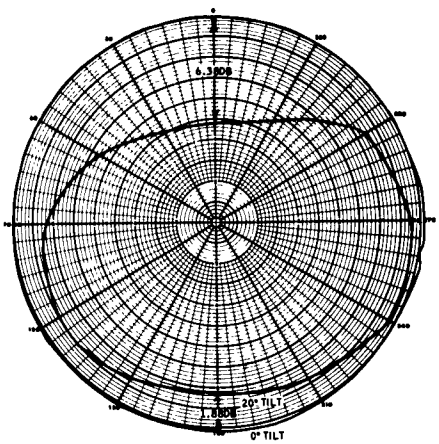

Figure 44. Radiation Angle 5°

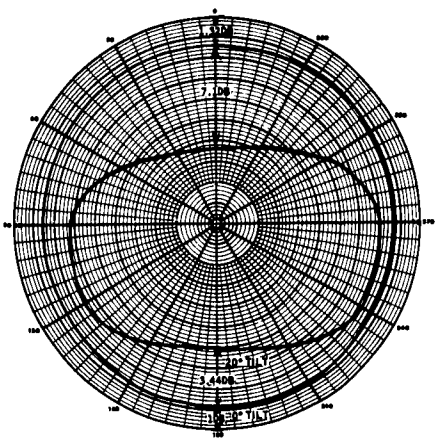

Figure 45. Radiation Angle 10°

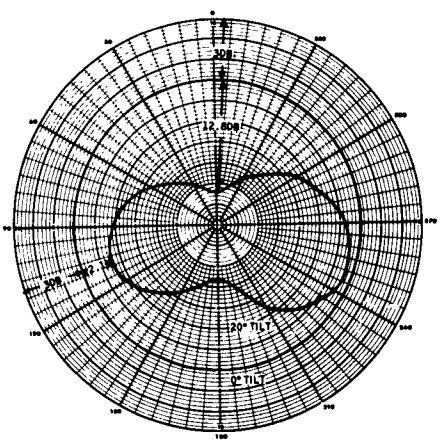

Figure 46. Radiation Angle 15°

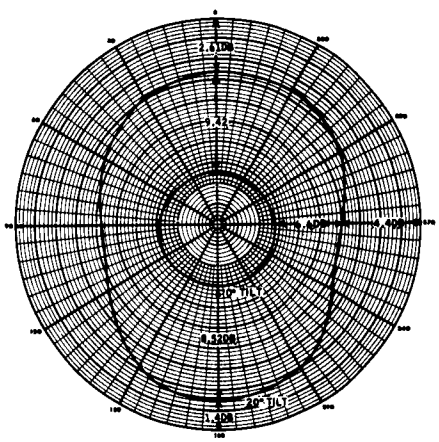

Figure 47. Radiation Angle 30°

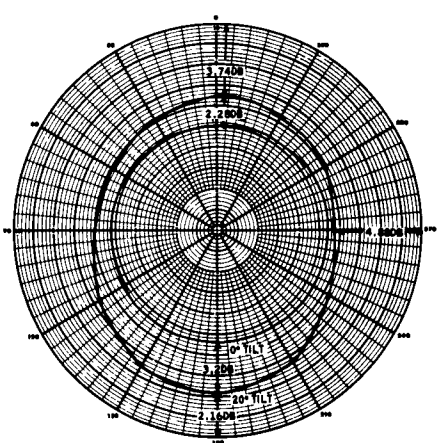

Figure 48. Radiation Angle 50°

Figure:	**Discone**
Design Frequency:	**2.3 mc**
Model Frequency:	**2,300 mc**
Scale Factor:	**100:1**
Polarization:	**Combined vertical and horizontal.**

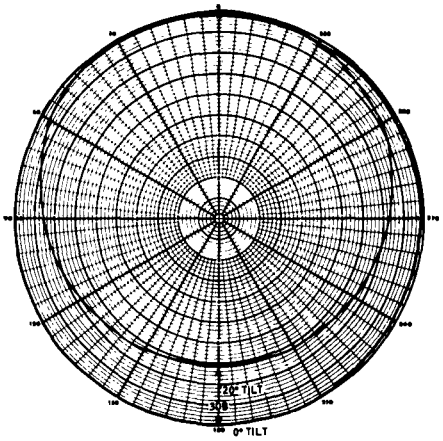

Figure 49. Radiation Angle 5°

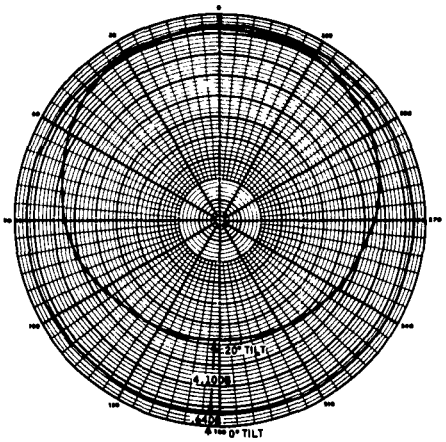

Figure 50. Radiation Angle 10°

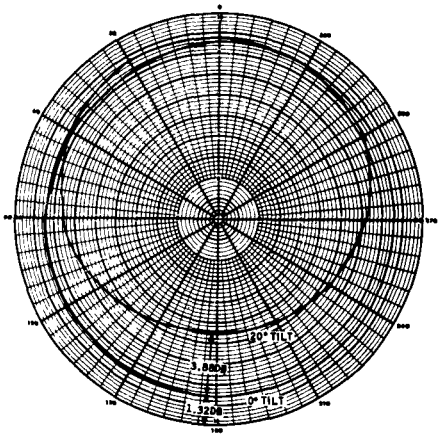

Figure 51. Radiation Angle 15°

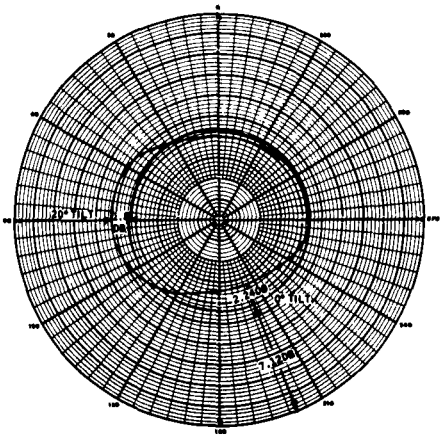

Figure 52. Radiation Angle 30°

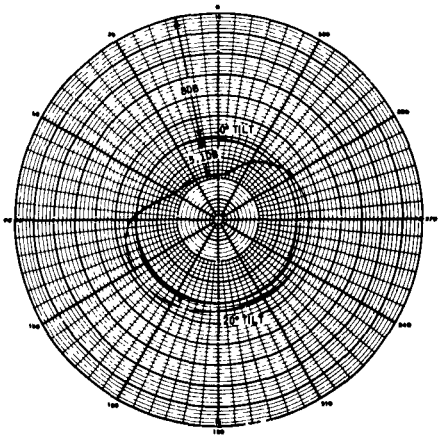

Figure 53. Radiation Angle 50°

Figure:	Whip
Design Frequency:	2.3 mc
Model Frequency:	2,300 mc
Scale Factor:	100:1
Polarization:	Combined vertical and horizontal

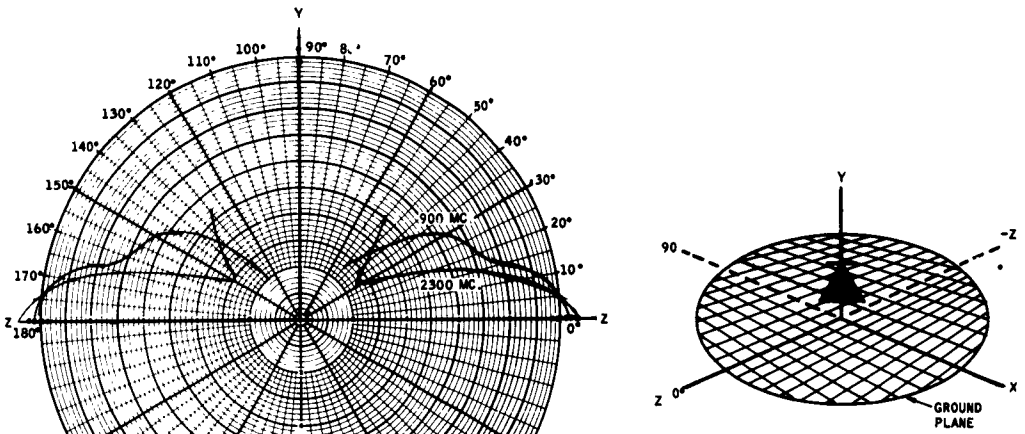

Figure 54. Discone

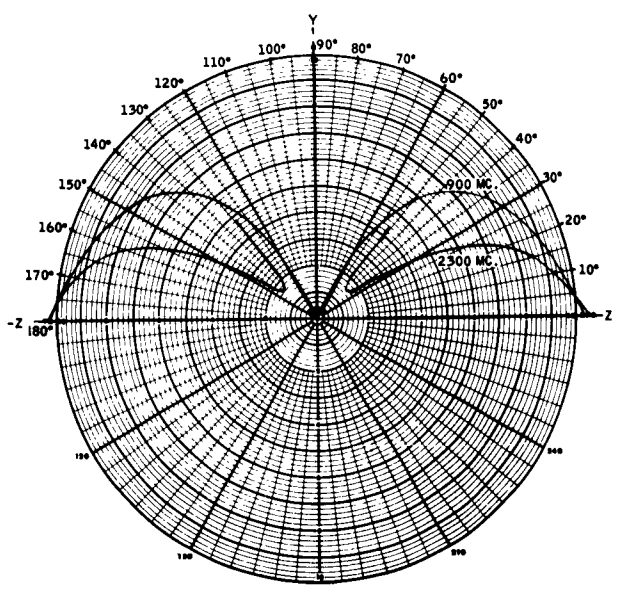

Figure 55. Whip

Design Frequency:	**9.0 - 2.3 mc**
Model Frequency:	**900 - 2,300 mc**
Scale Factor:	**100:1**
Tilt Angle:	**0°**
Polarization:	**Combined vertical and horizontal.**

efficiencies. Using this method, plus prior knowledge of the two antennas, it is indicated that 2 db should be subtracted from the 900-mc discone curves when comparing them to the quarter wave whip at 900 mc. The patterns made at 2,300 mc are not complete enough to allow the calculation of scale factors, and can be compared only on a qualitative basis.

3.5 DISCONE AT 900 MC

Figures 34 through 38 are discone patterns run at 900 Mc. Figure 34 shows the relative energy radiated at a (radiation) angle of 5° for azimuth angles of 0° to 360°. The outer circle is for the discone vertical (0° tilt) and the inner circle is for the discone tilted 40°. This means that if one is interested in transmitting RF energy at a radiation angle of 5° he will experience a variation of 2.5 db to 3.6 db where the antenna tilts as much as ±40° from the vertical.

Figure 35 is similar to Figure 34 except that here an examination is made of the energy radiated out at an angle of 10° rather than 5°. It is noted that with the antenna vertical (0° tilt) the energy transmitted is from .36 db to .64 db, less than it was for the 5° situation. With a ±40° tilt, the energy can be down an additional 3.14 db to 3.66 db. Figure 37 is for a radiation angle of 30°. Here the radiated energy is down 3.88 db for 0° tilt, as compared to the 5° radiation angle. Under ±40° tilt conditions, the pattern is no longer circular, and at right angles to the plane in which the antenna is tilted there is practically no difference between 0° tilt and 40° tilt. However, in the axis of the tilt plane there is a 3.24 to 3.66 db variation between the 0° and 40° tilt conditions.

Figure 38 is for a radiation angle of 50°. With the antenna vertical the power is down 12 db, as compared to the 5° or reference condition. It should be noticed here that with the antenna tilted 40°, the radiated power is at least 5.12 db, and as much as 8.2 db better at any azimuth angle than it was when the tilt angle was 0°. This shift is due to the greatly increased horizontally polarized component. However, this increase is considered to be of little consequence in that a continuous tilt angle of 40° is not expected to occur.

3.6 WHIP AT 900 MC

Figures 39 through 43 are whip patterns run at 900 mc. Figure 39 shows the relative energy at a radiation angle of 5°, with tilt angles of both 0° and 40°. The 0°-tilt, 5°-radiation angle setting is used as a full-scale reference since the maximum energy output occurs under these conditions. This figure compares to Figure 34 for the discone; however, all of the discone patterns must be increased by 2 db when comparison is made with the whip patterns (as discussed previously).

Variation in the whip patterns vs. tilt are similar to the discone patterns, with the following exceptions. The changes are less for the whip at low radiation angles and get even smaller at high radiation angles. The whip patterns stay circular at high radiation angles instead of eliptical as is the case with the discone. The whip produces very little horizontal polarization even at 40° tilt, whereas this becomes predominant in the case of the discone at large radiation and tilt angles.

3.7 DISCONE AT 2,300 MC

At this higher frequency both the whip and discone antennas were studied with tilt angles of 0° and 20°, rather than 0° and 40°. The effects of tilt become much worse because both antennas developed secondary lobes at this higher frequency.

Since buoy tilt angles exceeding 20° are not expected, this smaller tilt value was used because of the higher sensitivity of the patterns to tilt.

Figures 44 and 49 are the 5° radiation angle, 0°, and 20° tilt patterns for the discone and whip respectively. When tilted 20°, the discone pattern became eliptical — being depressed 6.38 db in the direction of tilt. The whip pattern changed to an off-center circle, being down 3 db in the exact opposite direction of tilt. In Figures 45 and 50, where discone and whip patterns were run at a radiation angle of 10°, the shapes previously discussed have become accentuated.

The 20° tilt curve is now down as much as 7.1 db from the 0° tilt curve for the discone (Figure 45), and down 4.1 db in the case of the whip (Figure 49).

Figure 46 is the discone pattern for a radiation angle of 15°. Here the 20° tilt curve has become peanut shaped, being down from the 0° tilt curve by as much as 12.8 db. The similar plot for the whip is shown in Figure 51. Here the effect of tilt is less than before (Figure 50), being down a maximum of 3.88 db, as compared to the 4.1 db.

Figure 47 shows the 30° radiation angle, 0°, and 20° tilt patterns. The 0° tilt pattern is down 10 to 12 db from the 0°-tilt, 5°-radiation angle pattern of Figure 44. The 20°-tilt angle pattern has blossomed out due to horizontal polarization. The maximum output is now along the tilt axis instead of at right angles to it. The similar plot for the whip (Figure 52) shows that the effects of tilt have been reduced, with the 20° tilt curve having some eccentricity. The 0° tilt pattern is still circular and is down 7.12 db from the 0° tilt pattern at 5° radiation angle.

Figure 48 shows the 50° radiation angle, 0° and 20° tilt patterns. The 0° tilt pattern is back up again, showing the effect of a secondary lobe. It is now down only 5 db from the 5° radiation angle plot. The 20° tilt plot is still greater than the 0° tilt plot, by as much as 2.28 db to 3.2 db. From the standpoint of pattern variation with tilt, this is less change than that found for the major lobe at low radiation angles.

The whip at 50° radiation angle (Figure 53) has changed slightly from its 30° situation. The 0° tilt pattern is down 8 db, as compared to the previous 7.1 db. However, the 20° tilt pattern has developed a flat side, putting it down 5.1 db from the 0° tilt case over about a 90° sector in azimuth.

Figures 54 and 55 are derived from Figures 34 through 53. These plots are in a plane perpendicular to the ground screen, directly above the center hole of the screen, and passing through the center of the parabolic reflector. This corresponds to the YZ plane shown in the small sketch in Figure 54.

Figure 54 shows the discone at 900 mc and 2,300 mc and Figure 55 shows the whip at 900 and 2,300 mc. Comparing the discone and whip at 900 mc it is noted that the discone pattern is flat while the whip pattern is humped up, almost semi-circular in shape. This means that the discone is concentrating its energy at low radiation angles relative to the whip. It has been estimated that the discone has a 2 db gain over the whip at low angles (0 - 7.5°). At 2,300 mc the main patterns of both the discone and whip are flatter than for 900 mc however, energy is being robbed from the low angle main lobe and put out at a high angle as noted by the formation of the secondary lobe. This situation does not seem advisable for general buoy use.

3.8 CONCLUSIONS

For a long range operation (1,000 mi. to 2,500 mi.) radiation angles required are in the range of 0° to 15°. The effect of tilt on the discone and whip antenna is a general reduction of radiated power in the 0° - 15° radiation angle range. At the low frequency end of its operating range (900 mc), the discone exhibited a loss of no more than 4.0 db at any azimuth angle when the antenna was tilted 40°. The loss was only 2.5 db in certain instances. The whip exhibited a loss that fell in the range of 1.92 to 2.38 db for a tilt variation of 0° to 40°.

It is necessary to subtract 2 db from the 900-mc discone patterns to bring them up to the same scale factor as the 900-mc whip patterns. When this is done, and the patterns are compared over the 0-15° radiation angle range, the following results are obtained: The discone has at least 2 db gain over the whip at 5° to 10° radiation angle and .88 db at 15° radiation angle, all at 0° tilt angle. When tilted 40° the discone has a gain of .32 db over the whip at 5° radiation angle, 1 db at 10° radiation angle and a loss of .84 db at 15° radiation angle.

Since a tilt angle greater than 20° is not expected, it is safe to say that the discone exceeds the whip for low angle (long distance) operation.

For short range work where high radiation angles (above 30°) may be used, the whip is definitely better than the discone both in terms of actual gain and variation of gain with tilt.

At 2,300 mc, both the discone and whip developed minor lobes at high radiation angles, and not enough information was obtained to define the pattern shapes at high angles. Because of this condition, the gain factor between discone and whip is not known. However, it can be seen from the radiation patterns that there is much less change due to tilt with the whip than with the discone. At a 5° radiation angle the whip had a 3 db variation, or compared to a 6.38 db variation for the discone for a tilt change from 0° to 20°. At 10° radiation angle it is 4.1 db vs 7.1 db. At 15° radiation angle it is 3.88 db vs 12.8 db. At 30° radiation angle it is 2.24 db vs 7.6 db., and at 50° it is 5.1 db vs 1.14 db.

Thus, for 0° to 20° tilt at 2,300 mc, the whip had at least 3 db less variation than the discone, except at the 50° radiation angle.

The patterns obtained at 2,300 mc are of interest, but multiple-lobed pattern antenna designs are not recommended for general use.

From a theoretical standpoint it was determined that the discone developed a secondary lobe for a different reason thanthe whip. The whip used in the test was longer than 5/8 wavelength, and it is known that at 5/8 wavelength and larger, a whip starts to develop minor lobes. The situation for the discone was different in that it was not mounted flush with the ground, but at a height of approximately 1 inch above the ground. Raising the discone this much above the ground screen caused lobing at the 2,300 mc test frequency. The model discone was positioned above the screen to simulate the actual conditions of a proposed design. The present design philosophy is to bring the skirt of the discone in contact with the ground plane. This will eliminate the secondary lobe at the higher frequencies, and from theoretical considerations, the pattern variations due to tilt should be similar to the whip and discone patterns at 900 mc.

It should be mentioned here that the discone has some practical advantages over the whip in that is is a wide-band device, and is fed at the top rather than near the bottom, thus avoiding the wet, salt-spray problem. The top of the discone can be grounded so that lights and instruments can be located there without effecting the pattern. Being grounded, the discone also gives lightning protection. Full-scale tests have not yet been run, but the 100:1 scale model tests indicate that the discone impedance varies much less than the whip as a function of tilt.

4 | ELECTRIC POWER SYSTEM TEST AT SEA

4.1 GENERAL

To supply electric power to an instrumentation package in a telemetering buoy intended to remain on station for as long as one year presents a serious problem. The quantity of energy required for the 100-channel equipment capability exceeds that which can be stored economically in chemical batteries for so long a time. It is estimated that to power all the equipment needed in the buoy, including the data-collection package, the data-storage package, the command receivers and telemetering transmitters, plus a collision-avoidance beacon, requires 1400 Watt-hours per 24-hour day. To last a year, a 28-volt chemical battery would have to have a capacity of 18,250 Ampere-hours to supply this demand. It would weigh of the order of 56,000 pounds, and would cost at least $1.00 per pound.

Obviously, other means of energy storage must be considered. As part of the task proposed, General Dynamics/Convair surveyed the entire field of energy conversion to find the best method that is suitable for this application, and that is presently available.

It soon became clear that the optimum system would include a means of energy storage to satisfy peak loads of short duration, involving a chemical battery charged by a device that would convert either fossil fuel or isotope fuel into electricity.

Steam-powered generators, solar cells, wind chargers, and methods of converting energy from currents and waves into electricity were considered but

discarded because of cost, or reliability, or problems of development, in sizes practical for this application. Small Diesel units were ruled out because of problems of starting this type engine if its cylinder bore is small, particularly at low temperature. Fuel cells were discarded because none is yet commercially available, and because at their present state of development would require cryogenic storage of fuel and oxidizer. Similarly, all the isotope-fuel devices were ruled out because of cost of development and cost of fuel. Thermoelectric generators and conventional piston-engine generators emerged as the most promising methods available now.

Attempts to obtain price quotations on thermoelectric generators in the range of 100 Watts continuous were unsuccessful. The few responses received involved development subcontract proposals.

From considerable study and previous experience it was felt that the conventional piston-engine generator burning propane fuel might possibly be reliable enough to charge chemical batteries, unattended, for 6 months to a year. It was proposed to select such a machine from among the many available on the commercial market, make minor modifications to suit it for unattended operation in a buoy, and actually operate it at sea to find its life expectancy and its major limitations. The work was begun in May 1962. Tests at sea were begun in October 1962 and are still in progress. The results obtained, as of February 1963, are presented here.

4.2 SURVEY OF AVAILABLE EQUIPMENT

Technical data were obtained from major manufacturers of small 4-stroke-cycle engine/generator plants in this country and abroad. Selection of the test specimen was accomplished as outlined in the following subparagraph.

4.2.1 PROCEDURE — Requests for technical data on small piston-engine generator plants, of 1 to 2 kilowatt rated output, were sent to major manufacturers of such units. The data obtained were carefully scrutinized, and each unit evaluated according to the following criteria:

4.2.1.1 Number of Moving Parts — It was considered to be of primary importance to select a unit having a minimum of moving parts, provided no serious engineering compromise were involved in making one part perform the function of two. Particular attention was given to parts that are normally expected to require periodic adjustment or replacement such as fan belts, ignition systems, water-pump seals, automatic chokes, fuel pumps, lubricating-oil pumps, and shaft couplings.

4.2.1.2 Engine-Design Compromise — It was considered important that a unit be selected whose engine was designed particularly for powering a generator. Engines designed for garden tractors, milk separators, lawn mowers, and the like, but adapted to a generator and offered for sale as an engine/generator, were considered to be undesirable. Engines found to have a great advantage in any one respect, resulting in disadvantages such as marginal cooling, poor starting because of radical cam design, and excessive temperatures, pressures, or rubbing speeds, were similarly weighted.

4.2.1.3 Modifications Required for Unattended Operation in a Buoy — The unit should require a minimum of modification to the lubrication system, cooling system, etc., for long-term unattended operation in a capsule in a buoy. Careful consideration was given to whether modifications would require redesign of a system. Redesign of a major system or component was considered unacceptable.

4.2.1.4 Simplicity of Operation — It was considered important that the unit be capable of starting, running, and stopping with a minimum of mechanical operations. For example, starting by means of motorizing the generator was considered acceptable, whereas starting by means of the conventional self-starter was not.

4.2.1.5 Adequate Cooling — Careful consideration was given to whether the air-cooled units would be capable of adequate cooling when cooling air and exhaust air would be moved through long runs of ducting, as from an engine/generator capsule to the open air through a long schnorkel. Units requiring

auxiliary electric blowers were considered to be undesirable.

4.2.1.6 Cost — Although not of primary importance, careful consideration was given to selecting a unit that would satisfy points 1 through 5 (covered in subparagraph 4.2.1.1 through 4.2.1.5), with minimum cost, including engineering and shop costs for modification and integration into a practical system.

4.2.2 FUEL — Propane was selected as the fuel to be used because of its clean-burning characteristics. Carbon deposits on the spark-plug center-electrode insulating porcelain, on combustion chamber walls and piston crown, under valve heads and on valve stems, and in the exhaust port and pipe, were expected to be serious problems if gasoline were used as fuel. It was felt that this could be avoided by using propane. Other advantages are —

a. No fuel pump required.

b. No float bowl required; fuel-air mixture ratio unaffected by vibration or attitude.

c. No choke or fuel-air mixture ratio change required for cold starts.

d. Fuel tank requires no ullage ventilation; accumulation of water cannot occur from condensation in tank as fuel is depleted.

e. Control of engine stop is easily accomplished by closing a solenoid valve at the fuel-storage tank — engine capsule or exhaust pipe then contain no raw fuel or explosive mixture.

f. Gas-phase fuel causes no dilution of lubricating oil, resulting in little contamination from products of combustion.

It was felt that a valid test of an engine/generator could be conducted only if the engine/generator would put energy into the same kind of load that it would face in actual operation in a telemetering buoy at sea. Also, to study automatic starting, it would be necessary to have a chemical battery in the system. It was decided to select a battery for the test that would fulfill both requirements.

Major manufacturers of chemical storage batteries were contacted. Technical data received were carefully studied. The following criteria were used:

a. Freedom from loss of electrolyte during long-term use involving many charge-discharge cycles.

b. Minimum variation of system voltage during charge-discharge cycle.

c. Freedom from evolution of gas.

d. Freedom from permanent loss of capacity at low temperature.

e. High efficiency of storage, with minimum loss because of self-discharge.

4.2.3 RESULTS — The engine/generator selected was a Kohler model 1CD1, having a rated cutput of 1000 watts continuous duty. Published specifications are as follows:

Manufacturer of engine	- Kohler Co., Kohler, Wisconsin.
Manufacturer of generator	- Kohler Co., Kohler, Wisconsin.
Engine type	- K161, 4-cycle, single-cylinder side valve. Piston displacement 16.2 c.i. (267 c.c.). Bore 2.87 in., stroke 2.5 in. 3.7 bhp at 1800 rpm. Compression ratio 6.1:1 to 6.4:1.
Generator type	- 1CD1, 1000 watt, shunt wound. Designed and built to ASA and NEMA standards for temperature rise. 36 volts at 28 amperes per terminal. Antifriction ball bearings.
Starting	- Generator motorized for cranking, using energy from battery to be charged.
Ignition	- Flywheel magneto with external points and condenser.
Cooling	- Air cooled by reverse-flow blower on crankshaft.
Fuel	- Adjustable-jet carburetors for either gasoline or propane.
Lubrication	- Splash.

Main bearings	- Anti-friction ball bearings.
Rod bearings	- Plain bearings.
Piston	- Low-expansion aluminum alloy.
Valves	- Forged steel alloy intake, stellite-faced exhaust, with valve rotators.
Valve seats	- Stellite inserts.
Crankshaft	- Heat-treated alloy steel forging, integral counterweights, induction-hardened crankpin.
Connecting rod	- Aluminum alloy casting, integral dipper.
Governer	- Precision flyball type in oil bath, external adjustment.
Size	- 16 x 17 x 23 inches.
Weight	- 165 pounds, dry.
Specific output	- 13.8 bhp/liter; 260 watts/bhp.

The battery selected was a nickel-cadmium, alkaline-electrolyte 28-volt, 19-cell bank manufactured by Britannia Batteries, Ltd., Redditch, Worcestershire, England, and represented in this country by Alkaline Batteries Company, 750 Natoma St., San Francisco, Calif. None of the lead-acid batteries considered was found to be satisfactory. This manufacturer of alkaline batteries was the only one who would furnish technical data of guaranteed accuracy. Battery specifications selected for the test are as follows:

Manufacturer of cells	- Britannia Batteries, Ltd.
Type of cell	- SV14, normal resistance, 140-A/hr.
Cell construction	- Double-pocket positive plate, single-pocket negative plate.
Cell container	- Welded steel, plated with cadmium and nickel.
Electrolyte	- Potassium hydroxide.
Number of cells in bank	- 19
Nominal discharge voltage	- 24

Capacity of bank	- 140 ampere-hours at 5-hour discharge rate.
Charge current	- 28 amperes to charge fully in 7 hours.
Size of bank	- 16 in. width, 38 in. length, 16 in. height.
Weight of bank	- 432 pounds.

4.3 STUDY OF TEST SPECIMENS ASHORE

An engine/generator set was purchased from the Kohler Company for preliminary testing on shore to verify its suitability for service in an electric power system to be tested at sea. A 19-cell battery bank was also purchased from Alkaline Batteries Company, who offered to refund the purchase price and accept the return of the battery if it were found to differ from guaranteed factory performance specifications and charge-discharge voltage curves.

From studies of test specimens ashore, the following design data were to be obtained:

a. Determine duct sizes required to conduct cooling air to the engine/generator, and hot air and exhaust gases away from the engine/generator, through a schnorkel 30 feet high.

b. Determine effects of engine load and speed upon cylinder-head temperature.

c. Determine the effect of introducing generator-windings coolant air into the capsule, upstream of the cooling-air inlet to the engine itself, upon the cylinder-head temperature.

4.3.1 PROCEDURE — The engine/generator unit was given a thorough inspection and functionally checked by running it in a static-test setup. All easily removed covers and plates were removed, and the internal construction and workmanship studied as thoroughly as possible, short of complete disassembly of the entire unit. It was determined that the unit was suitable for testing, and that modification for this purpose would not be difficult. As an aid in modifying the

lubricating-oil sump and in testing the actual design to verify its successful operation, a bare block with crankcase, sump and crank was obtained from the Kohler representative in San Diego.

Design of the lubricating-oil sump modification was accomplished with no difficulty. As shown in Figure 59, the system consisted of a remote reservoir for lubricating oil, an electric pump to transfer oil into the existing engine oil sump periodically after shutdown, and a carefully designed overflow standpipe fitted to the bottom of the oil sump to return oil to the remote reservoir and maintain proper level in the sump. The modification was accomplished on the bare-block-with-crank, and sump operation at various attitudes in a special test stand was verified visually by looking into the sump through the open cylinder bore. Clearance between crankshaft and standpipe was verified to be adequate.

The test stand was designed and built especially for these studies. It permitted observation and running of the engine/generator at angles up to plus-or-minus 35° in both horizontal axes in increments of 5°.

With the oil-sump modification installed on the test specimen, the completely instrumented engine/generator was run in the tilt stand at 0° tilt, to obtain baseline data, then at increments of 5° to ±35° to verify that proper running occurred at all angles in both planes. The engine/generator was run at each angle for five minutes, a much more severe condition than would be encountered at sea.

The engine/generator was then tested with long ducts attached to the cooling blower outlet, to determine the effects of various lengths and diameters of duct upon cooling efficiency. An enclosure was then placed over the engine/generator, with the long outlet duct and the exhaust pipe protruding from it — simulating the enclosure proposed for the test capsule and schnorkel.

During all shore tests a variable resistance bank was used as a load for the engine/generator.

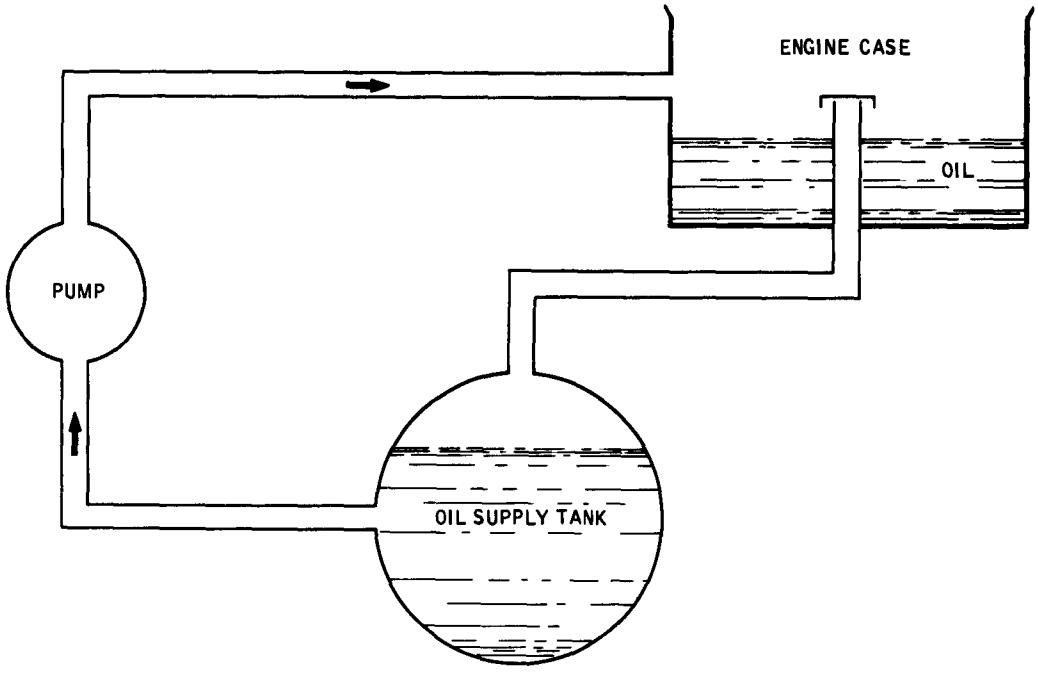

Figure 56. Lubricating Oil Replenishment System

Data from all tests were tabulated, plotted, and analyzed sufficiently to permit the design of the electric power system to be tested at sea.

The battery arrived in the uncharged condition, which is not harmful to nickel-cadmium cells. In the laboratory, the battery was completely charged and discharged twice, according to factory instructions, before evaluation of battery performance was begun.

Charge and discharge characteristics of the battery were determined, the data plotted and compared to the factory curves used for predesign of the system.

4.3.2 RESULTS — Baseline data were obtained in the test stand with the completely-instrumented engine/generator. The following items are considered to be particularly important.

Cranking speed at expected start voltage (22.9)	- 510 rpm.
Time to start (average) at 22.9 volts	- 6 seconds.
Cylinder-head temperature (maximum), no load	- 275° F.
Engine speed, no load	- 1850 rpm
Cylinder-head temperature (maximum) full load	- 438° F.
Engine speed, full load	- 1760 rpm
Current required to crank, overnight cold engine	- 18 Amperes
Current drawn with crankshaft locked	- 48 Amperes
Manifold pressure variation, unrestricted line	- 2 in. Hg., no load to full load.
Manifold pressure variation, restrictor-check in line	- 10 in. Hg., no load to full load.
Cranking pressure, open throttle, overnight cold	- 114 psi.
Cranking pressure, open throttle, hot	- 118 psi.

Baseline data were obtained using lubricating oil SAE No. 30 — the viscosity recommended in the Kohler specifications.

During these tests it was observed that manifold-pressure readings were surprisingly close to ambient pressure, when read with the indicator connected to the inlet pipe and using unrestricted line. A brief study revealed that this is to be expected in a 4-stroke cycle, single-cylinder engine where the inlet valve is open only a small percentage of time during the cycle. A restrictor-check valve was placed in the line between the inlet pipe and the manifold pressure indicator. It acted as a diode with a high resistance across it, giving indication of peak manifold vacuum with the penalty of a small time-constant in indicator response to pressure changes toward ambient.

Performance of the engine/generator in the tilt stand was satisfactory. The lubricating-oil sump modification performed as expected. There was no evidence of a lack of lubrication at any angle of tilt in either plane, up to plus or minus 35° (limits set for the test).

Some variation in engine speed occurred, caused by increasing effects of gravity as the flyball governor was tilted on its axis. At 35° generator up, engine speed had fallen from 1,800 rpm to 1,760 rpm; at 35° generator down, engine speed had risen to 1,825 rpm. Engine speed also fell to 1,790 rpm as the engine/generator was tilted about the shaft axis, 35° carburetor up.

When the engine/generator was tilted so that the crankcase breather port was near the level of the lubricating oil inside the sump (at 35° carburetor down), oil mist issued from the breather. At this time the air was entering the overflow standpipe, which was open. The oil mist stopped when the overflow standpipe was connected to the lubricating oil reservoir. A similar situation would exist when the engine condition is such as to allow considerable blow-by past the piston.

The engine/generator was then run in a level position to study the effects of ducting and enclosure upon cooling-blower operation and engine temperature.

The static-pressure probes installed in the engine cooling-blower shroud assembly measured variations in pressure at the blower inlet and the blower outlet as a function of change in cooling air mass flow. The pressure data were plotted as a function of cylinder-head temperature, since temperature should vary in relation to mass flow. An actual air mass flow calibration was not considered necessary. Figure 57 shows pressure variation as a function of cylinder-head temperature, at 1,800 rpm engine speed with 80% (800 watts) load on the generator.

The effect of injecting engine combustion exhaust gases into the outlet duct of the schnorkel was studied by making plots of cylinder-head temperature as a function of air mass flow with data obtained from tests conducted with the engine exhaust being piped into the 6-inch duct. Comparison of cylinder head

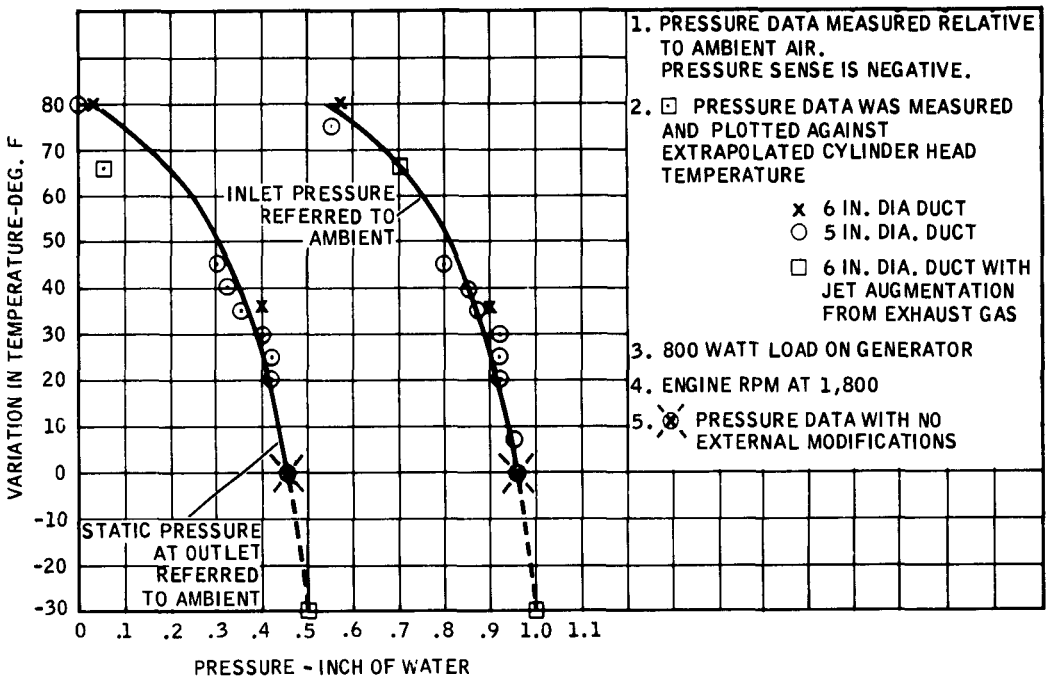

Figure 57. Variation in Cylinder Head Temperature from Normal Vs. Static Pressure at Inlet and Outlet

temperature curves as a function of air mass flow shows that some improvement may be obtained from jet-pump action. Figure 57 shows the inlet and outlet pressures plotted to an extrapolated point of cylinder head temperature. This extrapolation was necessary because no temperature measurement was made at this particular pressure point.

Engine cooling system performance data are presented in Figure 58. These data indicate that the capsule and schnorkel should be designed such that the duct losses would not exceed those encountered with 30 feet of 5-inch duct attached to the blower outlet, nor less than those encountered with 30 feet of 6-inch duct attached to the outlet. If the capsule and schnorkel design fell within these limits, the engine cylinder head temperature would be in an optimum range for the tests at sea.

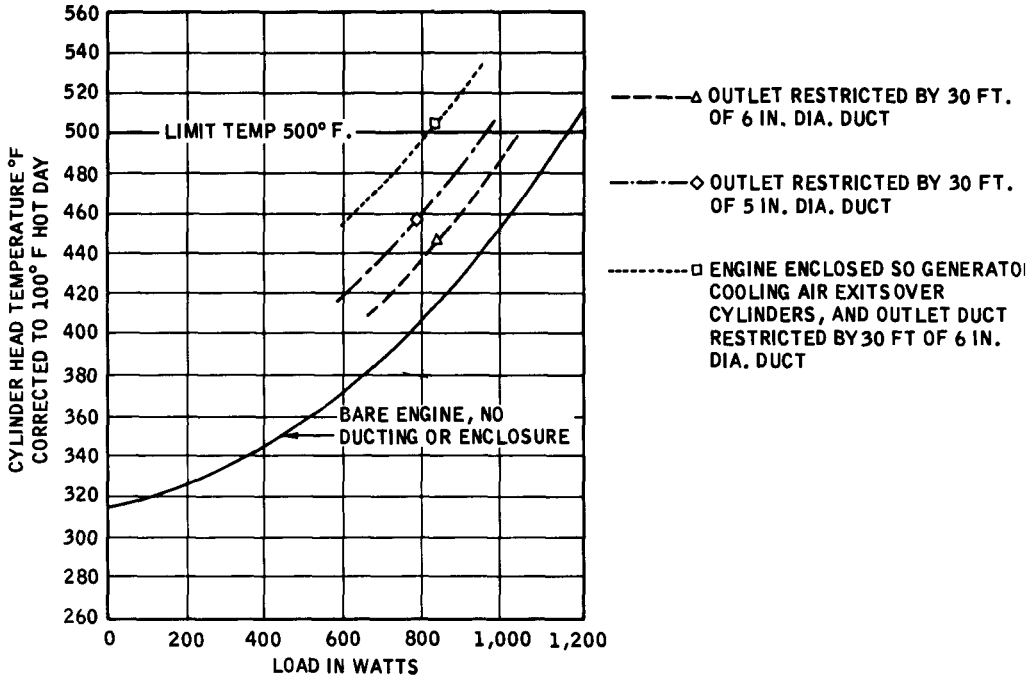

Figure 58. Cylinder Head Temperature as a Function of Engine Load

The data shown in Figure 58 are corrected to a 100° F hot day. Extrapolation from test data was accomplished by assuming a 1 degree rise in cylinder head temperature for every 1 degree difference between 100° and the ambient temperature measured at the time of the test. Based upon this one-to-one correction, the "boiler-plate" schnorkel designed for the tests at sea probably would not provide adequate cooling in 100° air. Test conditions in the San Diego area were expected to give a maximum ambient temperature of 70°, which would leave ample margin of safety.

Some of the maximum cylinder head temperatures observed were considered to be rather close to the factory-specified maximum of 500° F, so it was decided to determine whether increasing engine speed could be counted upon to solve a marginal cooling problem if it should arise. The engine/generator was run at various speeds and the differential pressure across the cooling blower recorded for each speed — with the following results:

Engine load	-	None
Engine speed	-	Δp across blower
1,700	-	-0.475 in. H_2O
1,800	-	-0.50
1,840	-	-0.525
1,900	-	-0.65
2,000	-	-0.70
2,100	-	-0.75

Although the occasion has not arisen to solve a problem of marginal cooling it is felt that these data indicate that increasing engine speed by adjusting the governer spring would be better than a mechanical re-design of the blower.

To obtain maximum efficiency from the engine/generator it must be operated near maximum rated output at all times. This requires constant-current charging of the battery. To charge batteries by this method, the electric output of the generator should be capable of considerable variation of voltage without any variation of current. Tests were made to determine what quality of current regulation the specimen generator could achieve. In spite of the fact that the literature describes the 1CD1 engine/generator as a shunt-wound machine it is actually compound wound as shown in Figure 59. There is a shunt-connected field winding and a separate series-connected field winding. (There is also a separate winding used only for starting.) Tests were conducted with the adjustable load bank across the P (L_1) and L_2 terminals — the normal load output. The test was then repeated with the load bank across terminals P and N, the normal battery charging output — first with the charge-rate control in the minimum position, then with it in the maximum position. Finally, a test was run with the load bank across terminals P and L_2 again, but this time with the series field connected with reversed polarity and the charge-rate control set at maximum. Results of these tests are shown in Figure 60. Although the desired output curve shape was achieved, the current was too low for this application. By shunting part of the current past the series

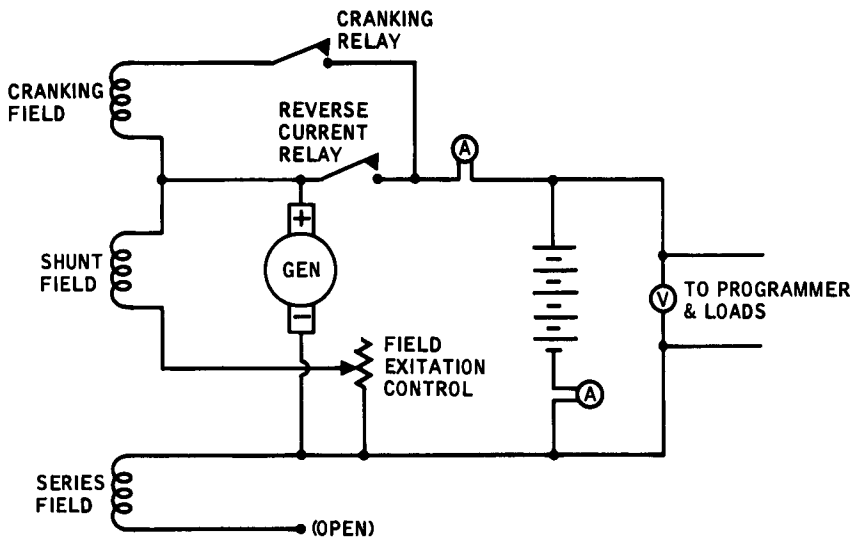

Figure 59. Generator Wiring Diagram

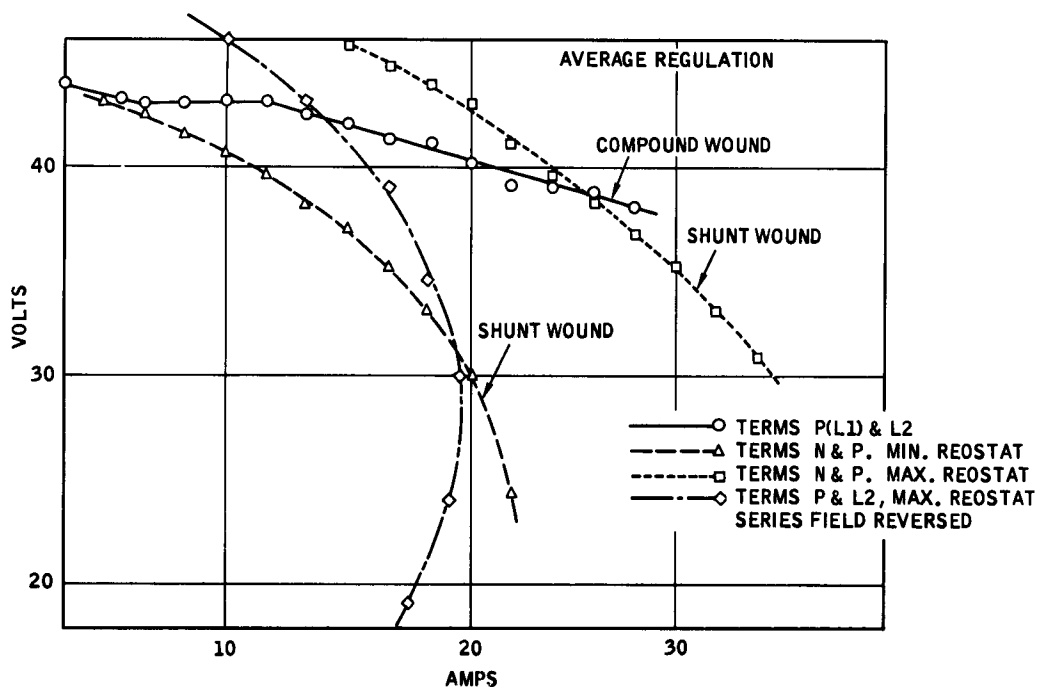

Figure 60. Current Regulation of Generator

field, the ideal situation could have been achieved, but the improvement over characteristic output from the battery charging terminals was not considered worth the cost of the modification for this test.

During this series of tests the reverse-current relay of the engine/generator failed in the closed position, causing minor damage to power cables. Inspection of the relay showed it to be welded closed at a small point of contact, resulting from extreme misalignment of the contacts during manufacture. The relay was repaired, the contacts aligned, and the relay pull-in voltage was re-adjusted to be compatible with a 28-volt system rather than the 36-volt system with which this unit would normally be used. This was accomplished by changing the combination of the spring tension and air gap. The relay was reinstalled and the tests continued. The relay was transfered to the boat test engine and operated satisfactorily.

The battery bank was charged in the laboratory, using a dc power supply, after being prepared by charging and discharging according to factory recommendations, and discharged at a constant rate to verify the factory discharge characteristic curves. The battery bank was then charged again up to the point of gassing, to verify the charge curve. Results of these tests and comparison to factory data are shown in Figure 61. It was noted that the nominal discharge voltage was 22 rather than 22.8, as computed from factory data of 1.2 volts per cell (times 19 cells) for "normal" discharge rates. The 23-ampere rate used in the test is evidently greater than "normal" and accounts for the difference.

At this time it was considered that the battery bank voltage might be marginal for operation of some of the equipment being put together for the unattended tests at sea. The advisability of purchasing one more SV14 cell, to raise the total voltage an additional 1.2 volt to 23.2, was debated. It was decided not to purchase the cell, partly because of the time required to ship it to San Diego.

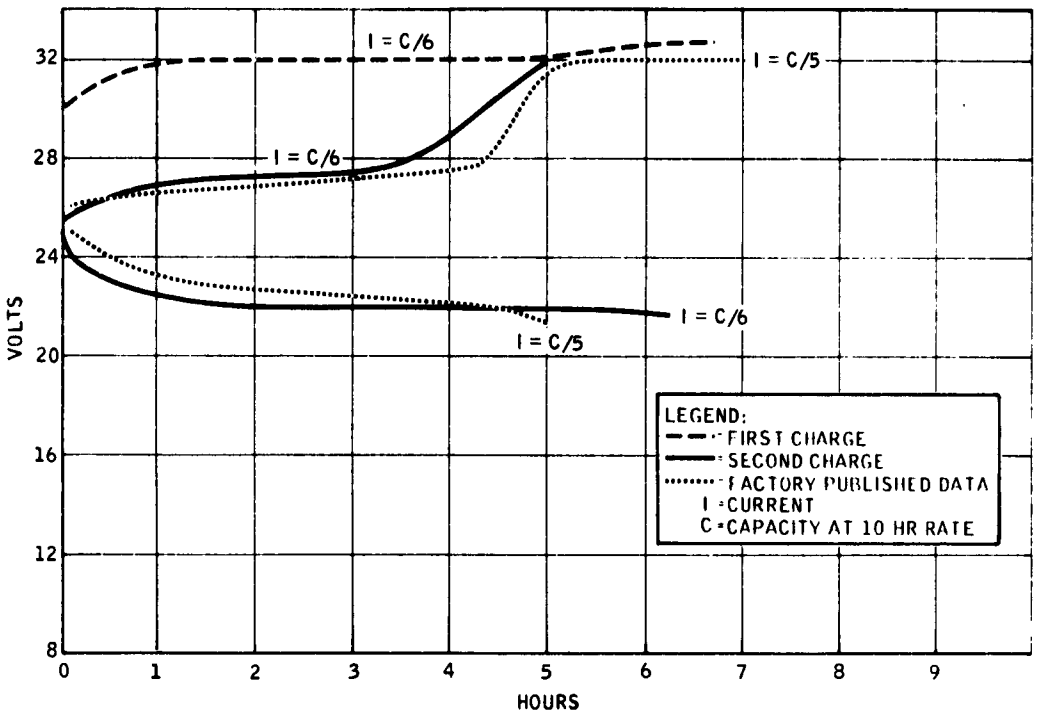

Figure 61. Battery Characteristics

4.4 ELECTRIC POWER SOURCE TESTS AT SEA

Tests at sea of a complete, unattended instrumented power system consisting of an engine/generator and its fuel supply, electronic equipment to start and stop the engine/generator at the proper time or system voltage, and the nickel-cadmium storage battery, were begun in October 1962. The tests were conducted in an unmanned 36-ft. hull converted for the purpose and moored off an exposed beach.

Test objectives for determining the life of the engine/generator in the capsule at sea were as follows:

a. Electric output from the engine/generator should be kept at 800 watts. This is the maximum available output from this particular generator at 28 amperes current density — the design maximum charge rate for the battery bank in this application.

b. The engine/generator should run for 3 hours per duty cycle of the system, with 4 duty cycles per 24 hours. This 3-on-and-3-off ratio would be permitted to vary slightly as a function of battery condition resulting from variation of load upon the electric power system, as from unscheduled telemetering, etc.

c. Engine cylinder-head temperature should be kept as close as possible to the maximum 500° F temperature quoted in factory specifications, to ensure a maximum heating and cooling during each duty cycle.

d. The engine/generator should be installed in a capsule and schnorkel that simulates as closely as possible its environment in an actual buoy. Fresh-air inlet should be at the top of the schnorkel, 30 ft. above the water. The outlet should be approximately 20 ft. above the water.

Artificial loads were placed across the output terminals of the storage battery, such that the entire system operated at four times the rate required of an actual buoy power source system in real calendar time. Instead of producing 2,400 watt-hours, the engine/generator produced approximately 9,600 watt-hours per day. In normal operation the system would be started only once or twice a day — during the tests it was started four times per 24-hour day. By February 1963 the equivalent of eight months of actual operation had been accumulated, based upon an operational system having only a single engine/generator. It is planned to use a system containing two engine/generators to improve reliability through redundancy. Based upon this system the tests to February represent 16 months of actual operation.

4.4.1 PROCEDURE — A fresh 1CD1 engine/generator with precision main bearings was purchased from Kohler and given visual inspection and functional check. The lubricating-oil sump and instrumentation were transferred from the first engine, and the unit installed in a "boiler-plate" capsule and schnorkel to simulate as closely as possible (at minimum cost in dollars and time) the installation in a telemetering buoy. The installation is shown in Figures 62 and 63.

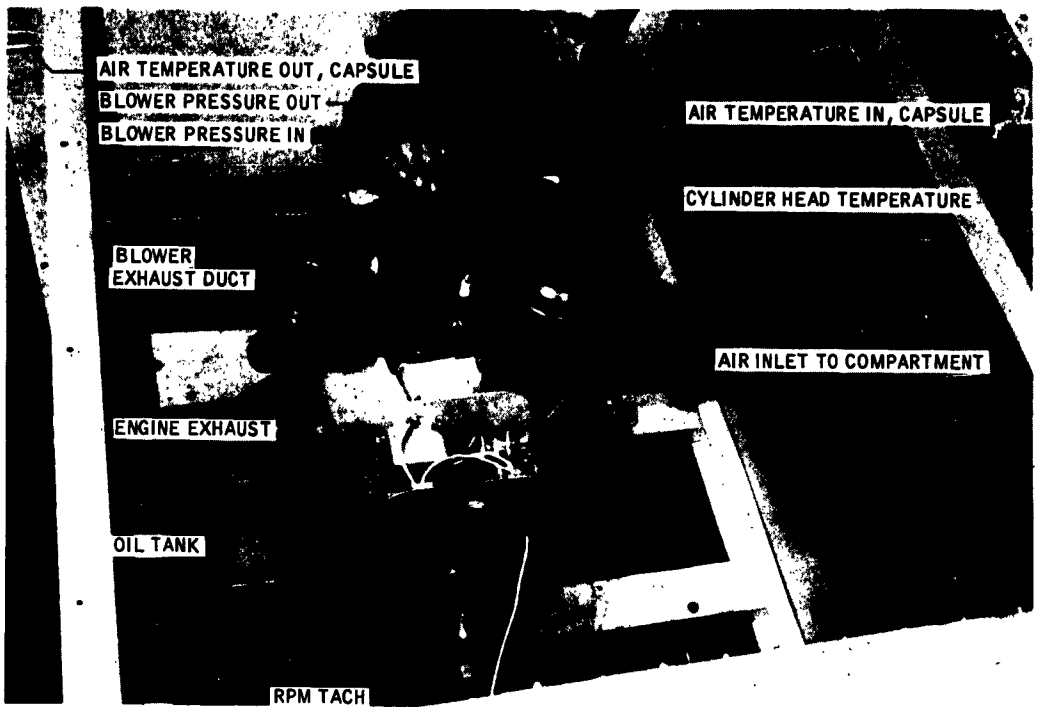

Figure 62. Engine/Generator Installed in Capsule

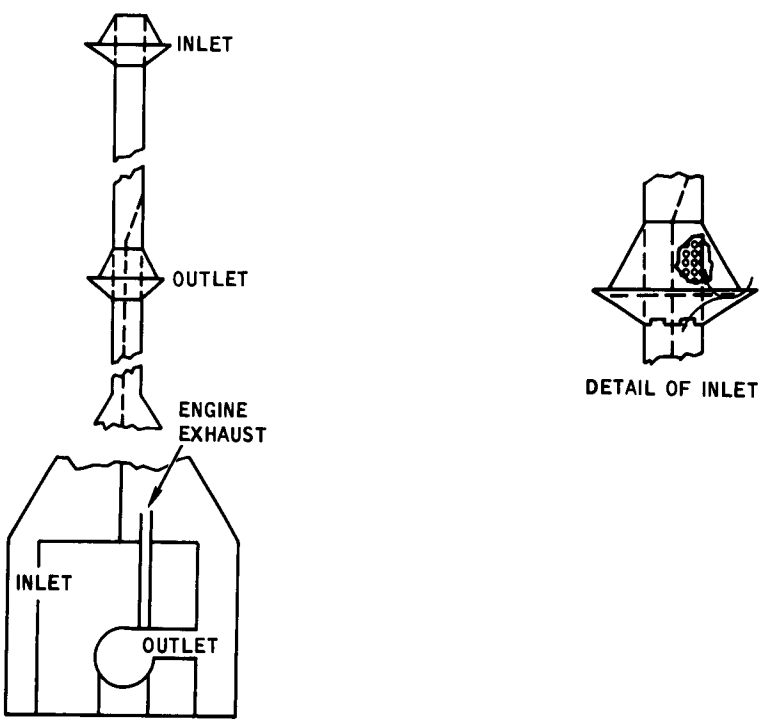

Figure 63. Capsule/Schnorkel

The capsule and schnorkel were installed in the cockpit of a surplus boat hull that had been prepared for the purpose. The battery bank was installed in a steel box on deck. A fuel tank storing a net volume of 150 gallons of propane was installed in the aft compartment, on what had originally been the main-propulsion engine mounts. Automatic control circuitry was mounted in standard racks installed in the cabin for that purpose. FM/FM telemetry equipment was also mounted in the racks. A completely instrumented photopanel was mounted on a bench installed in the cabin. The electric power source was completely instrumented. In addition, certain environmental measurements such as wind speed and direction, motion of the boat hull in roll and pitch, etc., were also instrumented. The complete measurements list is presented in Table 1.

The test hull was equipped with a high-intensity strobe light, flashing 10 times per minute, and the hull painted Coast Guard orange, in an effort to avoid collisions by making the vessel conspicuous.

The test hull was moored 0.8 mile off Mission Beach, 0.8 mile north of the Navy Electronics Laboratory Research Tower, on 29 October 1962. The test hull on station at sea is shown in Figure 64.

All operations aboard the test hull were controlled by an automatic programmer designed and built especially for the tests. The programmer is a system of relays controlled by a 28-volt dc chronometric motor rotating a camwheel which actuates a microswitch. The engine was started by this "clock," and stopped by a system-voltage sensor adjusted to a potential just beyond that at which battery gassing occurred. The programmer also controlled the Automax ciné camera which photographed the photopanel at certain times during the cycle. The chronological order of programmer events is discussed in the following subparagraph and presented in Table 2.

Table 1. Instrumented Environmental Conditions

	Photo Panel	Tele-metry	Mast Lite Blue	Mast Lite White	Ramp Test
Data correlation	X				
Time of day	X				
MAP	X				X
RPM	X				X
Temperature, cylinder head	X	X			X
Temperature, inlet air (upper stack)	X				
Temperature, exhaust air (upper stack)	X				
Temperature, exhaust air (lower stack)	X				X
Volts, battery	X	X			
Amps, battery (charge and discharge)	X				
Pressure, cooling "A"	X				
Pitch angle	X	X			
Roll angle	X	X			
Magnetic heading	X				
Pressure, cooling "B"	X				
Engine running		X	X		
Bilge level				X	
Fail start				X	
Fail stop				X	

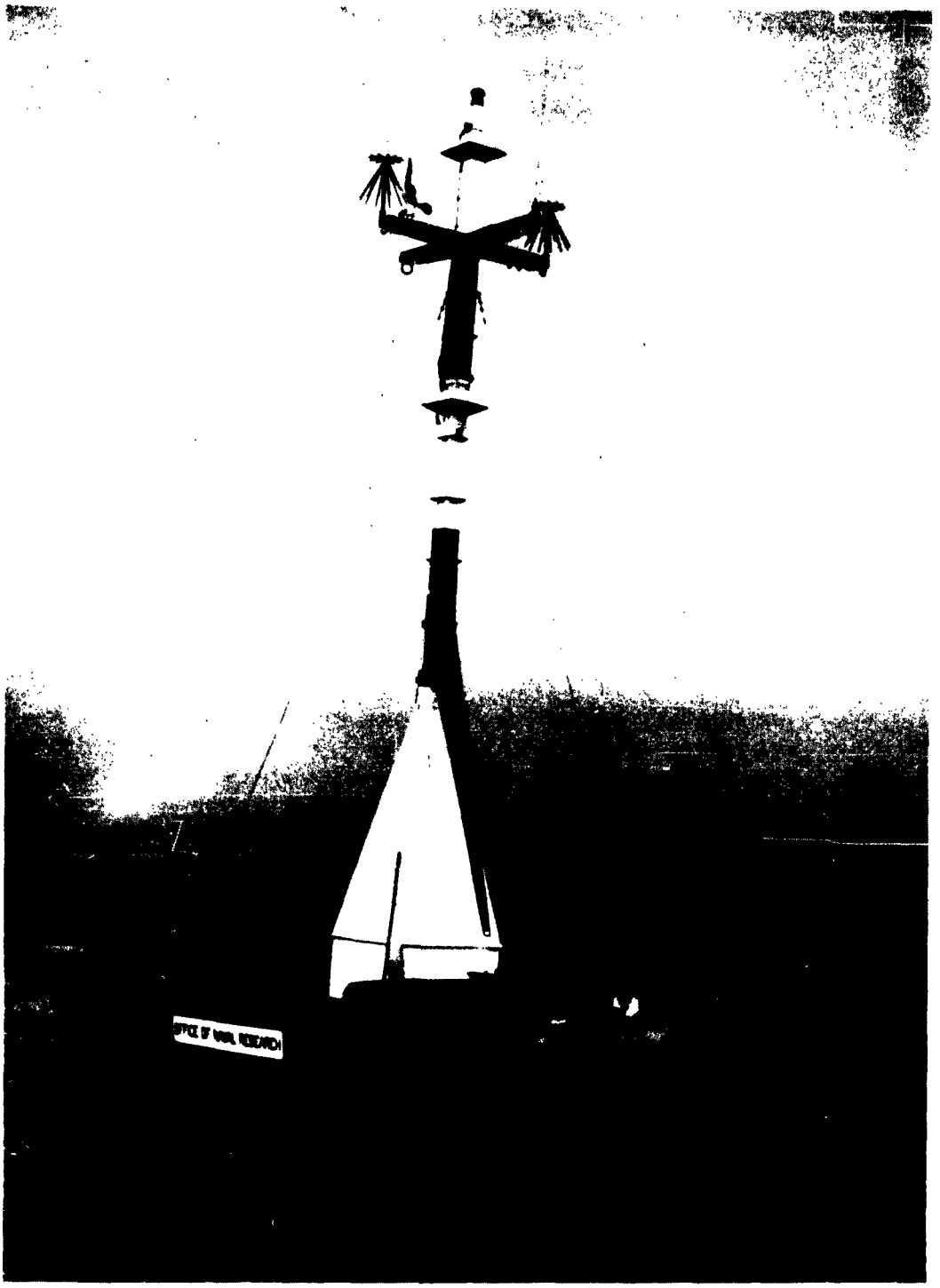

Figure 64. Electric Power Source Test Hull, On Station

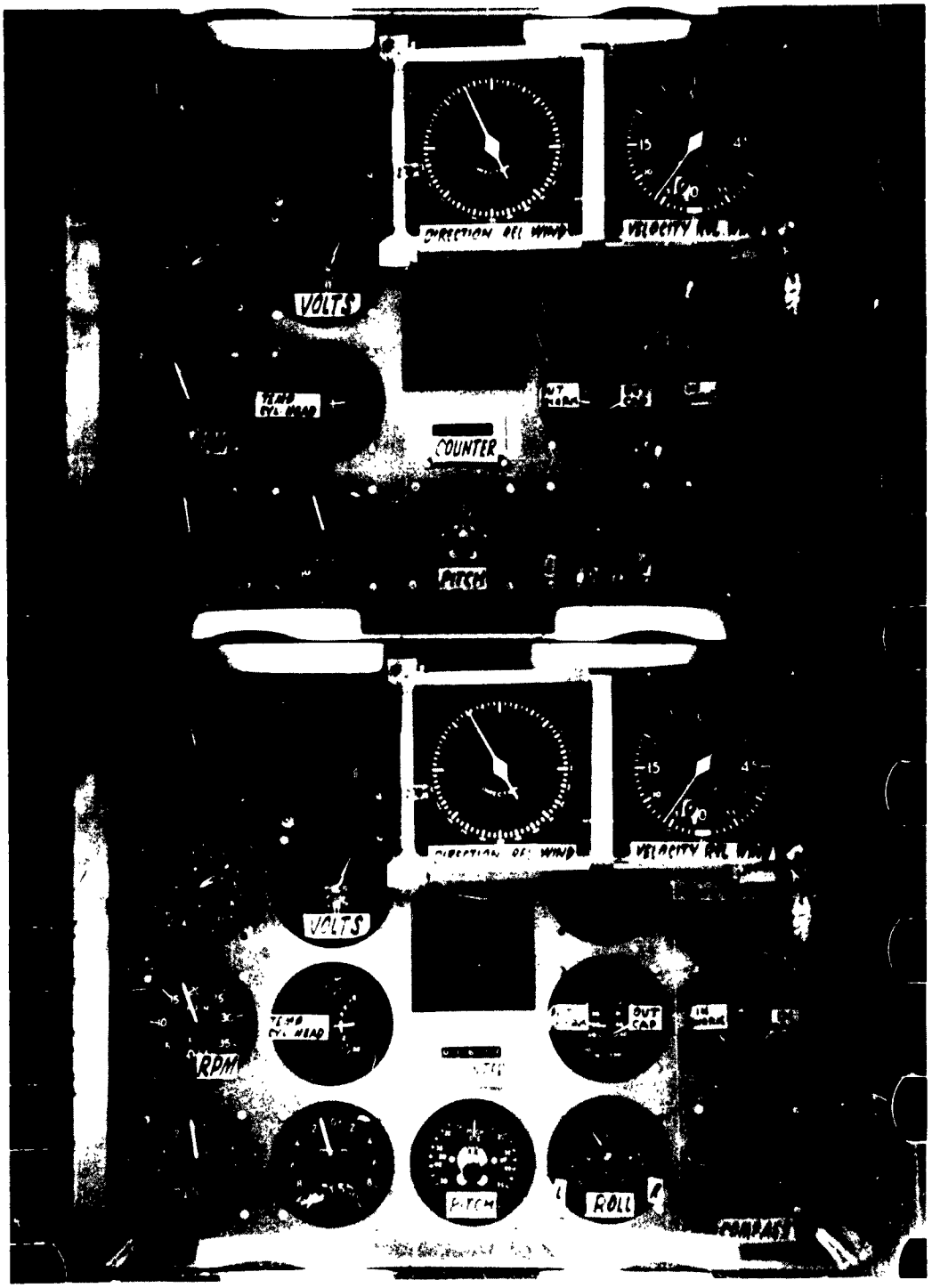

Figure 65. Two Photopanel Frames, Taken One Second Apart, From 10 February Storm

Table 2. Programmer Action Sequence

Minutes From	Action
T--O	
1	Ledex A steps from position 1 to 2.
12	Fuel valve opens. Camera motor starts. (approx. 1 min.) Engine cranks.
12 (-) .5 sec.	Photopanel pulse starts.. Photopanel lites ON.
12 (?) sec.	"Engine running" light ON.
13 (&) 30 sec.	Camera stops. Camera lights OFF.
24	30-second photo record.
36	Fail-start relay energized - if the engine is not running.
48	30-second photo record.
72	30-second photo record.
84	Photo limit relay energized.
120	30-second photo record.
180	30-second photo record.
192 (approx.)	Cutoff signal from voltage sensing circuit. (The cutoff voltage is 28.25 volts. The variable load for the battery will be adjusted by trial until the charge time approximates 3 hours.) Photo panel system activated. (90-sec. record.) Fuel valve denergized. Engine stops.
240	Overrun cutoff relay energized - if the engine is still running. Fuel valve closes. Breaker points are shunted to ground.
360	Photopanel counter advances 1 count. System reset relay energized. Capsule purge blower ON. (12 minutes).

4.4.1.1 Programmer Description — The test is programmed on a 6-hour cycle. The programmer consists of three multi-deck, 12-position Ledex switches used in tandem.

Ledex A steps 12 positions/12 minutes.

Ledex B steps 10 positions/120 minutes. (10, 11, and 12 bussed).

Ledex C steps 12 positions/360 minutes.

A 28-volt dc, chronometric-controlled motor with cam-actuated switch steps Ledex A once per minute.

The programmer can be reset to "home" position by the Reset switch when required in order to maintain sync with clock time.

The photopanel-camera film magazine capacity was 500 feet of 35mm film. At the rate of framing used, and because of the number and length of each burst commanded during each cycle by the automatic programmer, it was necessary to change film once a week. Film data were tabulated and analyzed.

Certain measurements were telemetered to shore upon command, as previously shown in Table 1. Telemetry was utilized occasionally as a check on system performance between regular visits to the hull to change film. During stormy weather, telemetry was used to obtain continuous records of hull motion and mooring loads. Data were recorded on Sanborn recorders in the government-owned data station at Convair.

4.4.2 RESULTS — Testing of the electric power system is still being conducted. From 29 December 1962 (when tests were started) until 15 February 1963, the engine/generator had been operated approximately 726 hours, involving 286 starts. The piston engine is still operating satisfactorily.

Analysis of photo panel data shows that cylinder head temperature has remained well below the maximum 500° F, with the engine/generator operating at sea in the capsule. The piston engine has suffered no ill effects from operating

in a marine environment — lubrication of all moving parts has been adequate regardless of the extreme pitch and roll of the test hull.

After one month of testing at sea, during which time the engine/generator was operated for 382 hours (involving 141 starts), the generator brushes failed abnormally. This test period is equivalent to 4.2 months of actual operation, based upon engine time alone, and assuming that the electric power source contained only one engine/generator.

The test hull was brought ashore and the fault corrected. At this time difficulties with the automatic programmer were discovered and remedied. Lubricating oil in the reservoir was changed from SAE No. 30 to SAE No. 10-30 to remedy a cold-starting failure situation discovered during system checkout at the dock. The old oil was found to have increased in viscosity. The propane tank was refilled. Tests at sea resumed on 30 January 1963 when the test hull was returned to its station.

On the weekend of 10 February, a severe storm system passed through San Diego. Wind velocities of 35 kt., with gusts exceeding 50 kt., were recorded at Lindbergh Field, San Diego. Unfortunately, the wind-velocity indicator on the photopanel in the test hull was not operative at the time, although the wind direction indicator and all other instrumentation operated satisfactorily. During the 3-day storm, heavy rainfall occurred. Wave heights exceeding 14 feet, trough to crest, were measured at the Mission Bay breakwater, which received considerable damage. Similar wave heights were observed at the NEL Research Tower. Roll angles recorded on the photopanel in the test hull repeatedly reached ±15°; pitch angles reached ±5°. These values were corroborated by continuous records obtained by telemetry. Typical photopanel frames are shown in Figure 68 and similar telemetry records appear in Section 2 of this report. The natural period of roll of the hull was 2.9 seconds. Sounds heard over the telemetry system's audio channel confirmed observations of slamming, as seen from the shore with binoculars. Observation of roll angle from shore consistently

indicated that ±15° is perhaps half of the actual roll because of overdamping in the roll sensor. The test hull made heavy weather of it for those three days; however, the electric power system functioned normally throughout that time.

The system operated satisfactorily for two weeks, until 15 February, when another malfunction of the automatic programmer caused system failure. The fault was found to be a relay in the voltage-sensing circuit that commands engine/generator cutoff. The relay was replaced and the system restarted. It operated satisfactorily, but with marginal battery voltage until 24 February, when system failure occurred again because of failure of the engine/generator start command from the automatic programmer. The test hull was returned to the dock on 27 February.

Sea tests of the engine/generator, operating in the "boiler-plate" capsule and schnorkel, revealed the following data:

a. Maximum cylinder head temperature recorded was 450° F.

b. Output of the engine/generator could not be held at 800 watts throughout the charging cycle because of poor current regulation characteristics of the generator. This effect is shown in Figure 66. The result was that maximum cylinder head temperature occurred 1 hour after charging was initiated, at which time generator output had fallen to 700 watts.

c. Temperature of air at the capsule inlet was 22° F. more than ambient measured at the schnorkel inlet, indicating transfer of heat from the exhaust duct to the inlet duct in the schnorkel. Temperature of outlet air mixed with engine combustion exhaust, as measured at the schnorkel outlet, was 140° F when this condition existed.

4.5 CONCLUSIONS

Data obtained during preliminary testing on shore and in the laboratory permitted successful design of the "boiler-plate" schnorkel and capsule, which has worked

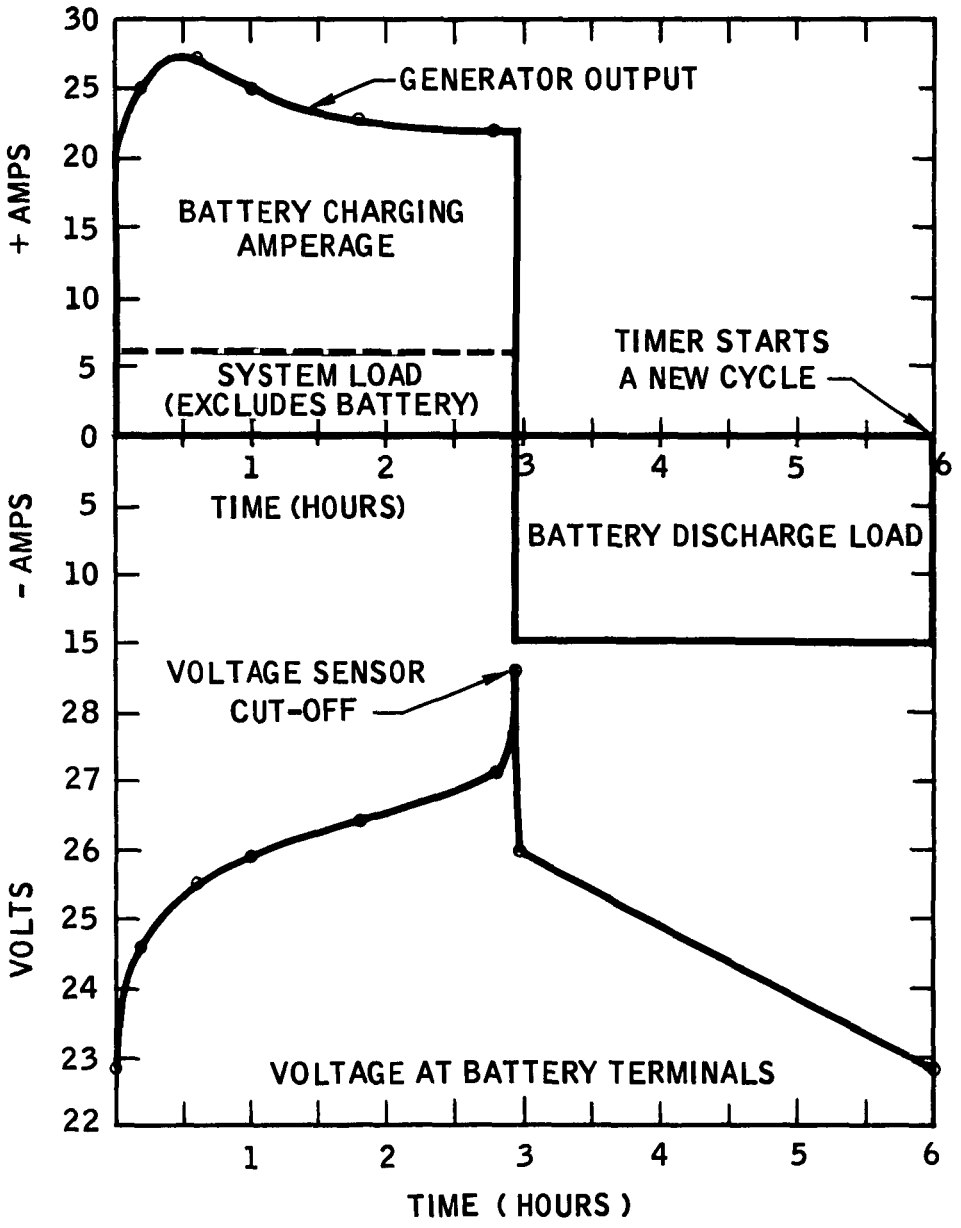

Figure 66. Six-Hour Power Cycle

out satisfactorily in the tests at sea. Sea tests of the complete electric power system indicate that the piston-engine/generator (burning propane fuel and charging nickel-cadmium batteries) is capable of long periods of unattended operation in a telemetering buoy. Available data indicate that such a device may easily operate for 382 hours — the time accumulated when the tests were first interrupted.

Difficulties with the automatic programmer, attributed to malfunction of certain relays, have caused the system to fail twice. A system failure also resulted from generator malfunctioning (caused by improper brush holder assembly), which burned the brushes and pitted the commutator. These events, each involving a deep discharge of the battery bank to the point where several cells reversed polarity, caused the bank to become unbalanced owing to divergence of individual cell potentials and capacity.

The fact that the piston-engine portion of the electric power system is still operating normally after more than 726 hours of operation at 80% output, and after more than 286 starts, is particularly interesting. At the outset it was felt that the system would eventually fail because of engine mechanical malfunction before trouble appeared in the system' s electric or electronic areas. Assuming that a system contains a single engine/generator, 726 hours of engine time is equivalent to more than 8 months of system operation.

When the system first failed, it was noted that the appearance of the engine/generator was the same as it was at initial installation in the capsule. The engine/generator was clean, free of oil, soot or corrosion, and sounded the same as when it was installed. The capsule' s interior was equally clean, except for some large oil spots on the bottom, caused by small leaks in the lubricating-oil transfer pump. (The pump has not been touched.) The plenum chambers in the capsule inlet and outlet were dry, and showed no indication of having had water in them. The sparkplug was removed, inspected, and immediately replaced. To avoid disturbing the electrode gap, it was not measured with

a feeler gage, but was estimated to have increased from 0.020 inch initially to 0.027 inch at time of inspection. The center-electrode porcelain was light straw in color, and there were no indications of carbon deposition. The gap was such that the engine would start at 300 rpm, but the lower limit is not known.

The cause of the generator malfunction could have been (and probably should have been) detected through a more thorough inspection before the tests were begun. Certainly, it is an extraordinary fault.

Battery bank imbalance was the result of operating the system beyond the battery design limits, which caused a difference in individual cell potentials. This difference has not yet been corrected; however, it can be accomplished by charging the battery bank three or four times to 200% capacity. It is believed that battery bank imbalance would not have occurred if the battery had been operated within its design limits. If the present system of beginning battery charging by clock command and stopping it by voltage sensor had been employed, the trouble would have been avoided — if the generator had not failed. In addition, if the battery bank were twice its present capacity, the battery bank would have given satisfactory performance even with the present cell-potential imbalance.

Modification of the engine/generator' s lubrication system has proved to be satisfactory in its functioning. Increase in oil viscosity may be eliminated by using another oil, or minimized by providing a larger oil reservoir. The possibility exists that the oil originally used was especially blended to become more viscous in service in order to counteract the dilution that normally occurs when gasoline is used as the fuel. The SAE No. 10-30 has not run long enough at this time to obtain data on its viscosity.

Difficulties with the automatic programmer stem partially from the fact that the programmer was designed and built around a particular relay that was available — a relay that worked satisfactorily in other applications but one that

is evidently marginal in this circuit. Some of the relays installed were not new, and had withstood many hours of service in another application. The difficulties may also be attributed to the fact that system voltage was lower than planned, because of the number of cells in the battery bank. In designing and building an operational system, neither of these situations should be permitted to exist. Lead time prevented procurement of a cam-operated mechanical programmer that would have been more reliable for this test.

Current regulation, over the voltage range required to charge batteries in this system, is not optimum with the specimen generator — its battery-charging terminals do not produce constant current with varying voltage. By connecting the series field with its polarity reversed, this situation was over-corrected. Minor rewiring which involves placing a suitable low resistance in parallel with the series field should produce satisfactory results.

Preliminary studies of cylinder head temperature and cooling system pressures with different duct diameters and lengths, and evaluation of data obtained from sea tests, indicate that duct size used in the 30-ft. "boiler-plate" schnorkel is larger than needed. Duct length and size apparently have less effect upon cylinder head temperatures measured in the capsule than does the contribution of heat into the capsule from the generator windings. A study will be made to determine the effects of ducting generator outlet air directly into the plenum that now receives engine outlet air. Evidently the generator's contribution to the capsule's heat budget is primarily responsible for the increase in cylinder-head temperature over the values obtained with the unenclosed engine/generator.

The fuel system, including engine/generator start and cutoff capability, functioned ideally. At no time has any fuel odor been detected from any part of the system. Engine/generator performance indicates no ill effects caused by using fuel shutoff to stop the engine.

The following points should be given further thought and study:

a. Heat from engine/generator exhaust and cooling outlet may be useful in removing ice from the schnorkel and antenna in locations where ice may be a problem.

b. Sensing the battery bank voltage or using series-connected pressure switches to detect gassing in all cells are both good methods of determining time for battery-charging cutoff. Perhaps using one as a back-up for the other is justified.

c. Watt-hour metering during the discharge cycle, with timer and voltage sensor backup, may be the optimum method of determining time for battery-charging start.

d. System design might be such that two or more levels of operation are possible, permitting use of a battery-condition sensor to remove less essential loads in the event of unusual demands upon the system, as from extra telemetry commands from shore, or in the event of degradation of electric-power system performance.

5 | INSTRUMENTATION SYSTEM STUDY

5.1 GENERAL

Part of the task proposed by Convair involved study of the types and amounts of equipment required to enable an oceanographic buoy to accept 100 channels of data, and to telemeter these data by ionospheric radio link from the buoy to a command and receiving station as far as 2,000 miles away. This phase of the task required considerable study of various methods for collecting data in the buoy, processing it for long-term storage in the buoy, and for short-term storage prior to telemetering from the buoy.

Every portion of the buoy system and the command and receiving station has been carefully investigated, together with a comparison of various methods for accomplishing each phase of buoy design and development. In some cases the choice of the optimum method for developing the buoy system was obvious; in other instances, selection involves trade-offs in flexibility or cost. This section of the report presents some of the factors considered thus far with regard to buoy system development. Concrete recommendations are also made in this report where the selection of a particular approach to the problem is obvious, together with a discussion of the relative merits of alternative methods, where a choice remains to be made.

5.2 SIGNAL CONDITIONING

In any sampled data system there is at least one and quite often more than one processing or conditioning operation that must be performed on the data signals before they can be passed through the sampling unit. Some of these operations include:

Scale factor adjustment and offset.

Bridge balance

Filtering

Linearization

Analog computation.

5.2.1 SCALE FACTOR — The data sampler (commutator) accepts signals from various sensors and sequentially feeds them into an encoder of some sort. In this case the data encoder is an A/D (analog to digital) converter. The encoder has certain limitations regarding input amplitude, offset and frequency response. For example, if the encoder has a full-scale input range of 0 to +5 volts, the signal conditioner must either amplify or attenuate the outputs of the individual sensors so that their full-scale outputs fall within this range. If the signal is allowed to exceed 5 volts, no answer will be obtained during that time when full scale is exceeded, except that it will be known that the input is full scale or greater. If the maximum output of the transducer is far below the allowable full scale, the resultant answers will suffer in terms of resolution. Sometimes the full-scale output to be expected is not known and it is necessary that an educated guess be made in setting up the scaling until test data are obtained. After instrumentation systems have seen some service it is usually desirable to reset the scale factors so that they are in closer agreement with the allowable full scale.

Off-set or zero setting is similar to full-scale adjustment in that it must agree with the zero level requirement of the encoder. Usually, the zero set point is zero volts, but sometimes it can have a positive or negative value. In any case, the offset or zero set circuit provides an adjustable voltage that is put in series with the data signal voltage, giving an arithmetic sum of the two voltages.

5.2.2 BRIDGE BALANCE — Where the sensing element in a sensor is a variable resistance element, such as a thermistor or strain gauge, the resistor is placed in a Wheatstone Bridge circuit to cause its variation (in response to a physical stimulus) to generate a voltage analog. In this case the bridge merely acts as a method of arriving at the zero offset required. In conjunction with the bridge balance controls there are other controls for varying the sensitivity and linearity of the gauge. All of these controls and associated fixed-resistive or reactive elements are usually considered to be in the signal conditioning area.

5.2.3 FILTERING — In any sampled data system it is necessary to examine the sensor system and determine if there are frequencies present that are too high for the sampling rate being used. If there are frequency components that exceed a certain limit, even if they are of no interest, they must be filtered out ahead of the data sampler to eliminate aliasing. Once data have been sampled there is no way of eliminating the errors due to aliasing. Elimination of these unwanted frequencies is accomplished by using either a passive or active electronic filter. Where the output of the sensor must be amplified, it is convenient to connect the amplifier as an analog low pass filter, thus killing two birds with one stone — amplification and filtering. If an amplifier is not being used, a simple RC filter network is quite often found to be sufficient; however, it is sometime necessary to use a sophisticated design such as a multi-stage M-derived filter. These are required only when desirable data frequencies are almost as high as the frequencies to be rejected.

5.2.4 LINEARIZATION — Variable resistance sensors can be linearized by means of fixed resistors inserted in series — parallel with the sensor element. The same is true of reactive element sensors. Sometimes the nonlinear characteristic of a semiconductor diode or varistor is used to linearize the action of a sensor. These operations are also considered as signal conditioning.

5.2.5 ANALOG COMPUTATION — Analog computer techniques are used to combine the outputs of two or more transducers to arrive at the desired answer directly.

In other instances it is necessary to integrate the output of a sensor over a period of time. Where the instantaneous output of a sensor does not provide a valid answer it is necessary to "look" at it over a period of time and take the average. Since the data storage system and radio link lacks the capability of handling continuous data, or many samples per channel, the analog computer technique may be recommended for generating a smoothed data point.

5.3 CALIBRATION AND TRANSDUCER SOURCE

A very accurate and stable power supply is needed to power all sensors except the self generating type. Bridge sensors can be operated with either dc or ac excitation, but in either case the voltage levels must be accurately stabilized. An accurate voltage is also needed to calibrate parts of the data encoder system. Between the sensors and data encoder there are usually units of one form or another that can drift or change gain. Since the transducer power supply already provides an accurate voltage source, this can be utilized to calibrate the rest of the system. If a large amount of dc reference power is required it can be obtained by running the unregulated dc through a solid-state regulator, using a temperature-controlled Zenner diode pack as a reference. An accurate amplitude-square wave voltage can be derived from the dc reference.

Accurate reference frequency wave forms used for clocks, gates and calibration of FM discriminators are derived from crystal-controlled oscillators.

5.4 MULTIPLEXING

At the present time, the mooring line sensor design philosophy is somewhat nebulous and it is recognized that an evolutionary process is involved. It is desirable that sensors be standardized as much as possible for ease in converting the data for storage. As sensor systems are developed and optimum

techniques are evolved, the methods of multiplexing and digitizing the data will undoubtedly change to be compatible with these improved methods.

5.4.1 HIGH/LOW VOLTAGE SENSOR SYSTEM — A proposed design describes a 100-channel digital data acquisition system. Of the 100 channels, 50 will be low level (±10 mv) and the remaining 50 will be high level (±2.5 V). The sampled information will be converted to digital binary form and will ultimately be recorded on magnetic tape in parallel word form for long-term storage, and in a magnetic core memory in parallel word form for temporary (24 hour max.) storage and eventual transmission over a HF radio link. The sampling of the 100 channels will take place once per hour and will be accomplished in approximately one second. Because total power consumption is a critical problem, it is desirable to turn on the system only during the sampling period and then turn it off again for the balance of the hour.

5.4.2 COMMUTATORS — A thorough investigation of three types of commutators for this application has been made, and the conclusions are that either a completely solid-state or reed-relay type commutator be used. This decision has been made primarily for reasons of life and reliability, and also because of channel synchronization when the system is turned on and off. Since a mechanical commutator of the rotating brush type requires a certain period of time to come up to speed it would be difficult to provide proper synchronization when the sampling of the 100 channels is begun. For this reason, and for purposes of wear and life, this type of commutator has been eliminated as a possibility.

5.4.2.1 All Solid-State Commutator — Two commutators (50 channels each) can be used for this application — one built for low-level operation and the other for high level. The low-level unit contains its own amplifier and draws a total of 8.5 watts.

The high-level commutator draws approximately 4 watts, and both units make use of transistor switches to gate the data into the A/D converter.

A single-pole double-throw transistor switch that will be included as part of the A/D converter package is used for sequentially gating the low-level and the high-level commutator into the A/D converter. In other words, the switch connects the low-level commutator to the A/D converter for the first 50 data channels, and the high-level commutator to the A/D converter for the last 50 channels.

5.4.3 FM SENSORS — Certain types of sensors are particularly suited to provide an output in the form of an ac voltage of constant amplitude but variable frequency, where the change in frequency is proportional to change in the physical stimulus. Signals in this form can be handled in a number of ways. They can be digitized directly by means of cycle-counting techniques, or they can be converted to a dc voltage by means of an FM discriminator and then inserted into an A/D converter. Where short samples (under 0.5 sec.) of FM data are to be taken there is an advantage in using the discriminator method because of the analog low-pass filtering capability at the output of the discriminator. If samples of 0.5 sec. or longer are to be taken, the averaging effect of the cycle counting method will probably be adequate to eliminate unwanted frequency components. Where FM sensors share a sampling sequence with sensors whose output is a dc voltage, it is convenient to change one into the form of the other before A/D conversion — otherwise, two types of A/D converter are required and the converter outputs must be combined. If the FM sensors can be normalized so they all operate in the same frequency range, they can be multiplexed into a common discriminator whose output is then fed to the A/D converter. The single FM discriminator can be easily calibrated by means of two reference frequencies, whereas multiple-channel discriminators operating in different frequency bands would each require its own calibration frequencies.

At the present time it is assumed that FM sensors as well as high level (0-5 V) and low-level (0-10 MV) voltage output type sensors will be required to do the job. In the area of FM sensors, both voltage controlled and the direct-conversion type sensors (such as the Vibratron) may be used.

A commutation and digital conversion system that can be used with both FM and voltage type sensors is shown in Figure 67. A number of FM oscillator-type data encoders, located at various positions along a mooring cable, are all operating simultaneously, and are connected to a pair of common wires running the length of the cable. They enter the buoy through a swivel joint which serves as a rotary electrical connection between the mooring cable and the buoy. The FM oscillators are all selected to operate on the same center frequency (F_x), and all have the same frequency deviation for full-scale data. The output of each FM oscillator is connected to a gate that is normally closed. Each gate is controlled by a discrete frequency which, when applied to the gate control input, causes the gate to open and allow the FM oscillator output associated with it to pass on through to the mooring cable wires. The discrete frequencies that operate the gates are generated in the buoy. An electronic programmer in the buoy starts a data-sampling sequence in the following manner: First, power is applied to the FM oscillators and other electronics allowing sufficient warm-up time for stable operation of the units. Then, a discrete frequency from the tone oscillator (i.e., F_a) is fed down the mooring cable, causing gate F_a to open — thus allowing the first FM oscillator to feed up the mooring cable wires through the electrical swivel to an FM discriminator. The discriminator output is fed to an A/D converter for quantitization in the form of a ten-bit, straight-binary code. After the quantitizing process has been completed, the ten-bit word is transferred from the A/D converter to a magnetic core memory and magnetic tape memory. At the end of this sequence the tone oscillator F_a is turned off, thus closing gate F_a — and tone oscillator F_b is turned on to open the FM oscillator gate F_b. As before, this channel is discriminated, converted to digital form and stored on magnetic core and tape.

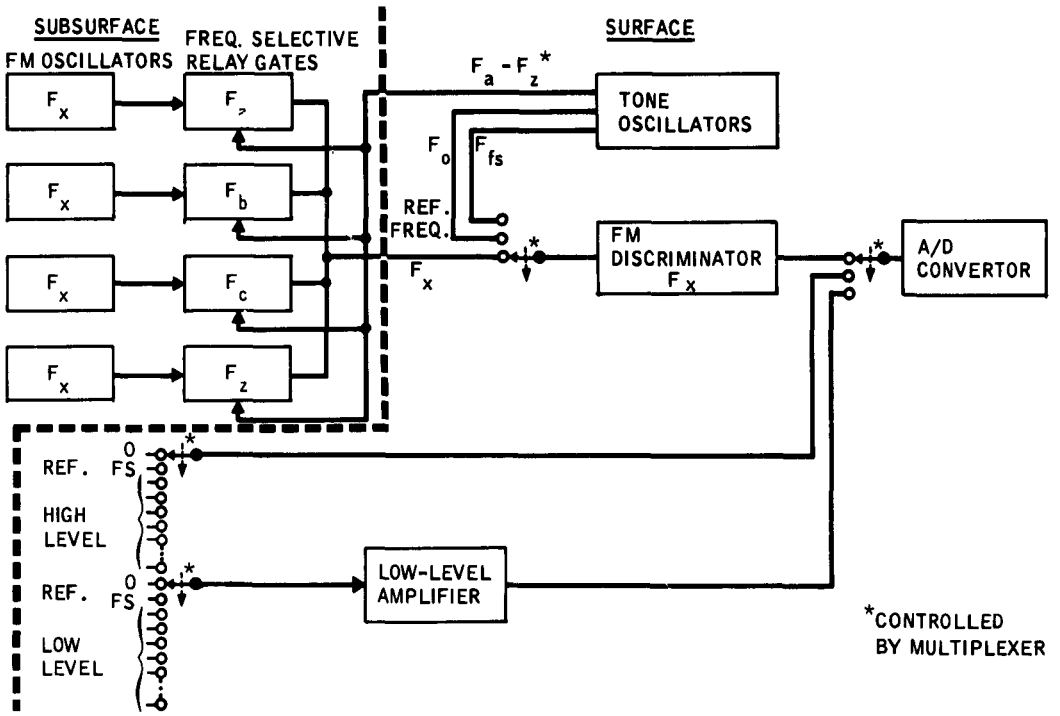

Figure 67. Possible Commutation and Digital-Conversion System

This process is repeated at a fixed rate until all of the FM oscillator channels have been digitized. Sometime during this sequence the FM discriminator is connected, in turn, to a zero and full-scale reference frequency to calibrate out any discriminator drift.

The A/D converter is then disconnected from the output of the FM discriminator and connected to the common output buss of the high-level voltage sensor multiplexer. As the multiplexer steps from one sensor to the next, the A/D converter generates a 10-bit, straight-binary code representing each voltage level and stores it on magnetic core and tape memories as before. Included with the high-level sensors are zero and full-scale voltage reference points that act as a check on the A/D converter. After sweeping through the high-voltage sensors, the low-level multiplexer starts its sequence. The output of the low-level multiplexer is fed through an amplifier before going to the A/D converter, but the digitizing action is the same as before. Ordinarily, low-level sensors

are differential in nature; consequently, the low-level amplifier not only increases the amplitude of the signals but also converts from differential input to single-ended output to be compatible with the A/D converter.

At the end of this data-gathering sequence, with all of the data stored in both magnetic core and magnetic tape memories, the equipment is turned off until the next warm-up period is called for by the buoy programmer.

5.4.4 ANALOG-TO-DIGITAL CONVERTER — The analog-to-digital converter (ADC) proposed is a completely solid-state unit using a reference oscillator, PDM Keyer type of design. This unit includes the single-pole, double-throw switch discussed in the previous subparagraph. This unit will have the following specifications:

Digitize rate	- 112.5 conversions/sec
No. of bits	- 10
Code type	- straight binary
Frame sync	- 20-bit word/alternate ones and zeros/per frame
Word sync	- a "one" bit at the beginning of each word
Temperature range	- -50 to + 100° C
Power	- 1.7 watts
Size	- 4 x 4 x 2

5.5 MASTER CLOCK, DIGITAL PROGRAMMER, DIGITAL SCANNING UNIT

Since the gathering of data on an hourly basis is controlled within the buoy itself it is necessary that the buoy has a very accurate source of time. A temperature-regulated, oven-type, crystal-controlled solid-state oscillator is used for this purpose. A unit of this type can be obtained having a stability of one part in 10^7 per week. This would amount to approximately a 1-minute error in 6 months. The oscillator frequency is made high enough so that it can be used for clock

pulses in the A/D converter, multiplexer, time code generator, digital scanning unit, magnetic-core storage unit and magnetic-tape storage unit. Low-frequency clock pulses are obtained from the primary frequency source by divider chains. A once-per-hour pulse derived in this fashion is used to generate a data-gathering sequence. The sequence may proceed as follows: 1) Turn on all electronic units associated with data gathering and storage, allowing sufficient time for warm-up; 2) Trigger the digital scanning unit which then sequentially transfers a frame-sync word, buoy ID, time code, and digital transducer words into the magnetic-core and magnetic-tape storage. The last position of the digital scanning unit is the output of the A/D converter. After arriving at this position, the digital scanner holds while the digital programmer commands the multiplexer to sequence through its series of operations. At the end of the multiplexing cycle, all of the units are turned off except the time-code generator and the master clock and digital programmer itself. This same sequence is repeated once per hour for one year.

5.6 DIGITAL DATA SOURCES

5.6.1 FRAME-SYNC WORD — Two ten-bit words are set up as zero-one voltage levels to be scanned out by the digital scanning unit at the beginning of its cycle.

5.6.2 TIME CODE GENERATOR — Using the output of the crystal oscillator master clock as a reference frequency, the time-code generator arrives at a binary representation of year, day, hour and minute through a series of binary dividers. Each of these four numbers are represented by a ten-bit, straight-binary code. Since all ten bits are not needed to represent the full range of the numbers, the extra bits will be used for redundancy. The last three decimal digits of "year" will be used, requiring all ten binary digits. "Day" will require three decimal digits (000 to 365) or nine binary bits. "Hour" requires two decimal digits (00 to 24) or five binary bits. "Minute" requires two decimal digits (00 to 60) or six binary bits. Four sets of wires (ten wires per set) feed

the binary voltage levels from the time code generator to the digital scanning unit for transfer into the memories during a data-sampling sequence.

5.6.3 BUOY ID — "Buoy ID" is represented by a ten-bit binary code that is set up initially for each buoy during manufacture of the instrumentation system. It is set up on a permanent basis and can be altered only by a hand-wiring change. The output of this unit feeds the digital scanning unit in the same manner as the other digital inputs.

5.7 TEMPORARY DATA STORAGE

The sensors used to convert the physical function being measured (temperature, pressure, current direction, velocity salinity, etc.) into voltage or current analogs are scanned once per hour, as determined by a timer-programmer located in the buoy. The data are converted into digital form by an AD conversion process at the rate of 100 channels per second. It is desired that this data be transmitted over a high-frequency radio link (3-30 Mc), and received and stored at a remote shore station (200 to 2,000 miles away). If the data were transmitted directly once per hour, the following problems would be encountered: 1) Radio contact may be impossible on an hourly schedule basis: 2) Data would have to be scanned out at a 10-second interval instead of 1 second (this is probably acceptable), because of the radio link bandwidth limitation: 3) More battery power would be consumed by transmitting 24 times a day for 10-second intervals vs. 6 times a day for 40 seconds, or once per day for 240 seconds.

In addition, running the transmitter for longer periods less often is a higher reliability mode. Turning vacuum tubes off and on repeatedly, letting them heat up and then cool off, is the worst thing that can be done from a reliability standpoint. Assuming transmission 24 times a day in ten-second bursts it would still be necessary to allow the transmitter to turn on and warm up a few minutes prior to actual RF emission. Of course, this would consist of filament power only during warm up, but compared to operation on a four-per-day basis an

extra hour of filament power would be used up — assuming a 2.5-minute warm-up period. The difference would be 50 minutes — comparing 24-per-day to 4-times-per-day transmission.

Although all but the first difficulty might be overcome, it is very unlikely that it would be possible (under most circumstances) to transmit once per hour over an HF radio link.

Because of these problems it is necessary to store the data gathered during the once-per-hour scanning cycles for later playback over the HF link. When the various equipment used for storage and playback of digital data is evaluated, magnetic tape and magnetic core stand out as the most promising. Storage requirements are as follows:

a. Read in and out at rates that differ by as much as ten to one.

b. Data in storage not erased by power being turned off and on.

c. High reliability.

d. Low power consumption.

e. Reasonable cost.

f. Reasonable size.

5.7.1 READ IN/OUT RATE — The high read-in and low read-out rate requirement is more easily met by the core memory than by the magnetic tape storage. The core memory read-in or read-out rate is changed by selecting different clock frequencies, whereas in tape storage it is necessary to make a belt or gear shift change, or somehow change motor speed. In addition, the tape storage needs a slewing speed to shuttle back and forth between locations on the tape. The core memory on the other hand can easily align itself with the starting point. Both the core and tape methods will retain the data with the power turned off.

5.7.2 COST — The cost of a core storage is about twice that of a tape storage — in terms of off-the-shelf type of equipment — with a lower limit price on a tape machine ($6,000) than on the core unit ($12,600). Once a core unit has been designed for this specific purpose its price would be more in line with the tape, although it would probably still be rather high.

5.7.3 POWER — The power drawn by a core unit would be somewhat less than that of a tape unit because of the motor power required in the tape unit. However, since the amount of power drawn here is so small compared to the buoy total, the difference in power drain could most certainly be ignored as a factor in selecting one mode over the other.

The relative size of the core unit vs. the tape unit is about the same. If specially designed units were built for use on oceanographic buoys, the sizes could be reduced but would still be comparable. In any case, for the intended use, size does not impose a significant problem.

5.7.4 RELIABILITY — If a core memory were packaged properly it would be much more reliable than a magnetic tape unit because it has no moving parts. Although tape recorders can be made with a high degree of reliability, the core units should last indefinitely. Because high accelerations and shock may be encountered during handling and operation, the core unit would definitely have the advantage.

5.7.5 EXPANDABILITY — One area where the magnetic tape unit has an advantage over the core unit is expandability. An increase in the capacity of the core memory would entail a proportional increase in size, complexity and cost, whereas the tape storage could be increased at no cost whatsoever by simply using a longer piece of tape.

5.8 RADIO REMOTE CONTROL

5.8.1 SSB TRANSCEIVER — It is assumed that a 3-30 mc, single-sideband transceiver will be used. The normal mode is receive — the transmit mode

being used only during identification or data transmission. The transmitter and receiver have a common frequency-determining section with a choice of three presettable frequencies. The frequency to which the transceiver is tuned at any time is selected by means of the remote control radio link.

The use of a single receiver is considered to be a compromise method as compared to a three receiver set-up which would be optimum. Three separate receivers operating simultaneously would guarantee buoy response if one of the frequencies were usable. Operation experience is required to determine the necessity for the three receivers.

5.8.2 DECODER — A decoder suggested for possible use in this system is a transistorized electro-mechanical decoder similar to the Secode Digital Recorder RFD-634. This unit is a single-tone pulse decoder which receives and decodes digital pulses from the output of the SSB receiver. The output of the decoder is a momentary contact closure which is used to actuate other circuitry. The heart of the unit is a pulse-operated, electro-mechanical decoding switch with over 360,000 possible combinations. Contacts close to complete an electrical circuit only after a predetermined sequence of input pulses has been received. The unit provides undercount and overcount protection and will not respond to the sum of the individual code digits. The basic units have up to five output contact closures available.

5.8.3 CONTROL LOGIC UNIT, BUOY PROGRAMMER — Momentary contact closures from the decoder actuate the control circuitry in the control logic unit. The control logic unit holds the information and passes on commands to the buoy programmer, which performs a sequence of operations. For instance, if a command is given at the shore station for an ID reply, the buoy programmer switches the SSB transceiver to the transmit mode. After a slight delay to allow switching transients to die out, the ID reply generator is triggered into operation. It puts out a train of pulses that consists of a frame-sync word followed by three 10-bit binary words that are coded to identify the particular

buoy. The time needed to transmit this code sequence is approximately 5 seconds. The transmitted signal is received at the shore station for a sufficient period of time to enable the station to check the radio link conditions and definitely identify the buoy. At the end of the ID reply transmission the buoy programmer would turn off the transmitter and return the receiver to the operate mode. If the signal conditions were bad, or the shore station decided that operation would be more efficient on the next higher frequency, it could send out a command to the buoy to change frequency. After a time delay sufficient to allow the shore station to shift the receiver to the new frequency, the buoy would transmit its ID reply on the new frequency. If this seemed satisfactory, the station could request a data playback on the new frequency; however, if the new frequency were above the MUF or very poor in quality, the station would reset it to another frequency.

After a satisfactory link had been set up, the station could request a data playback of the last 6 hours, or a playback of the last 24 hours. By requesting a 24-hour data playback every 6 hours, the data would be repeated 4 times before being erased from the magnetic core memory. This is a form of redundancy that appears to have advantages over other forms of redundancy when used on HF radio circuits.

For a data playback over the radio link, the sequence would be as follows:

1) A command from the shore station is stored in the control logic unit; 2) the control logic unit in turn feeds a command to the buoy programmer which starts its sequence; 3) and the SSB transceiver is switched to the transmit mode.

An interlock between the buoy programmer and digital programmer prevents transmission during data sampling and storage. If data sampling is in progress when an RF transmission is called for, the RF transmission is delayed until the data sample has been completed. With this condition satisfied, the magnetic core memory is scanned out into the FSK modulator, which shifts back and forth between two frequencies in accordance with the 0/1 binary levels as they emerge

serially from the core memory. The FSK modulator amplitude modulates the SSB transmitter whose emission is picked up at the shore receiving station.

5.8.3.1 Modulator — The modulator is a voltage-controlled oscillator that is shifted between two frequencies by the voltage pulse train generated during a readout of the magnetic core storage. The core storage is loaded one word (10 bits) at a time, but is read out in serial fashion (1 bit at a time). The serial output is in binary NRZL form. For example, the "zeros" are all at a -5 volt level and the "ones" are at a +5 volt level. Although optimum frequency deviations and bit rates have not been determined at this time, the following example shows the type of condition that can be expected: The "zero" level (-5 volts) causes the FSK and modulator to oscillate at 1,250 cps, and the "one" level (+5 volts) makes it oscillate at 1,750 cps. The bit rate of 100 bits per second causes the modulator to shift back and forth between the two frequencies at a rate of 100 times each second — if the data were such that alternative bits were "ones" and "zeros." The PCM waveform would be a 50 cps square wave. The main limiting factors on bit rate are multipath conditions and bandwidth available in the 3-30 mc/s radio spectrum.

Another type of FSK Modulator that can be used is the two-frequency type. An electronic switch controlled by the binary data selects the output of one of two crystal oscillators. The result is a waveform similar to that generated by voltage-controlled oscillator method. This method is advantageous in that the two frequencies generated can be very accurate, but it also has disadvantages in that a discontinuity is generated during the switchover from one frequency to the other. The discontinuity makes the generated frequency spectrum spread out, and it causes a ringing to occur in the demodulation process. The voltage-controlled oscillator method allows shaping of the waveform before modulation, which is an added advantage. Consequently, the voltage-controlled oscillator method is preferred at this time.

5.9 SHORE STATION

The purpose of the shore station is to control as many as five functions in each buoy by means of an HF radio-command link, and to receive telemetry signals transmitted by the buoys. (Figure 67 is a block diagram of the shore station.)

A telephone-dial controlled coder operating into a SSB transmitter serves as the radio remote control unit for the buoys. By selecting a three-digit dial code, up to five functions can be controlled individually on up to 1,000 buoys. The planned shore station is mobile, so that it can be readily moved from one location to another. Two collapsible antennas are stored on board the mobile station, and are used in conjunction with the diversity receivers. One antenna is set up directly over the station and the other at least 600 feet away. The WWV receiver uses a simple whip antenna that can be easily assembled and disassembled.

The two telemetry receivers are HF/SSB units operating in the range of 3-30 mc — their outputs are recorded on tape and also passed through a diversity combiner and demodulator to the input of a digital data-handling system. The digital system records the data in both digital and analog form. The raw signals on the tape can be used at a later time, substituting for the receiver output.

5.9.1 ANTENNAS — It is believed that the omnidirectional discone antennas set up in space diversity are the best for use in conjunction with a portable command and receiving station. They are wide-band devices that can operate over the required frequency range without matching networks; therefore, the station can switch rapidly from one frequency to another without difficulty. Since the antennas are omnidirectional, reception from buoys at different locations can be accomplished without the necessity for antenna orientation. The use of high-gain antennas would be better from a signal to noise standpoint, if the noise were originating from a direction other than the direction of the signal. It is assumed that the mobile trailer can be located in a quiet (low noise) area, where the noise is the same, looking in all directions. A directive antenna will be an

improvement only if the ambient noise level is not detectable by the omnidirectional antenna. The loss in gain due to nondirectionality could easily be recovered, by means of the diversity gain. If directive antennas of a broadband nature were easily rotatable, and easily put up and taken down, it would reasonable to use a pair of them in dual-space diversity, since directivity in itself is not a penalty and can give an appreciable amount of improvement in certain instances. The "log periodic" is an antenna that might fall into this category. This antenna is similar in appearance to the Yagi, and its longest element is one-half wavelength at the lowest frequency to be used. Antennas of this type would have to be pointed in the direction of the buoys if the buoys were at widely scattered locations; however, the antenna would probably cover a 50° sector without rotation. For general purpose use, the directive antenna is not considered necessary; however, for a specified application, the directional antenna may be worth considering.

5.9.2 COMMAND TRANSMISSION SYSTEM

5.9.2.1 Command Coder - The coding system suggested for use in this remote-control HF radio link makes use of the Secode Digital Code Sender TGS-715B2. This unit is an electronic, digital, tone oscillator which modulates a radio carrier with interrupted signaling pulses.

A telephone dial on the front panel functions as the digital encoding device. When operated, the instrument turns on the transmitter and modulates it with a pure audio tone. As the dial is released, the pulsing contacts alternately open and close the output circuit of the oscillator, thus causing the tone signal to be interrupted. As a result, the Digital Code Sender TGS-715B2 produces digital tone pulses which agree, in number, with the particular digits dialed. The pulse interruptions occur at a rate of 10 per second. If a mistake is made in dialing, the dialing of a "1" will reset the decoder on the receiving end. A pause, during dialing, of 4 seconds will also cause a reset of the decoder.

5.9.2.2 SSB Command Transmitter — The command transmitter is a single-sideband unit capable of 500 watts peak envelope power output. The unit can be set to any frequency in the 3-30 mc range. Modulation input is derived from the command coder (described previously). The transmitter shares an antenna used by one of the two SSB receivers. During a command transmission the two receivers are automatically switched to the transmit mode.

5.9.3 MAGNETIC TAPE RECORDER — The magnetic tape recorder is a four-track analog (as opposed to digital) machine commonly used in telemetry ground stations. It records the raw output of the two SSB receivers in the form of FSK audio carriers. This raw storage is then available for playback through the diversity combiners and the rest of the data recovery system at a later date. The tape storage acts as a back-up for protection against possible momentary failure in the downstream portion of the station. Also, such pre-detection recording offers the possibility of optimizing demodulation in the presence of unique signal and noise conditions.

The raw signals recorded on magnetic tape are also useful for obtaining information on propagation characteristics, for future optimization of buoy operation.

5.9.4 WWV RECEIVER — The WWV receiver output recorded on tape gives accurate time information to which the buoy time code can be compared. During complete fade-outs of buoy transmission, the WWV signal will serve as a continuing time reference. It will also give propagation information that can be compared to the buoy link.

5.9.5 DIVERSITY COMBINER — The outputs of the two receivers are in the form of FSK audio carriers. The purpose of the diversity combiner is to accept the best of the two signals and suppress the other. This action can be accomplished by combining the two carriers in proportion to the quality of their signals. It can be done also in digital fashion, where one signal is accepted and the other completely rejected. This second method has been used successfully

in FSK radioteletype work, and is accomplished as shown in Figure 68.

The two receivers "see" the same radio frequency carrier, but their outputs are translated down to two different frequencies f_1 and f_2 that are mixed together and passed through a common amplifier-limiter. The output of the amplifier-limiter will be f_1 or f_2, depending upon which one has the greater amplitude. Two filter-discriminator units, one tuned to f_1 and the other tuned to f_2, are connected to the output of the limiter amplifier. One of the two discriminators will be operative, depending upon which frequency (f_1 or f_2) is present. The discriminator outputs are mixed forming a continuous signal being derived from the strongest of the two signals.

5.9.6 DEMODULATOR — As discussed in paragraph 5.9.5, an FM discriminator can be used as a demodulator for the FSK audio signal. Modern telemetry FM discriminators are much better than the older type of unit because of their linear phase characteristics and wide detector bandwidth. This is especially important from the standpoint of radio propagation multipath interference rejection. The pulse-averaging type FM discriminator is in common usage for telemetry work, but in certain instances the newer phase-locked-loop discriminator offers an improvement on threshold signals. Further study and test may show that an improvement could be obtained by using the phase-locked-loop discriminator for this purpose.

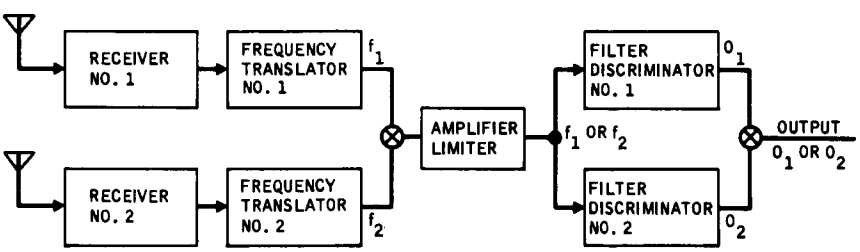

Figure 68. Diversity Combiner

5.9.7 DIGITAL UNIT — The digital unit accomplishes the following: 1) Takes the series of NRZ (non-return-to-zero) binary pulses from the output of the demodulator; 2) Generates sync pulses; 3) Decommutates the data channels; 4) Converts selected channels to analog form; 5) Provides a serial-digital channel output in BCD or straight binary form; 6) Provides a visual indication of data error rate; 7) Provides a visual indication of buoy identification reply; and 8) Feeds a paper tape punch that makes a BCD tape of all the data in real time as it is received.

5.9.7.1 Synchronizer - The data arrives in the form of NRZL (non-return to zero level), straight-binary code. One word of data in this form is shown in Figure 72. The waveform at the top (labeled "clock") is the reference frequency used to generate the binary code shown below it. The decimal equivalent of the binary word shown is 790. Since the binary code alone is transmitted over the radio link, it is the job of the synchronizer to re-establish the clock waveform by means of a frame-sync word arriving ahead of the data words. The data

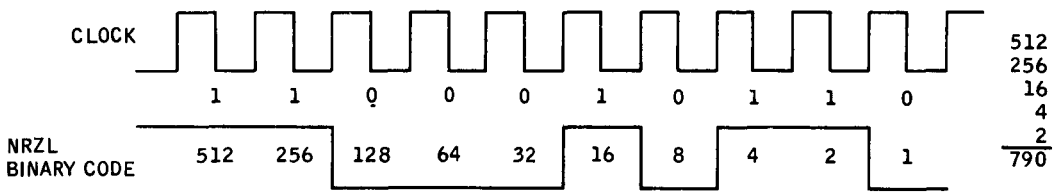

Figure 69. NRZL Straight-Binary Code, One Word

words themselves are then used to keep the synchronizer in sync until the next frame-sync word arrives. The reason for using a NRZ code is that for a given data rate one-half the bandwidth is required or, conversely, for a given bandwidth, twice the data rate can be used.

5.9.7.2 Decommutator and DAC (Digital to Analog Converter) — The decommutator allows up to eight selected words out of a frame to be channelled into a DAC for oscillographic presentation. Magnetic-tape playback is required if

analog presentation is required on other channels of the frame.

5.9.7.3 Error-Rate Indicator — When loss of sync occurs, and by detecting errors in the data words, the error-rate indicator counts (at the word rate) the number of erroneous data words. For a given run, the errors accumulated are presented visually to the operator. Word errors are also indicated on the digital print-out by means of an identifying mark.

5.9.7.4 Paper Tape Punch and Digital Printer — The paper tape punch accepts data from the digital unit in groups at the rate of 3 BCD characters per word. All of the data coming in over the radio link are punched out in real time, assuming that the maximum rate will not exceed 10 words per second. Ten words per second is equivalent to 30 characters (or 30 punching operations) per second on the paper tape punch. The punched tape is then used to generate a decimal listing of the data points, but at a slowed-down rate as compared to real-time data.

The punched tape can then be taken to a computer facility for conversion to digital magnetic tape and entry into a digital computer.

5.10 MODULATION SCHEME — Pulse code modulation (PCM) on a frequency shift-keyed (FSK) subcarrier is the modulation scheme now preferred for transmitting data from oceanographic buoys to shore. This method is preferred over other types of coding because of its noise rejection characteristics and high accuracy. An FSK carrier has a 10 db advantage over off-on keying of a carrier in terms of transmitter power required for a given error rate in the received signal. The PCM/FSK signal is used to modulate a single-sideband (SSB) suppressed-carrier transmitter which offers high efficiency and bandwidth conservation, as compared to standard AM. The difference amounts to 6 db in terms of transmitter radiated power.

At the receiving end, the SSB signal is less subject to heterodyne beat interference and to complete loss of data due to selective carrier fade out.

Frequency modulation of a carrier directly with the PCM waveform generates the same carrier spectrum as PCM/FSK/SSB, and is somewhat more efficient in terms of power drain, due to Class C operation of the finals, but it is limited to this single mode of modulation. The SSB system, on the other hand, is almost as efficient, and is much more flexible in terms of accepting changes in modulation scheme. For instance, subcarrier frequency multiplexing or subcarrier frequency diversity methods are also compatible with the SSB system, and it is felt that either or both of these schemes may find applications in the future.